STRUCTURE/CALCIUM AFFINITY RELATIONSHIPS OF CALMODULIN SITE III: TESTING THE ACID-PAIR HYPOTHESIS USING CALMODULIN MUTANTS

by

XIAOCHUN WU

B.Sc., West China University of Medical Sciences, 1983
M.Sc., West China University of Medical Sciences, 1986

A THESIS SUMBITTED IN PARTIAL FULFILLMENT OF
THE REQUIREMENTS FOR THE DEGREE OF
DOCTOR OF PHILOSOPHY

in

THE FACULTY OF GRADUATE STUDIES
Division of Pharmaceutical Chemistry
Faculty of Pharmaceutical Sciences

We accept this thesis as conforming
to the required standard

THE UNIVERSITY OF BRITISH COLUMBIA
July 1997

In presenting this thesis in partial fulfilment of the requirements for an advanced degree at the University of British Columbia, I agree that the Library shall make it freely available for reference and study. I further agree that permission for extensive copying of this thesis for scholarly purposes may be granted by the head of my department or by his or her representatives. It is understood that copying or publication of this thesis for financial gain shall not be allowed without my written permission.

Department of Pharmaceutical Sciences

The University of British Columbia
Vancouver, Canada

Date July 8, 1997

DE-6 (2/88)

ABSTRACT

The overall objective of this study was to test the Acid Pair Hypothesis in the calcium binding site III of calmodulin using calmodulin mutants. The Acid Pair Hypothesis was proposed to predict calcium binding affinity of a helix-loop-helix calcium binding motif based on the number and the location of acidic amino acid residues in chelating positions [Reid & Hodges, (1980) *J. Theor. Biol. 84*, 401-444]. This hypothesis states that a site will have a higher affinity for calcium if the anionic ligands are paired on the axial vertices of a near octahedron than if they are unpaired. The mutants were designed so that there were either three or four acidic chelating residues with acid-pairs on the X and/or Z axis. The F92W/D133E mutations were maintained in all mutants. Tryptophan was introduced as a fluorescent label into site III to monitor the calcium-induced structural transitions in the C-terminal domain. The D133E mutation in the +Z position of site IV was designed to inactivate this site with respect to calcium binding therefore eliminating the cooperative interactions between sites III and IV. The calcium affinity of site III increased when the number of the acidic chelating residues increased from three to four, when the number of acid-pairs increased from zero to one and further to two, and when the location of the acid-pair was changed from the X axis to the Z axis. These results are consistent with the prediction of the Acid Pair Hypothesis. The fact that the D133E mutation drastically reduced calcium affinity of site IV indicates that the type of acidic residue in chelating positions also plays a role in dictating calcium affinity of the helix-loop-helix site. Conclusions drawn from earlier studies using synthetic models of a single helix-loop-helix calcium binding site describing the effect of the number and location of acidic residues on calcium affinity appear to be applicable to the multisite protein.

TABLE OF CONTENTS

ABSTRACT ii

TABLE OF CONTENTS iii

LIST OF TABLES ix

LIST OF FIGURES xi

LIST OF ABBREVIATIONS xiv

LIST OF AMINO ACID CODES xvi

LIST OF GENETIC CODE xvii

LIST OF OLIGODEOXYNUCLEOTIDES xviii

LIST OF BACTERIAL MEDIA xx

MUTANT NOMENCLATURE xxi

ACKNOWLEDGMENT xxii

CHAPTER 1

INTRODUCTION

1.1. THE HELIX-LOOP-HELIX CALCIUM BINDING MOTIF 1

1.1.1. Calcium binding sites in proteins 1

1.1.2. Structure overview of the hlh calcium binding motif 3

1.1.3. Calcium binding affinity of hlh calcium binding motifs in proteins 4

1.1.4. Prediction of calcium binding affinity of the hlh motif or paired motifs 11

1.1.5. Acid-pair hypothesis 12

1.1.6. Calcium binding in the single site hlh peptide model 13

1.2. HELIX-LOOP-HELIX CALCIUM BINDING PROTEINS 16

1.2.1. Calmodulin 16

1.2.2. Troponin C 26

1.2.3. Parvalbumin 29

1.2.4. $Calbindin_{9K}$ 32

1.2.5. Calcyclin 35

1.3. VU-1 CALMODULIN 36

1.3.1. The synthetic CaM gene and the pVUCH-1 CaM expression vector 36

1.3.2. The amino acid sequence of VU-1 CaM 37

1.4. STUDIES ON STRUCTURE/CALCIUM AFFINITY RELATIONSHIPS USING ENGINEERED PROTEINS 41

1.4.1. Mutation at the invariable +X and -Z positions 41

1.4.2. Mutation at the +Y position 42

1.4.3. Mutation at the -Y position 43

1.4.4. Mutation at the -X position 43

1.4.5. Mutation of charged residues on the surface 44

1.4.6. Mutation of non-chelating residues in the loop 45

1.4.7. Mutation of non-polar residues that become more solvent-exposed upon calcium binding 45

1.4.8. Mutation of Gly92 at the center of the central helix of skeletal troponin C 46

1.4.9. Mutation of the entire calcium binding loop or the entire hlh motif 47

1.5. FLUORESCENCE LABELING OF HLH CALCIUM BINDING PROTEINS 48

1.5.1. T26W, T62W, F99W, and Q135W calmodulins 49

1.4.2. F102W parvalbumin and F102W oncomodulin 50

1.4.3. F29W and F105W troponin C 51

1.6. OBJECTIVES 51

CHAPTER 2

INTRODUCING A FLUORESCENT LABEL INTO VU-1 CALMODULIN AND CREATING A CALMODULIN MUTANT INACTIVATED AT SITE IV WITH RESPECT TO CALCIUM BINDING CAPACITY

2.1. MATERIALS 54

2.2. METHODS 55

2.2.1. Preparation of competent *E. coli* cells 55

2.2.2. Transformation of *E. coli* cells 56

2.2.3. Isolation of plasmid DNA pVUCH-1 56

2.2.4. Quantitation of plasmid DNA 57

2.2.5. Sequencing the CaM gene in pVUCH-1 58

2.2.6. Construction of F92W CaM expression vector pf92w 58

2.2.6.1. *Stu* I/*Xma* III digestion of pVUCH-1 60

2.2.6.2. Separation of digested fragments on agarose gel..... 60

2.2.6.3. Purification of double-cut pVUCH-1 from agarose gel..... 60

2.2.6.4. Dephosphorylation of double-cut pVUCH-1..... 61

2.2.6.5. Semi-quantitative agarose gel electrophoresis..... 62

2.2.6.6. Phosphorylation of DNA cassette..... 62

2.2.6.7. Ligation of DNA cassette with double-cut pVUCH-1..... 63

2.2.6.8. Introduction of ligated plasmid DNA into *E. coli* cells..... 63

2.2.6.9. Identification of the pf92w clone..... 64

2.2.6.10. Storing the positive clones in glycerol culture..... 65

2.2.7. Construction of F92W/D133E CaM expression vector pd133e..... 65

2.2.8. Expression of VU-1, F92W and F92W/D133E calmodulins..... 67

2.2.9. Purification of VU-1, F92W and F92W/D133E calmodulins..... 68

2.2.10. Preparation of the CaM binding peptide W4I-M13..... 69

2.2.11. SDS-polyacrylamide gel electrophoresis of calmodulins..... 70

2.2.12. Amino acid composition analysis and determination of the extinction coefficient of F92W CaM..... 71

2.2.13. Molecular weight determination by mass spectrometry..... 72

2.2.14. Far UV circular dichroism spectroscopy..... 72

2.2.15. Fluorescence spectroscopy and calcium titration..... 73

2.2.16. Effect of W4I-M13 CaM binding peptide on calcium binding affinity of calmodulins..... 73

2.2.17. Calcium titration data analysis..... 74

2.2.18. Phosphodiesterase stimulation assay 75

2.3. RESULTS 77

2.3.1. Confirming the DNA sequence of the CaM gene in pVUCH-1 77

2.3.2. Identification of the pf92w clone 77

2.3.3. Identification of the pd133e clone 80

2.3.4. Identification of VU-1, F92W, and F92W/D133E calmodulins 82

2.3.5. Determination of the extinction coefficient of F92W CaM 85

2.3.6. Identification of W4I-M13 CaM-binding peptide 86

2.3.7. Far-UV CD spectra of VU-1, F92W, and F92W/D133E calmodulins 87

2.3.8. Fluorescence spectra of VU-1, F92W, and F92W/D133E calmodulins 89

2.3.9. Calcium titration of VU-1, F92W, and F92W/D133E calmodulins 91

2.3.10. Effect of W4I-M13 CaM binding peptide on calcium affinity of VU-1, F92W, and F92W/D133E calmodulins 94

2.3.11. Phosphodiesterase stimulation assay 97

2.4. DISCUSSION 103

CHAPTER 3

TESTING THE ACID-PAIR HYPOTHESIS USING F92W/D133E CALMODULIN AS A WHOLE PROTEIN MODEL

3.1. MATERIALS 111

3.2. METHODS 111

3.2.1. Construction of the expression vectors for 3xCaM, 3zCaM 4xCaM, 4zCaM, and 4xzCaM 111

3.2.2. Expression and purification of CaM mutants 114

3.2.3. Characterization of CaM mutants 115

3.3. RESULTS 115

3.3.1. Identification of the p3zcam and p4zcam clones 115

3.3.2. Identification of the p3xcam, p4xcam, and p4xzcam clones 118

3.3.3. Identification of 3xCaM, 3zCaM, 4xCaM, 4zCaM, and 4xzCaM 121

3.3.4. Far UV CD spectra of CaM mutants 124

3.3.5. Fluorescence emission spectra of CaM mutants 126

3.3.6. Calcium titration of CaM mutants 128

3.3.7. Effect of W4I-M13 CaM-binding peptide on calcium affinity of CaM mutants 131

3.3.8. Phosphodiesterase regulation by CaM mutants 135

3.4. DISCUSSION 139

CONCLUSIONS 145

FUTURE STUDIES 147

REFERENCES 150

APPENDIX 168

LIST OF TABLES

Table Page

1. Calcium dissociation constants of hlh calcium binding proteins.....7

2. CaM-binding proteins..... 22

3. Amino acid compositions of VU-1, F92W, and F92W/D133E calmodulins..... 84

4. Molecular weight of VU-1, F92W, and F92W/D133E calmodulins..... 85

5. Amino acid composition of W4I-M13 CaM-binding peptide..... 86

6. Molar ellipticity of VU-1, F92W, and F92W/D133E calmodulins..... 87

7. Calcium dissociation constants of VU-1, F92W, and F92W/D133E calmodulins..... 93

8. Calcium dissociation constants of VU-1, F92W, and F92W/D133E calmodulins in the presence of W4I-M13 CaM-binding peptide 97

9. Phosphodiesterase stimulation activity of VU-1, F92W, and F92W/D133E calmodulins..... 100

10. Amino acid compositions of CaM mutants..... 123

11. Molecular weight of CaM mutants..... 124

12. Molar ellipticity of CaM mutants..... 126

13. Calcium dissociation constants of CaM mutants and synthetic hlh calcium binding peptides..... 129

14. Calcium dissociation constants of CaM mutants in the presence of W4I-M13 CaM-binding peptide.....134

15. Phosphodiesterase stimulation activity of CaM mutants..... 137

16. One-site model fitting 168

17. One-site model fitting (+W4I-M13) 169

18. Two-site model fitting 170

19. Two-site model fitting (+W4I-M13) 172

20. Three-site model fitting 174

21. Three-site model fitting (+W4I-M13) 176

22. Four-site model fitting 178

23. Four-site model fitting (+W4I-M13) 181

LIST OF FIGURES

Figure Page

1. The EF hand 2
2. A schematic drawing of the loop region of a hlh calcium binding motif 3
3. Summary of the sequences of the loop of 567 EF hands 5
4. Amino acid sequences of chicken skeletal troponin C and bovine brain CaM 18
5. Ribbon diagram of the crystal structure of rat testis CaM 19
6. A general model of regulation of a target enzyme by CaM 24
7. Amino acid sequences of carp parvalbumin 4.25 and rat oncomodulin 30
8. Amino acid sequences of bovine calbindin$_{9K}$ and rabbit calcyclin 33
9. Sequence of the synthetic CaM gene 38
10. Structure of pVUCH-1 CaM expression vector 39
11. Amino acid sequences of VU-1 CaM and bovine brain CaM 40
12. Schematic diagram for construction of pf92w 59
13. Schematic diagram for construction of pd133e 66
14. Agarose gel electrophoresis of restriction enzyme digested pf92w 79
15. Agarose gel electrophoresis of restriction enzyme digested pd133e 81
16. SDS-PAGE of VU-1, F92W, and F92W/D133E calmodulins 83
17. Far-UV CD spectra of VU-1, F92W, and F92W/D133E calmodulins 88
18. Fluorescence emission spectra of VU-1, F92W, and F92W/D133E calmodulins 90
19. Calcium titration curves of VU-1, F92W, and F92W/D133E calmodulins 92

20. Fluorescence emission spectra of VU-1, F92W, and F92W/D133E calmodulins in the presence of W4I-M13 CaM-binding peptide..... 95

21. Calcium titration curves of VU-1, F92W, and F92W/D133E calmodulins in the presence of W4I-M13 CaM-binding peptide..... 96

22. Time-course of the amount of cAMP hydrolyzed by PDE..... 98

23. Phosphodiesterase stimulation curves of bovine brain CaM and VU-1 calmodulins..... 101

24. Phosphodiesterase stimulation curves of F92W and F92W/D133E calmodulins..... 102

25. The amino acid sequences of the calcium binding loop of site III of CaM mutants..... 112

26. Schematic illustration of the DNA cassettes used for constructing p3xcam, p3zcam, p4xcam, p4zcam, and p4xzcam..... 113

27. Agarose gel electrophoresis of restriction enzyme digested p3zcam and p4zcam..... 116

28. Agarose gel electrophoresis of restriction enzyme digested p3xcam, p4xcam, and p4xzcam..... 119

29. SDS-PAGE of 3xCaM, 3zCaM, 4xCaM, 4zCaM, and 4xzCaM..... 122

30. Far-UV CD spectra of 3xCaM, 3zCaM, 4xCaM, 4zCaM, and 4xzCaM..... 125

31. Fluorescence emission spectra of 3xCaM, 3zCaM, 4xCaM, 4zCaM, and 4xzCaM..... 127

32. Calcium titration curves of 3xCaM, 3zCaM, 4xCaM, 4zCaM, and 4xzCaM..... 130

33. Fluorescence emission spectra of CaM mutants in the presence of W4I-M13 CaM-binding peptide 132

34. Calcium titration curves of CaM mutants in the presence of W4I-M13 CaM-binding peptide 133

35. PDE stimulation curves of CaM mutants at low calcium concentration 136

36. PDE stimulation curves of CaM mutants at high calcium concentration 138

LIST OF ABBREVIATIONS

APH.....Acid-Pair Hypothesis

ATP..... adenosine 5'-triphosphate

CaM..... calmodulin

cAMP..... adenosine 3',5'-cyclic monophosphate

CD..... circular dichroism

DTT.....dithiothreitol

EDTA..... ethylenediamine tetraacetic acid

EGTA..... ethylene glycol bis-(β-aminoethyl ether) N, N, N',N'-tetraacetic acid

hlh.....helix-loop-helix

h..... hour

HPLC..... high performance liquid chromatography

IPTG..... isopropyl-β-D-thiogalactoside

L..... liter

min..... minute

MW..... molecular weight

MOPS..... 3-(N-morpholino)propanesulfonic acid

NZCYM.... a bacterial culture medium. See page xx for the recipe.

PAGE..... polyacrylamide gel electrophoresis

PDE.....3',5'-cyclic nucleotide 5'-phosphodiesterase

PMSF..... phenylmethylsulfonylfluoride

SDS..... sodium dodecyl sulfate

sec..... second

S.O.C..... a bacterial culture medium. See page xx for the recipe.

TEMED..... N,N,N',N'-tetramethylethylenediamine

TFA..... trifluoroacetic acid

Tris..... tris(hydroxymethyl)aminomethane

LIST OF AMINO ACID CODES

Amino Acid	3 Letter Code	1 Letter Code
Alanine	Ala	A
Arginine	Arg	R
Asparagine	Asn	N
Aspartic Acid	Asp	D
Cysteine	Cys	C
Glutamic Acid	Glu	E
Glutamine	Gln	Q
Glycine	Gly	G
Histidine	His	H
Isoleucine	Ile	I
Leucine	Leu	L
Lysine	Lys	K
Methionine	Met	M
Phenylalanine	Phe	F
Proline	Pro	P
Serine	Ser	S
Threonine	Thr	T
Tryptophan	Trp	W
Tyrosine	Tyr	Y
Valine	Val	V

LIST OF GENETIC CODE

1st position	2nd position				3rd position
(5' end)	U	C	A	G	(3' end)
	Phe	Ser	Tyr	Cys	U
	Phe	Ser	Tyr	Cys	C
U	Leu	Ser	Stop (Ochre)	Stop (Umber)	A
	Leu	Ser	Stop (Amber)	Trp	G
	Leu	Pro	His	Arg	U
	Leu	Pro	His	Arg	C
C	Leu	Pro	Gln	Arg	A
	Leu	Pro	Gln	Arg	G
	Ile	Thr	Asn	Ser	U
	Ile	Thr	Asn	Ser	C
A	Ile	Thr	Lys	Arg	A
	Met	Thr	Lys	Arg	G
	Val	Ala	Asp	Gly	U
	Val	Ala	Asp	Gly	C
G	Val	Ala	Glu	Gly	A
	Val	Ala	Glu	Gly	G

LIST OF OLIGODEOXYNUCLEOTIDES

primer 1 (18 mer):	5'-GGC TTT CTC TCT GTT TGA-3'
aatII-1 (19 mer):	5'-CGA TGG TGA GGG CCA GGT T-3'
aatII-2 (38 mer):	5'-CAG CTT CGC GAA TCA TTT CGT CAA CTT CTT CGT CAG TA-3'
hind-1 (46 mer):	5'-AGC TTA CTG ACG AAG AAG TTG ACG AAA TGA TTC GCG AAG CTG ACG T-3'
hind-2 (51 mer):	5'-GTT TCA TCG ACG CCG CTG AAC TGC GTC ACG TTA TGA CTA ACC TGG GTG AAA-3'
hind-3 (51 mer):	5'-AGC TTT TCA CCC AGG TTA GTC ATA ACG TGA CGC AGT TCA GCG GCG TCG ATG-3'
hpaI-1 (23 mer):	5'-AAC CTG GCC CTC ACC ATC GAC GT-3'
stuI-1 (40 mer):	5'-CCT TCC GTG TTT GGG ACA AAG ACG GTA ACG GTT TCA TCT C-3'
stuI-2 (40 mer):	5'-CCT TCC GTG TTT GGG ACA AGG ACG GTG ACG GTT TCA TCT C-3'
stuI-3 (40 mer):	5'-CCT TCC GTG TTT GGG ACA AGA ACG GTG ACG GTT TCA TCA C-3'
stuI-4 (30 mer):	5'-CCT TCC GTG TTT GGG ACA AGG ACG GTA ACG-3'
stuI-5 (34 mer):	5'-AAA CCG TTA CCG TCC TTG TCC CAA ACA CGG AAG G-3'
stuI-6 (30 mer):	5'-CCT TCC GTG TTT GGG ACA AGA ACG GTA ACG-3'
stuI-7 (34 mer):	5'-AAA CCG TTA CCG TTC TTG TCC CAA ACA CGG AAG G-3'

stuI-8 (30 mer):	5'-CCT TCC GTG TTT GGG ACA AGA ACG GTG ACG-3'
stuI-9 (34 mer):	5'-AAA CCG TCA CCG TTC TTG TCC CAA ACA CGG AAG G-3'
xma-1 (44 mer):	5'-GGC CGA GAT GAA ACC GTT ACC GTC TTT GTC CCA AAC ACG GAA GG-3'
xma-2 (44 mer):	5'-GGC CGA GAT GAA ACC GTC ACC GTC CTT GTC CCA AAC ACG GAA GG-3'
xma-3 (44 mer):	5'-GGC CGA GAT GAA ACC GTC ACC GTT CTT GTC CCA AAC ACG GAA GG-3'

LIST OF BACTERIAL MEDIA

1. LB broth

   Per liter:

SELECT peptone 140 (pancreatic digest of casein)	10.0 g
SELECT yeast extract, autolyzed, low sodium	5.0 g
NaCl	5.0g

2. M9 minimal salts

   Per liter:

Na_2HPO_4 (anhydrous)	6.0 g
KH_2PO4 (anhydrous)	3.0 g
NH_4Cl	1.0 g

3. NZCYM medium

   Per liter:

SELECT peptone 140 (pancreatic digest of casein)	10.0 g
SELECT yeast extract, autolyzed, low sodium	5.0 g
Pepton 5 (casamino acids)	1.0 g
NaCl	5.0g
$MgSO_4$ (anhydrous)	0.98 g

4. S.O.C. medium

   2% tryptone, 0.5% yeast extract, 10 mM NaCl, 2.5 mM KCl, 10 mM $MgCl_2$, 10 mM $MgSO_4$, 20 mM glucose

MUTANT NOMENCLATURE

F92W CaM: F92W VU-1 calmodulin.

F92W/D133E CaM: F92W/D133E VU-1 calmodulin.

3xCaM: F92W/D95N/S101D/D133E VU-1 calmodulin.

4xCaM: F92W/S101D/D133E VU-1 calmodulin.

3zCaM: F92W/D95N/N97D/D133E VU-1 calmodulin.

4zCaM: F92W/N97D/D133E VU-1 calmodulin.

4xzCaM: F92W/D95N/N97D/S101D/D133E VU-1 calmodulin.

F92W CaM: This mutant was designed to have a fluorescent label in site III of VU-1 calmodulin to monitor the calcium induced structural changes in the C-terminal domain.

F92W/D133E CaM: This mutant was designed to inactivate at site IV with respect to calcium binding capacity.

3xCaM: This mutant was designed to have three acidic residues in the chelating positions in site III with one pair of acidic residues on the X axis.

4xCaM: This mutant was designed to have four acidic residues in the chelating positions in site III with one pair of acidic residues on the X axis.

3zCaM: This mutant was designed to have three acidic residues in the chelating positions in site III with one pair of acidic residues on the Z axis.

4xCaM: This mutant was designed to have four acidic residues in the chelating positions in site III with one pair of acidic residues on the Z axis.

4xzCaM: This mutant was designed to have four acidic residues in the chelating positions in site III with one pair of acidic residues on the X axis and the other one on the Z axis.

ACKNOWLEDGMENT

I would like to express my sincere thanks to my supervisor, Dr. Ronald Reid, for his guidance and support throughout the course of my Ph. D. training. I would also like to acknowledge my supervisory committee members, Drs. Stelvio Bandiera, Kathleen MacLeod, Robert Molday, and Robert Thies, for their constructive suggestions. Special thanks to Drs. Thomas Lukas and Marty Watterson at Northwestern University, Chicago, for generously providing the calmodulin expression vector, pVUCH-1, and the *E. coli* K12 UT481 strain; to Dr. Stelvio Bandiera for technical support and allowing me to use the gel-drier and electrophoresis equipment in his lab; to Dr. Grant Mauk in the Department of Biochemistry for allowing me to use his spectropolarimeter; to Dr. Loida Escote-Carlson in the Biotechnology Teaching Laboratory for technical support and allowing me to use the ultra-sonicator, UV-transllumilator, instant camera, and bacterial incubator; to Drs. Julian Davies and Robert Hancock in the Department of Microbiology for allowing me to use the 37° walk-in room, bacterial shaker, UV-transllumilator and camera.

Thanks are also extended to Mr. Roland Burton for performing the mass spectrometry of calmodulin and calmodulin mutants; to Dr. Krystyna Piotrowska at the Nucleic Acid and Protein Service (NAPS) Unit and Ms. Sandy Kielland in University of Victoria for performing the amino acid composition analysis; to Ms. Tracy Evans, Ms. Tracy Farr, and Ms. Debbie Neufeld at the NAPS Unit for performing the automated DNA sequencing and oligodeoxynucleotide synthesis; to Mr. Bryn Coventry and Mr. Gary Lesnicki in the Fermentation Pilot Plant, Biotechnilogy Labortory for performing the large scale (20 liter) fermentation.

I would also like to thank my colleagues, Mr Patrick Franchini, Dr. Spyros Potamianos, and Dr. Ric Procyshyn for their assistance in the lab and stimulating discussion.

I am also grateful to my husband, Haikun Ren, and my parents, Shufany Fang and Yongxi Wu, for their support, encouragement and understanding throughout the years.

Financial assistance was provided by the PMAC-HRF/MRC Graduate Student Scholarship. This research was funded by the Medical Research Council of Canada.

CHAPTER 1

INTRODUCTION

1.1. HELIX-LOOP-HELIX CALCIUM BINDING MOTIF

1.1.1. Calcium binding sites in proteins

The known calcium binding sites in proteins can be divided into two major groups. One group includes those sites consisting of calcium chelating residues that belong to different segments or discontinuous regions of a polypeptide chain. The second group includes those sites consisting of calcium chelating residues located on a continuous 12-14 residue region of a single polypeptide. The former is found in many extracellular enzymes such as thermitase, subtilisin, proteinase K, thermolysin, and phospholipase A2 (reviewed in McPhalen *et al.*, 1991). The later is exemplified by the calcium binding sites in such intracellular proteins as calmodulin (CaM), troponin C, parvalbumin, and calbindin$_{9K}$ (reviewed in Strynadka, *et al.*, 1989; reviewed in McPhalen *et al.*, 1991). While the thermitase group of calcium binding proteins utilize calcium to stabilize the protein structure for enzyme activity through enhanced thermal stability or resistance to proteolytic degradation upon calcium binding, the activity of calmodulin superfamily of calcium binding proteins are regulated by fluctuating levels of calcium within a cell.

The common calcium binding structural unit in the CaM superfamily is the helix-loop-helix (hlh) calcium binding motif, also termed EF hand by Kretsinger when his group elucidated the structure of carp parvalbumin (Kretsinger & Nockolds, 1973). The index finger refers to the E helix, the curled middle finger refers to the loop, and the thumb refers to the F helix of carp parvalbumin EF site (Figure 1). A typical hlh calcium binding site has its

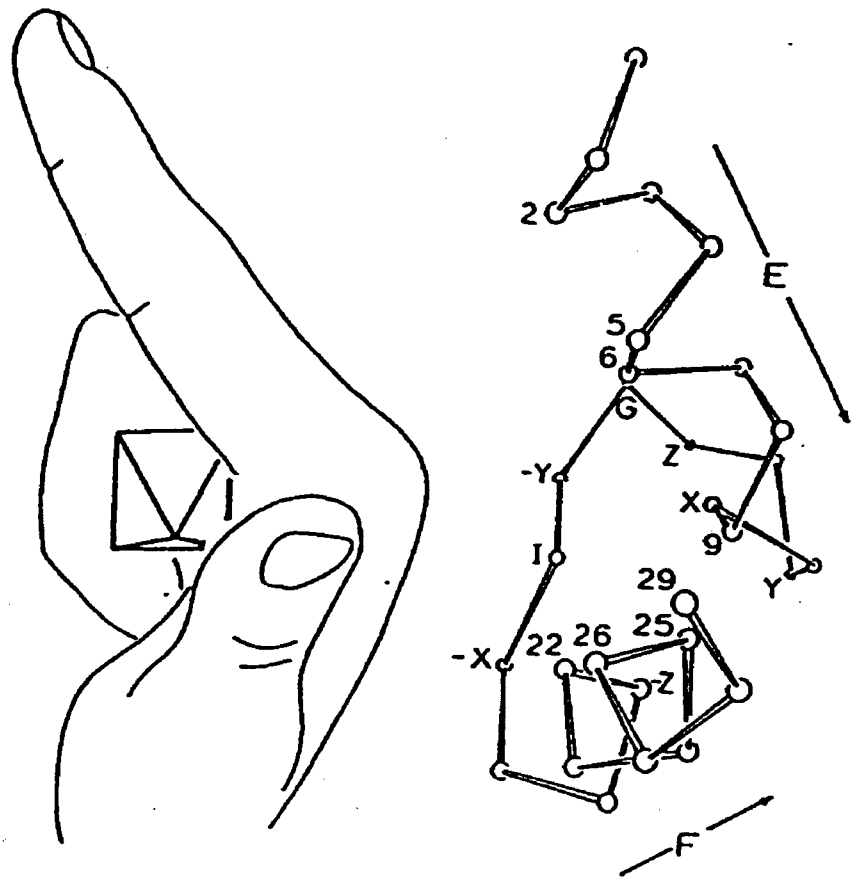

Figure 1. The EF Hand. The index finger and the thumb represent the E and F helices, respectively. The vertices of the octahedral coordination shell about the calcium ion is designated by +X, +Y, +Z, -Y, -X, and -Z. (Taken from Kretsinger, 1980)

oxygen ligands coming from a continuous 12-residue region of a polypeptide chain. This typical hlh calcium binding site is different from another similar calcium binding structural unit such as site I of calbindin$_{9K}$ and S100 proteins which have the oxygen ligands originating from a 14-residue region of a polypeptide and are called "pseudo" EF hands.

1.1.2. Structure overview of the hlh calcium binding motif

A typical hlh calcium binding motif usually spans 28-32 residues, and contains a loop flanked by two α-helices. A 12-residue region comprising the loop and the N-terminal end of the second helix contains most of the oxygen ligands. The term "loop" will be used in the thesis as referring to this entire 12-residue region. The calcium ion is coordinated by seven oxygens in a pentagonal bipyramid arrangement, and most often with a water molecule as one of the ligands. Six residues located at positions 1, 3, 5, 7, 9, and 12 of the loop provide, either directly or indirectly, the seven oxygen ligands. These six positions are denoted for historical reasons as the +X, +Y, +Z, -Y, -X, and -Z positions on the axes of a near-octahedral coordination shell (Figure 2). Among the seven oxygen ligands, three are from

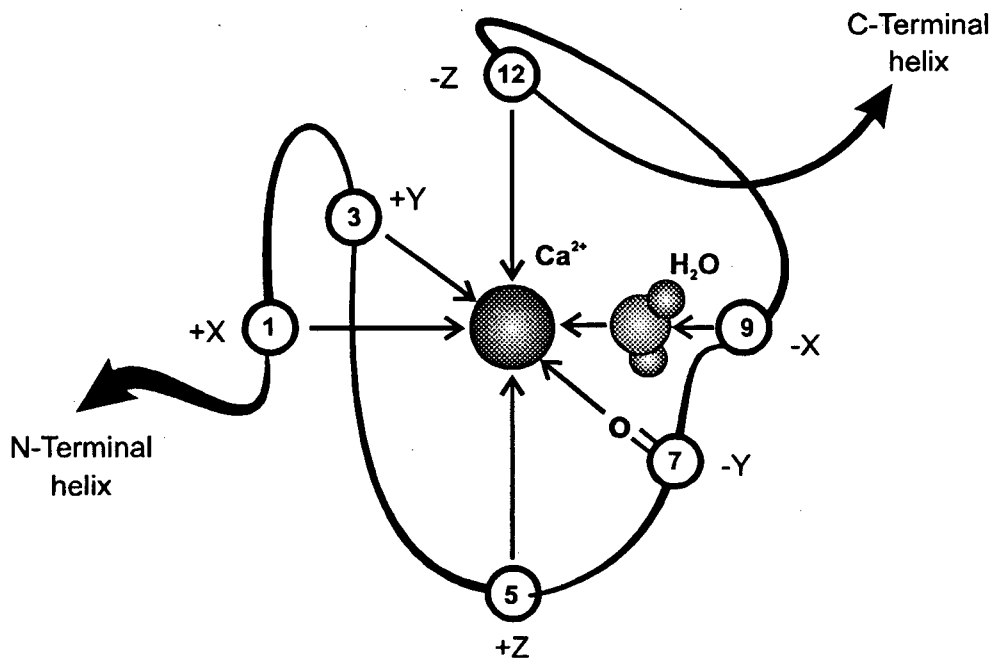

Figure 2. A schematic drawing of the loop of a hlh calcium binding motif. The chelating residues are numbered 1, 3, 5, 7, 9, and 12, and these six positions are denoted as the +X, +Y, +Z, -Y, -X, and -Z on the axes of a near octahedral coordination shell.

the side chain oxygen of the monodentate residues at the +X, +Y, and +Z positions; one is from the backbone carbonyl oxygen of the residue at the -Y position; one is usually from a water molecule which is hydrogen-bonded to the side chain oxygen of the residue at the -X position; and the last two are from the bidentate Glu at the -Z position. In the case of parvalbumin CD site, the side chain oxygen of a Glu at the -X position interacts directly with the calcium, and no water molecule is involved (Kretsinger & Nockolds, 1973). While the chelating residues provide the oxygens to chelate the calcium, the non-chelating residues in the loop provide hydrogen bonding via main-chain NH groups to stabilize the geometry of the loop required for calcium binding (reviewed in Strynadka & James, 1989).

Marsden *et al.* examined the frequency of occurrence of each amino acid in each of the 12 positions in the calcium binding loop (1990). Among 276 EF hands in the calcium binding proteins they examined, there are 165 unique sequences of the 12-residue loop. Position 1 (+X), 6, and 12 (-Z) are almost always occupied by Asp, Gly, and Glu, respectively. Position 3 (+Y) is occupied by either Asp or Asn, and position 8 is usually occupied by Ile. Other positions show relative variability. Falke *et al.* also summarized 567 sequences of EF hands found in the protein data bank using PROSITE sequence analysis software (reviewed in Falke *et al.*, 1994). They examined amino acid occurrences in each position of the 9-residue N-terminal helix, the 12-residue loop, and the 11-residue C-terminal helix. A summary of the loop sequences is shown in Figure 3.

1.1.3. Calcium binding affinity of hlh calcium binding motifs in proteins

Although the sequences of the hlh calcium binding motif are highly homologous, especially in the calcium binding loop, the calcium dissociation constants of the hlh calcium

Ligand coordinate:	+X		+Y		+Z		-Y		-X			-Z
Position in the loop:	1	2	3	4	5	6	7	8	9	10	11	12
Preferred :	**D**	K	D	G	D	**G**	T	I	D	F	E	**E**
occurrences %	**100**	29	76	56	52	**96**	23	68	32	23	29	**92**
Observed:	D567	K163	D432	G319	D295	G541	T130	I384	D181	F131	E164	E523
		A67	N130	K69	S131	D9	F90	V94	S116	Y64	D108	D44
		Q54	S5	R48	N123	N8	K70	L74	T79	A59	K70	
		T54		N47	T9	K4	Q54	M11	E65	T53	A54	
		V46		Q22	G8	R2	Y51	C4	N57	L44	P47	
		I39		A15	E1	H2	E36		G56	V43	N35	
		S36		H13		Q1	R27		Q9	E37	Q24	
		E32		S11			S26		C4	K35	S20	
		R30		D7			I15			S19	R7	
		L16		E7			C13			P17	G7	
		F9		T5			D11			I14	T7	
		M8		M3			L11			R13	Y7	
		Y5		C1			V11			G10	L5	
		N3					A8			W7	V5	
		C3					H6			N5	H4	
		D1					M5			Q5	M3	
		G1					N3			M5		
										D3		
										C2		
										H1		

Figure 3. Summary of the sequences of the loop of 567 EF hands. The consensus sequence (bold for conservation > 90%) and observed amino acid distribution for each position of the loop are shown.

binding sites in proteins range from 1 nM to 1 mM (Table 1). It is evident not only that the primary structure of the site determines the calcium affinity of the site but that other factors such as ionic strength, pH, and the presence of Mg^{2+}, also affect calcium affinity of the site (reviewed in Linse & Forsén, 1995). A high concentration of salts decreases the calcium affinity due to non-specific electrostatic interactions. The macroscopic calcium dissociation constants of the four sites in CaM increase from 0.4, 0.31, 0.1, and 0.025 (μM) in the absence of KCl to 40, 12.7, 2.5, and 0.25 (μM) in the presence of 100 mM KCl, respectively (Linse *et al.*, 1991a). A similar effect of KCl on the calcium binding constants of CaM, parvalbumin, $calbindin_{9K}$, and S100 proteins has also been reported (Svensson *et al.*, 1993; Haiech *et al.*, 1979; Kesvatera *et al.*, 1994; Baudier *et al.*, 1985; Baudier *et al.*, 1986). The magnitude of the effect varies depending on the protein and the type of salt (Svensson *et al.*, 1993). It is believed that the calcium affinity is affected by pH in at least some pH ranges (reviewed in Linse & Forsén, 1995). This is because the total charge of the protein varies with pH due to the presence of ionizable side chains (Asp, Glu, His, Lys, and Arg). As a result, higher pH leads to a higher calcium affinity due to higher negative charge of the protein. However, the calcium affinity often remains unchanged within a certain pH range. The calcium affinity of calmodulin at pH 6.4, 7.5 and 8.3 has been found to be virtually identical (Svensson *et al.*, 1993). Magnesium competes with calcium in binding to many hlh calcium binding sites. As a result, the calcium affinity of proteins is lower in the presence than in the absence of magnesium (Haiech *et al.*, 1979; Moeschler *et al.*, 1980; Drabikowski & Brzeska, 1982; Ogawa & Tanokura, 1984; Ogawa, 1985; Durussel *et al.*, 1993; Cox *et al.*, 1977; Baudier *et al.*, 1985; Baudier *et al.*, 1986). Recently Linse *et al.* (1995) demonstrated that the protein concentration has a significant effect on ion binding. A 94% reduction in

calcium affinity of site II of the N56A calbindin$_{9K}$ mutant was observed when the protein concentration was increased from 27 μM to 7.35 mM. A 13 fold reduction in the average magnesium affinity of the N-terminal domain of CaM was also observed when the protein concentration was changed from 0.325 mM to 3.25 mM (Linse *et al.*, 1995).

Table 1. Calcium Dissociation Constants of hlh Calcium Binding Proteins

Protein[a], site	Solvent conditions salt[b]/buffer (mM)/(mM; pH)	Method[c] used	K_d (μM)	Reference
BHCaM, 1 site	-/50; 7.5	GF	3.0	Teo & Wang, 1973
BHCaM, 2-3 sites	3 mM Mg^{2+}		7.14	
BBCaM, 3 sites	-/25; 8.0	ED	3.45	Lin *et al.*, 1974
BBCaM, 1 site			17.9	
BBCaM, 3 sites	-/10; 7.4	ED	0.2	Wolff *et al.*, 1977
BBCaM, 1 site			1.0	
BBCaM, 4 sites	100/10; 7.5	ED	22.2	Crouch & Klee, 1980
			8.3	
			3.33	
			1.16	
BBCaM, 4 sites	100/10; 7.55	FD	62.5	Haiech *et al.*, 1981
			7.1	
			2.0	
			1.9	
BBCaM, 4 sites	150/10; 7.2	ED	83	Keller *et al.*, 1982
			22	
			5.3	
			3.6	
BBCaM, (single site model)	100/50; 7.0	TyrFluo	0.7	Drabikowski *et al.*, 1982
BBCaM, (single site model)	-/20; 7.0	CDTitr (θ_{222})	0.3	

Table 1. (Continued)

Protein[a], site	Solvent conditions salt[b]/buffer (mM)/(mM; pH)	Method[c] used	K_d (μM)	Reference
BBCaM, 3 sites	-/5; 7.9 (12-50°)	TyrFluo	7.7 0.2 0.08	Permyakov *et al.*, 1985
RCaM, 2 sites	100/20; 6.8 5 mM Mg^{2+}	ED	6.3	Yazawa *et al.*, 1978
RCaM, 2 sites			31.2	
CCaM, (single site model)	100/10; 7.7 1 mM Mg^{2+}	FD	12.5	Putkey *et al.*, 1986
STCaM, 4 site	100/20; 7.0	FD	16.7 7.7 2.8 2.9	Minowa & Yagi, 1984
WGCaM, 4 site	100/20; 7.0	FD	7.7 5.9 4.0 3.8	Minowa & Yagi, 1984
VU-1 CaM	-/50; 7.5	FD	0.7 1.4 3	Haiech *et al.*, 1991
BBCaM, I, II	100/2; 7.5	Br_2BAPTA	40.0 12.6	Linse *et al.*, 1991a
BBCaM, III, IV	100/2; 7.5	Br_2BAPTA	2.5 0.25	Linse *et al.*, 1991a
BCTnC, II	100/20; 7.0 0.1 mM EGTA	ED	50.0	Potter *et al.*, 1977
BCTnC, III, IV			0.08	
BCTnC, II	50/25; 7.5 2 mM EGTA	Ca^{2+} electrode	10-100	Leavis & Kraft, 1978
BCTnC, III, IV		TyrFluo	0.03	
BCTnC, (single site model)	150/50; 7.5 1 mM EGTA	CDTitr (θ_{221})	0.14	Burtnick & Kay, 1977
BCTnC, III, IV (single site model)	-/50; 7.0 2 mM EGTA	TyrFluo	0.017	Barskaya & Gusev, 1982
RSTnC, I, II RSTnC, III, IV	100/10; 7.0	ED	3.33 0.05	Potter & Gergely, 1975

Table 1. (Continued)

Protein[a], site	Solvent conditions salt[b]/buffer (mM)/(mM; pH)	Method[c] used	K_d (μM)	Reference
RSTnC, I, II RSTnC, III, IV	100/20; 6.8	Metal-I	15.6 0.22	Ogawa, 1985
RSTnC, I, II RSTnC, III, IV	300/25; 7.5 1 mM EGTA	FluoTitr (IAE-Cys98)	10 2.5 0.1 0.025	Wang, & Cheung, 1985
CPV4.25, 2 sites	100/20; 7.0 0.1 mM EGTA	ED	0.004	Potter *et al.*, 1977
CPV4.25, 2 sites	80/25; 7.4 1 mM EGTA	ED	0.00037	Moeschler *et al.*, 1980
CPV4.25, 2 sites	30/50; 7.0 5 mM EGTA	FluoTitr (dansyl-Cys)	0.025	Iio & Hoshihara, 1984
FPV4.50, 2 sites	60/30; 6.7 2 mM Mg^{2+}, 1 mM EGTA	ED	0.2	Benzonana *et al.*, 1972
FPV4.50, 2 sites	150/25; 7.55	FD	0.002	Haiech, *et al.*, 1979
FPV4.88, 2 sites	150/25; 7.55	FD	0.0077	Haiech *et al.*, 1979
HPV4.36, 2 sites	60/30; 6.7 2 mM Mg^{2+}, 1 mM EGTA	ED	0.1	Benzonana *et al.*, 1972
PPV4.2, 2 sites	-/50; 8.1	TyrFluo	1.45 0.0038	Permyakov *et al.*, 1983
PPV5.0, 2 sites	-/50; 8.1	TyrFluo	0.0023 0.0016	Permyakov *et al.*, 1983
RPV, 2 sites	150/25; 7.55	FD	0.0067	Haiech *et al.*, 1979
RPV, 2 sites	80/25; 7.4 0.1 mM EGTA	ED	0.001	Cox *et al.*, 1977
RPV, 2 sites	80/25; 7.4 0.1 mM EGTA 2 mM Mg^{2+}	ED	0.4	Cox *et al.*, 1977
RTPV, CD site RTPV, EF site	150/10; 7.5	^{1}H NMR	0.011 0.006	Williams *et al.*, 1986
RTPV, 2 sites		FD	0.002	Rinaldi *et al.*, 1982
WPV, 2 sites	-/50; 7.5	TyrFluo	0.002 0.17	Permyakov *et al.*, 1980

Table 1. (Continued)

Protein[a], site	Solvent conditions salt[b]/buffer (mM)/(mM; pH)	Method[c] used	K_d (μM)	Reference
ROnCo, CD site ROnCo, EF site	-/NA[d] ; 7.4	FD	0.77 0.042	Hapak *et al.*, 1989
$BCaD_{9K}$, 2 sites	150/1; 6.8	ED	1	Fullmer & Wasserman, 1977
$PCaD_{9K}$, 2 sites	20/30; 7.2	GF	0.18-0.28	Hitchman & Harrison, 1972
$BCaD_{28K}$, 4 sites	150/1; 6.8	ED	0.5	Bredderman & Wasserman, 1974
$BCaD_{9K}$, 2 sites	100/2; 7.5	Quin2	0.31 0.16	Linse *et al.*, 1991b
$BCaD_{9K}$, 2 sites	-/2; 7.5	Quin2	0.006 0.0025	Linse *et al.*, 1991b
$PCaD_{9K}$, 2 sites	-/2; 7.5	Quin2	0.0125 0.0056	Linse *et al.*, 1987
HCLP, 4 sites	150/50; 7.5	FD	250 167 100 30.3	Durussel *et al.*, 1993
HCLP, 4 sites	-/60; 7.5	FD	83.3 20.4 5.3 2.6	Rhyner *et al.*, 1992
Calcineurin (single site model)	100/50; 8.1 1 mM Mg^{2+}	GF	1	Klee *et al.*, 1979
BS100αα, 2 sites	-/20; 8.3	FD	10 3.3	Baudier *et al.*, 1986
BS100b, 2 sites	-/60; 7.6	ED	1000 50	Callisano *et al.*, 1974
BS100b; 2 sites	-/100; 8.5	CDTitr ($\theta_{268.5}$)	58.8 20	Mani *et al.*, 1983
BS100b, 2 sites	-/20; 8.3	FD	20 4.0	Baudier *et al.*, 1986
BS100a, 2 sites	-/20; 8.3	FD	16.4 3.0	
RS100b, 2 sites	-/20; 7.5	FD	100 20	Baudier *et al.*, 1985

[a] Abbreviations for proteins in the table: BHCaM, bovine heart CaM; BBCaM, bovine brain calmodulin; RCaM, rabbit calmodulin; CCaM, chicken calmodulin; STCaM, scallop testis calmodulin; WGCaM, wheat germ calmodulin; BCTnC, bovine cardiac troponin C; VU-1 CaM, a recombinant calmodulin encoded by a synthetic calmodulin gene; RSTnC, rabbit skeletal troponin C; CPV4.25, carp parvalbumin pI 4.25; CPV3.95, carp parvalbumin pI 3.95; FPV4.50, frog parvalbumin pI 4.50; FPV4.88, frog parvalbumin pI 4.88; HPV, Hake parvalbumin; PPV4.10, pike parvalbumin pI 4.10; PPV5.0, pike parvalbumin pI 5.0; RPV, rabbit parvalbumin; RTPV, rat parvalbumin; WPV, whiting parvalbumin; ROnCo, rat oncomodulin; $BCaD_{9K}$, bovine $calbindin_{9K}$; $PCaD_{9K}$, pig $calbindin_{9K}$; $BCaD_{28K}$, bovine $calbindin_{28K}$; HCLP, human calmodulin-like protein; BS100αα, bovine S100 protein, chains αα; BS100b, bovine S100 protein, chains ββ; BS100a, bovine S100 protein, chains αβ; RS100b, rat S100 protein, chains ββ.

[b] KCl or NaCl.

[c] Methods used for determining the calcium binding constants: ED, equilibrium dialysis; FD, flow dialysis; Br_2BAPTA, calcium titration in the presence of the calcium chelator, tetrapotassium salt of 5,5'-dibromo-1,2-bis(2-aminophenoxy)ethane-N,N,N',N'-tetraacetic acid (A_{263} was monitored during calcium titration); Quin2, calcium titration in the presence of the fluorescent calcium chelator, tetrapotassium salt of Quin2 (λ_{ex} = 339 nm, λ_{em} = 500 nm); CDTitr, calcium titration monitored by ellipticity change at the specified wavelength; TyrFluo, calcium titration monitored by Tyr fluorescence change; GF, gel filtration method; FluoTitr (IAE-Cys98), fluorescence titration of the 5-iodoacetamidoeosin labelled troponin C at Cys98. Metal-I, metallochromic indicator (tetramethylmurexide) method.

[d] Not available.

1.1.4. Prediction of calcium binding affinity of the hlh motif or paired motifs

Several investigators tried to predict calcium binding properties of the hlh proteins on the basis of their amino acid sequences. Potter *et al.* (1977) found that a Gly residue is usually located between chelating residues at the +Y and +Z positions in loops with low calcium affinity such as the loops of CaM sites I, II, III and IV, skeletal troponin C sites I and II, and cardiac troponin C site II. However, there are exceptions such as a Gly residue found at the same position in the parvalbumin EF site, which is a high affinity site. Vogt *et al.* (1979) examined 29 sequences of the hlh motifs from troponin C, myosin light chain,

parvalbumin and calmodulin. They found that the position and linear density of "β-turn forming" residues in the loop are correlated with the site's ability to bind calcium. A high propensity of "β-turn forming" residues in the first and third tetrapeptides of the loop indicates possible calcium binding to the site. This criterion appears to be able to identify the loops that bind calcium, but, it can not predict the binding affinity. Boguta *et al.* (1988) have proposed a method to estimate calcium binding constants based on the secondary structure of the hlh motif. In their procedure, the estimation points are first calculated based on the predicted frequencies of helix, reverse turn and random coil formation of the residues in a single hlh motif or paired hlh motifs, and then a calcium binding constant is assigned to the site or the paired sites based on the calculated estimation points. This method allows a prediction of calcium binding constants of typical hlh motif and paired motifs with a precision of one order of magnitude. Another quantitative structure/affinity relationship (QSAR) method has been established after analyzing six different two-site domains: the N- and C-domains of rabbit skeletal troponin C, the N- and C-domains of rabbit CaM, carp parvalbumin, and the C-domain of bovine cardiac troponin C (Sekharudu & Sundaralingam, 1988). This method relates the calcium binding affinities ($1/K_d$) of the hlh proteins with the net ligand charge of the two calcium binding loops, the hydrophobicity of the β-sheet segment of the loops and the hydrophobicity of the four helices.

1.1.5. Acid-Pair Hypothesis

Reid and Hodges (1980) proposed the Acid Pair Hypothesis (APH) to correlate the nature of the chelating residues in the loop with calcium affinity of the hlh calcium binding motif. The APH predicts the calcium affinity of the hlh calcium binding motif based on the

number and location of acidic amino acid residues in chelating positions. This hypothesis states that a hlh calcium binding site will have a higher affinity for calcium if the anionic ligands in the loop are paired on the axial vertices of a near octahedron than if they are unpaired. Implicit in this hypothesis is the suggestion that a high affinity calcium binding site will have a maximum of four acidic residues in positions 1, 3, 5, 9 or 12 in the loop, and these four acidic residues will be paired on the vertical axes (i.e., the X and Z axes: note that there cannot be a side chain pair on the Y axis since the peptide carbonyl oxygen chelates in the -Y position by definition).

1.1.6. Calcium binding in the single site hlh peptide model

Synthetic peptides comprising fragments of a single hlh motif from the 12 residue loop to the entire motif of 33-34 residues corresponding to troponin C sites II and III and CaM site III have been used to examine the structure/cation affinity relationships (Reid *et al.*, 1980; Reid, *et al*, 1981; Reid, 1987a; Reid, 1987b; Malik *et al.*, 1987; Marsden *et al.*, 1988; Reid, 1990; Shaw *et al.*, 1991; Procyshyn & Reid, 1994a; Procyshyn & Reid, 1994b; Reid & Procyshyn, 1995). Calcium binding to the 12-residue fragment of the calcium binding loop of troponin C site III is undetectable (Reid *et al.*, 1980). However, lanthanum (La^{3+}) is able to bind to 13 residue peptide analogs of site III of rabbit skeletal troponin C (Marsden *et al.*, 1988). These peptide analogs cover the 12-residue calcium binding loop and have an extra Leu at the C-terminus. The primary sequence of these peptide analogs represent all possible combinations having Asp and Asn at the +X, +Y, and +Z positions, and the lanthanum dissociation constants range from 4 μM to 1.1 mM monitored by high-field ^{1}H NMR. It is observed that those analogs with the larger number of acidic chelating residues result in the

higher association constants, however, the presence of acidic residues in neighboring positions at either the +X and +Y, the +Y and +Z, or the +X and +Y and +Z positions have been shown to decrease the association constant due to dentate-dentate repulsion.

When the sequence of the 12 residue peptide analogs of the loop of troponin C site III is extended to include either the 9 residues from the C-terminal α-helix, the 9 residues of the C-terminal α-helix plus 5 residues of the N-terminal α-helix, or the entire hlh region of troponin C site III, these three peptides (21, 26, and 34 residues, respectively) have been found to bind calcium monitored by CD spectroscopy (Reid *et al.*, 1981; Reid, 1987a). The 34 residue peptide had a 750 fold higher calcium affinity than the 21 residue peptide, and the 26 residue peptide had a 115 fold higher calcium affinity than the 21 residue peptide (Reid *et al.*, 1981; Reid, 1987a). A similar study using synthetic peptide analogs of skeletal troponin C site II has also been reported (Malik *et al.*, 1987). A 12 residue peptide analog corresponding to the loop of site II of skeletal troponin C with changes of G/A and F/Y in positions 6 and 10, respectively, binds calcium with a dissociation constant of 100 mM monitored by Tyr fluorescence (Malik *et al.*, 1987). When the 12 residue peptide was extended to include 11 residues of the N-terminal helix, this 23 residue peptide showed a 4 fold higher affinity for calcium (Malik *et al.*, 1987). Another similar 23 residue peptide analog without the G/A mutation in position 6 but the F/Y in position 10 exhibited 4 fold higher affinity for calcium than the former 23 residue peptide. This is in agreement with the fact that position 6 in the loop is almost always occupied by Gly (Figure 3). Since the success of these early studies, synthetic hlh peptides of 33-34 residues in length have been used as a single site model to study the mechanisms by which calcium binds to the hlh motif in proteins.

A wealth of information has been obtained with respect to the structure/cation affinity relationships in the hlh calcium binding motif using the synthetic single site peptide model. Increasing the number of acidic chelating residues from 3 to 4 by substituting Asp for Asn at the +Y position increases the calcium affinity of the models by 2 to 38 fold (Procyshyn & Reid, 1993). Increasing the number of acid-pairs from 0 to 1 or from 1 to 2 increases the calcium affinity of the models by 1.4 to 27 fold (Reid, 1990; Procyshyn & Reid, 1993). Changing the position of the acid-pair from the X axis to the Z axis increases the calcium affinity of the models by 1.4 to 9 fold (Procyshyn & Reid, 1993). These results are in agreement with the prediction of the Acid-Pair Hypothesis (section 1.1.5, page 12). It is also found that the calcium affinity of peptide models containing an X axis acid-pair are reduced when the +Z residue is changed from Asn to Ser. A similar reduction in calcium affinity is observed in the Z axis acid-paired peptides when the -X residue is changed from Ser to Asn (Procyshyn & Reid, 1993). It is interesting that a Glu in the -X position is unfavorable for calcium affinity of the peptide models derived from CaM site III (Procyshyn & Reid, 1995). A Glu at the +Z position is detrimental to both calcium and magnesium binding to the peptide models (Reid & Procyshyn, 1995).

Using 34 residue synthetic peptide analogs derived from skeletal troponin C, Shaw *et al.* (1991) demonstrated that the peptide corresponding to site III with chelating residues identical to site II has a 2.7 fold lower affinity for calcium than the peptide corresponding to site III. However, the former peptide has a 2667 fold higher affinity for calcium than the peptide corresponding to site II. These results indicate that the non chelating residues significantly affect calcium binding affinity of the hlh motif.

It has been noted that the calcium binding affinity of a single site peptide model is always lower than that of the same site in the protein. This fact is possibly due to the large number of interactions which can occur in the larger multisite calcium binding proteins.

1.2. HELIX-LOOP-HELIX CALCIUM BINDING PROTEINS

The hlh calcium binding proteins are a family of highly homologous intracellular proteins the activities of which are regulated by the calcium binding event. While some proteins such as CaM and troponin C function as enzyme regulators, others such as parvalbumin and calbindin$_{9K}$ act as calcium buffers in regulating the intracellular calcium concentration. Although most members of the family have no known enzymatic activity, calpain (calcium protease), calcineurin (phosphatase 2B), diacylglycerol kinase and a calcium-dependent protein kinase from *Plasmodium falciparum* are a few examples of enzymes with EF hands (Ohno *et al.*, 1984; Klee *et al.*, 1979; Sakane *et al.*, 1990; Zhao *et al.*, 1994). While the calcium binding domain is covalently linked to the catalytic domain in calpain, diacylglycerol kinase and the calcium-dependent protein kinase, the calcium binding domain in calcineurin is not covalently linked to the catalytic domain but exists as the B subunit of the protein.

1.2.1. Calmodulin

CaM was first discovered as an activator of the bovine brain cAMP-phosphodiesterase (Cheung, 1970). Subsequently, it was demonstrated to be a calcium binding protein that confers calcium sensitivity to bovine heart cAMP-phosphodiesterase (Teo and Wang, 1973). CaM is a small acidic protein of a 148 amino acids in length with a molecular weight of 16.7

kDa. It is present in all eukaryotes and mediates a variety of physiological processes in a Ca^{2+}-dependent manner (reviewed in Klee & Vanaman, 1982; reviewed in Wylie & Vanaman, 1988).

The amino acid sequence of calmodulin from different species (protozoan to mammalian) has been found to be highly homologous through evolution (reviewed in Wylie & Vanaman, 1988). The amino acid sequence of bovine brain CaM is shown in Figure 4. Two post-translational modifications have been found in bovine brain CaM with Ala at the N-terminus being acetylated and Lys115 trimethylated (Watterson *et al.*, 1980). Both the crystal and solution structures of Ca^{2+}-bound CaM resemble a dumbbell, in which two structurally similar globular domains, the N- and C-terminal domains, are linked by a central helix (Babu *et al.*, 1985; 1988; Seaton, *et al.*, 1985; Heidorn & Trewhella, 1988; Matsushima *et al.*, 1989; Ikura *et al.*, 1991; Barbato *et al.*, 1992). Although the central helix (residues 65-91) is a continuous eight-turn α-helix in the crystal structure, residues 77-80 of the central helix adopt a nonhelical conformation with considerable flexibility in the solution structure (Seaton *et al.*, 1985; Heidorn & Trewhella, 1988; Ikura *et al.*, 1991; Barbato *et al.*, 1992). Each domain consists of a pair of hlh calcium binding sites, and the four sites are numbered I to IV from the N-terminus (Figure 5). Sites I and II are located in the N-terminal domain, and sites III and IV are located in the C-terminal domain. Short β-strands are found in each calcium binding loop (residues 26-28 in site I, residues 62-64 in site II, residues 99-101 in site III, and residues 135-137 in site IV), and two β-strands from each paired site form an antiparallel β-sheet in each domain (Figure 5). The solution structure of apo-calmodulin also shows two globular domains similar to those observed in the Ca^{2+}-bound form (Zhang *et al.*, 1995; Kuboniwa *et al.*, 1995; Finn *et al.*, 1995). However, the structure of the Ca^{2+}-bound

```
         1                   10                  20
TnC  Ac A S M T D Q Q A E A R A F L S E E M I A E F K A A F D
CaM     - - - - - - - - - -Ac A D Q L T E E Q I A E F K E A F S
                             1                  10

           30                  40                  50
TnC   M F D A D G G G D I S T K E L G T V M R M L G Q N P T
CaM   L F D K D G D G T I T T K E L G T V M R S L G Q N P T
          20                  30                  40

                 60                  70                  80
TnC   K E E L D A I I E E V D E D G S G T I D F E E F L V M M
CaM   E A E L Q D M I N E V D A D G N G T I D F P E F L T M M
                 50                  60                  70

                     90                  100                 110
TnC   V R Q M K E D A K G K S E E E L A N C F R I F D K N A D
CaM   A R K M K D T D - - - S E E E I R E A F R V F D K D G N
                     80                  90

                         120                 130
TnC   G F I D I E E L G E I L R A T G E H V T E E D I E D L M
CaM   G Y I S A A E L R H V M T N L G E K L T D E E V D E M I
          100                 110                 120

        140                 150                 160
TnC   K D S D K N N D G R I D F D E F L K M M E G V Q
CaM   R E A D I D G D G Q V N Y E E F V Q M M T A K -
              130                 140
```

Figure 4. Amino acid sequences of chicken skeletal troponin C and bovine brain CaM. The calcium binding loops are underlined, and the chelating residues are in bold type. Dashes represent deletions. K115 in bovine brain CaM is trimethylated.

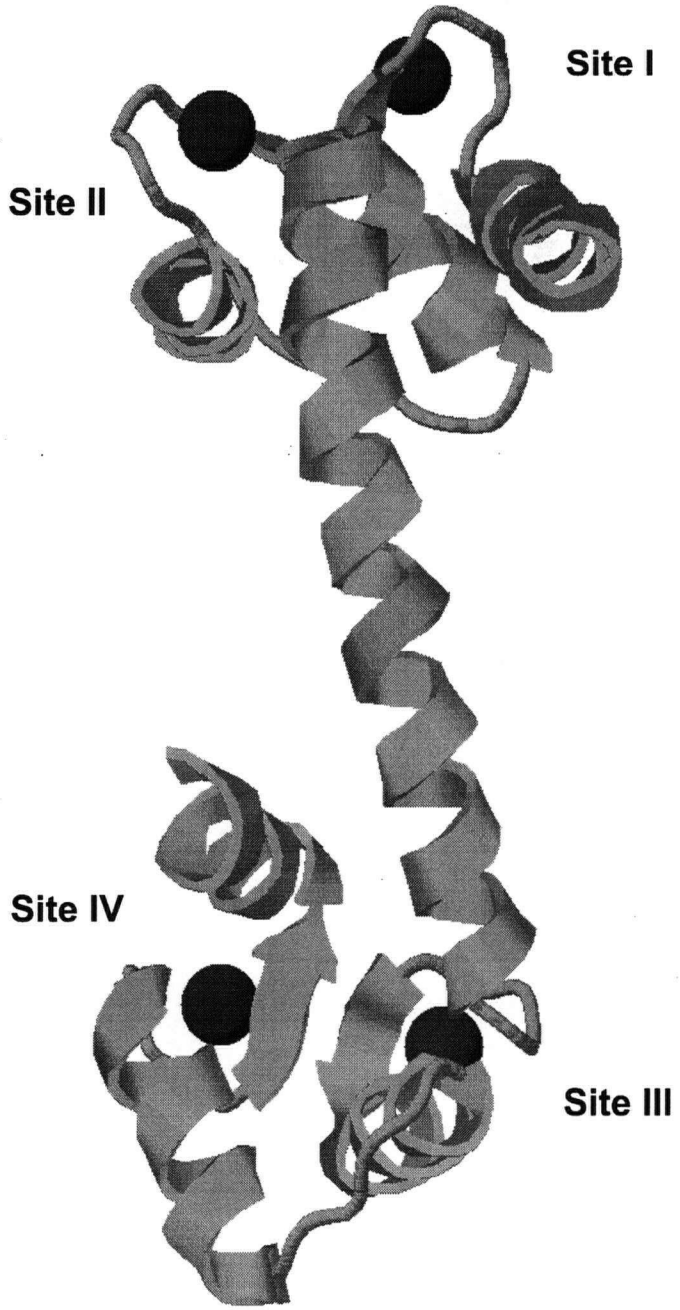

Figure 5. Ribbon diagram of the crystal structure of rat testis CaM. The structure information was obtained from the Protein Data Bank, Brookhaven National Laboratory using the ID code 3CLN. The model was created using the Rasmol program (version 2.6, Roger Sayle, 1995). The solid circles represent the bound calcium ions, and the arrows represent the β-strands. The crystal structure of CaM was determined at 2.2 Å (Babu *et al.*, 1988).

form is different from that of apo-CaM in terms of the interhelical angles and the solvent-accessible hydrophobic areas (Zhang *et al.*, 1995; Kuboniwa *et al.*, 1995; Finn *et al.*, 1995). Binding of calcium induces a change in the interhelical angles leading to the exposure of the hydrophobic core in each globular domain, which enables CaM to interact with a target enzyme, thereby regulating enzyme activity (Ikura *et al*, 1992; Meador *et al.*, 1992).

Calcium binding to CaM has been examined using a variety of methods including equilibrium dialysis, flow dialysis, gel filtration, circular dichroism spectroscopy, fluorospectrometry, and UV-spectrophotometry (Teo & Wang, 1973; Lin *et al.*, 1974; Wolff *et al.*, 1977; Yazawa *et al.*, 1978; Crouch & Klee, 1980; Haiech *et al.*, 1981; Keller *et al.*, 1982; Drabikowski *et al.*, 1982; Minowa & Yagi, 1984; Permyakov *et al.*, 1985; Putkey *et al.*, 1986; Linse *et al.*, 1991a). The calcium dissociation constants of the four sites in CaM range from 0.08 μM to 83 μM depending on the method and the conditions used for the calcium binding experiments (Table 1). At near physiological salt concentrations (100-150 mM), the calcium dissociation constants range from 0.25 μM to 83 μM (Table 1). Most investigations of calcium binding to CaM suggest the presence of two classes of sites, with one pair having 3-10 fold greater affinity than the other (Teo & Wang, 1973; Watterson *et al.*, 1976; Crouch & klee, 1980; Haiech *et al.*, 1981; Linse *et al.*, 1991a; Brown *et al.*, 1997). However, there is no consensus concerning which pair of sites has higher affinity for calcium. Studies from intact CaM and trypsin-digested fragments each containing two of the Ca^{2+}-binding sites suggest that calcium binding to one domain does not affect calcium binding to the other (Linse *et al.*, 1991a; Minowa & Yagi, 1984). However, other studies suggest that interdomain interactions are evident (Seamon, 1980; Wang *et al.*, 1984; Kilhoffer *et al.*, 1992; Pedigo & Shea, 1995; Shea *et al.*, 1996), but it is unknown to what extent these

interactions may affect the calcium binding affinity of each domain. It appears that these interdomain interactions do not significantly affect the calcium affinity of each domain. However, positive cooperativity occurs between paired sites (Crouch & Klee, 1980). The calcium affinity of CaM decreases in the presence of either magnesium or potassium (Crouch & Klee, 1980; Haiech *et al.*, 1981; Drabikowski, 1982; Linse *et al.*, 1991a). However, the calcium affinity of CaM increases in the presence of the CaM binding peptide, mastoparan or caldesmon fragment (Yazawa *et al.*, 1987).

CaM has also been found in yeast (Hubbard *et al.*, 1982). Unlike the vertebrate and plant calmodulins, the CaM isolated from yeast has three functional calcium binding sites (Matsuura *et al.*, 1991; 1993; Starovasmik *et al.*, 1993). Due to mutations at the highly conserved positions, +X and -Z (Ser and Gln are found at the two positions, respectively) and a deletion at position 2, site IV of yeast CaM does not bind calcium. The calcium dissociation constants of the three sites in yeast CaM are 5.2, 3.3, and 2.3 μM, respectively, determined by flow dialysis in the presence of 1 mM $MgCl_2$ and 100 mM KCl at pH 7.6 (Starovasnik *et al.*, 1993). These values indicate that the three sites in yeast CaM have similar calcium affinity to those of vertebrate CaM (Table 1).

CaM functions as a regulatory protein to modulate the activity of a variety of enzymes involved in cellular signaling pathways (Table 2). These include cyclic nucleotide metabolism, protein phosphorylation and dephosphorylation, cation transport, cytoskeletal organization and gene expression. CaM acts both directly, through interaction with key target enzymes, and indirectly, via specific kinases or phosphatases.

Table 2. CaM-Binding Proteins

Proteins	References
Adenylate cyclase	Brostrom *et al.*, 1975
cAMP phosphodiesterase	Cheung, 1970; Cheung *et al.*, 1975
Nitric oxide synthase	Schmidt *et al.*, 1989; Zhang & Vogel, 1994
Myosin light chain kinase (smooth muscle)	Sherry *et al.*, 1978
Myosin light chain kinase (skeletal muscle)	Blumenthal & Stull, 1980
Phosphorylase kinase	Cohen *et al.*, 1978
CaM-dependent protein kinase I	Sheng *et al.*, 1991
CaM-dependent multiprotein kinase II	Kennedy *et al.*, 1983; Sheng *et al.*, 1991 Wegner *et al.*, 1992
Calcineurin (protein phosphatase 2B)	Klee *et al.*, 1979; Stewart *et al.*, 1982; 1983
Plasma membrane Ca^{2+}-ATPase	Carafoli & Zurini, 1982
Sacoplasmic reticulum ryanodine receptor Ca^{2+} channel	Menegazzi *et al.*, 1994; Guerrini *et al.*, 1995
Ca^{2+}-dependent Na^{+} channel of *Paramesium*	Saimi & Ling, 1990
Plasma membrane Na^{+}/H^{+} exchanger isoform 1	Bertrand *et al.*, 1994
Rod photoreceptor cell cGMP-gated channel	Hsu & Molday, 1993
Nicotinamide adenine dinucleotide kinase from plant and sea urchin	Muto & Miyachi, 1977; Anderson *et al.*, 1980; Epel *et al.*, 1981
The basic hlh transcription factor	Corneliussen *et al.*, 1994
Cytoskeletal proteins (spectrin, β-adducin, caldesmon)	reviewed in Crivici & Ikura, 1995
Brush border myosin-I	reviewed in Crivici & Ikura, 1995
Neuromodulin	Alexander *et al.*, 1987; 1988

In most cases, CaM modulation of target proteins is calcium dependent, however, bacterial adenylate cyclase binds to and is stimulated by CaM in the absence of calcium (Greenlee *et al.*, 1982). Phosphorylase kinase exists as a calmodulin complex in the absence of calcium, however, calcium stabilizes the complex between the γ-subunit and calmodulin (δ-subunit), and the activation of the enzyme is dependent on calcium (Cohen, 1988). Neuromodulin binds to CaM with higher affinity in the absence than in the presence of calcium under conditions of low ionic strength (Alexander *et al.*, 1987; Alexander *et al.*, 1988). A possible role of this protein is suggested as a plasma membrane-associated CaM trap that releases CaM into the cytosol in response to an increase in calcium concentration (Liu & Strom, 1990).

CaM regulates target enzymes by binding to the CaM binding domain located in or near the inhibitory domain of the target enzymes. A general model of regulation of a target enzyme by CaM has been suggested (Figure 6). In response to an increase in intracellular calcium concentration, CaM binds calcium first. Calcium binding to CaM induces a conformational change leading to an exposure of the hydrophobic patches in CaM. Subsequently, Ca^{2+}-bound CaM binds to the CaM binding domain of a target enzyme through hydrophobic and electrostatic interactions. CaM binds to a target enzyme with high affinity (K_d: 0.1 μM to 10 pM) (Klee, 1988) and induces a conformational change in the target protein that relieves autoinhibition allowing full activation of the target enzyme. Constitutive Ca^{2+}-CaM-independent activity can be induced *in vitro* by proteolytic cleavage of the regulatory domain, which includes the autoinhibitory domain and the CaM-binding domain, or by cleavage of the autoinhibitory domain only (reviewed in Cohen & Klee, 1988). The

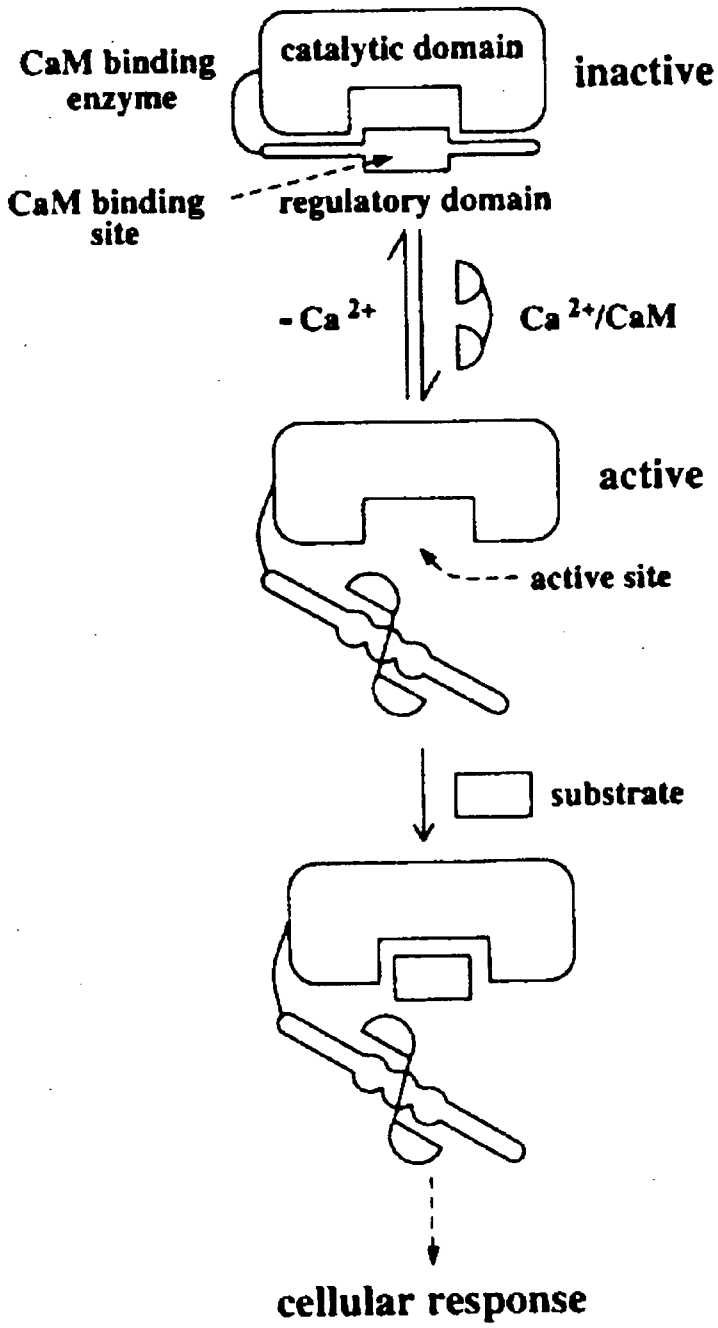

Figure 6. A general model of regulation of a target enzyme by CaM. (Taken from Crivici & Ikura, 1995)

autoinhibitory domain and CaM-binding site overlap in the myosin light chain kinases and CaM-dependent protein kinase II (Colbran *et al.*, 1989) but are separated by 50-60 residues within the A subunit of calcineurin (the B subunit of calcineurin is also a CaM-like calcium binding protein) (Cohen, 1989; Hashimoto & Perrino, 1990).

The CaM binding domain has been identified in a number of CaM binding proteins (reviewed in Crivici & Ikura, 1995). It is a short region of 14-26 residues in length that has a propensity to form a basic amphiphilic α-helix, and several consensus hydrophobic and basic residues are found in all known CaM-binding sequences (reviewed in O'Neil & DeGrado, 1990). However, residues in the primary sequences of known CaM-binding domains do not always exhibit a propensity to form an amphiphilic α-helix but rather adopt a helical conformation upon complex formation (reviewed in Crivici & Ikura, 1995). The CaM-binding fragment from phosphorylase kinase is predicted to form an extended β-turn-β-sheet structure (Dasgupta *et al.*, 1989). The three-dimensional structure of Ca^{2+}-CaM complexed with M13, a 26 residue peptide corresponding to the CaM binding site of skeletal muscle myosin light chain kinase, was solved using multidimensional NMR (Ikura *et al.*, 1992). Almost at the same time, the crystal structure of Ca^{2+}-CaM complexed with smM13, a 20 residue peptide corresponding to the CaM binding site of smooth muscle myosin light chain kinase, was determined (Meador *et al.*, 1992). The third structure of CaM/target peptide complex solved to date is the crystal structure of CaM complexed with a 25 residue peptide fragment of CaM-dependent multiprotein kinase II (Meador *et al.*, 1993). In these CaM/target peptide complexes, the two globular domains of CaM remain essentially unchanged. The long central helix (residues 65-93) is disrupted into two helices connected by a flexible loop (residues 74-82 in the solution structure of CaM/M13 complex, residues

73-77 in the crystal structure of CaM/smM13 complex), thereby enabling the two domains to clamp the bound peptide, which adopts a helical conformation. Both hydrophobic and electrostatic interactions that occur in the CaM/target peptide complexes are similar but not identical (Ikura *et al.*, 1992; Meador *et al.*, 1992; Meador *et al.*, 1993; reviewed in Clore *et al.*, 1993; reviewed in Crivici & Ikura, 1995). The arrangement of hydrophobic and basic residues in CaM-binding domains may be an important determinant in the mode of CaM recognition of its target (reviewed in Crivici & Ikura, 1995). A recent study indicates that the binding of a CaM-binding peptide to CaM is driven by negative changes in enthalpy (Wintrode & Privalov, 1997). Another study indicates that subtle changes in the CaM-binding peptide sequence can have significant effects on both the peptide dissociation rates and also the dissociation pathway which could contribute to the variety of regulatory behavior shown by CaM with different target enzymes (Brown *et al.*, 1997).

1.2.2. Troponin C

Troponin C is also a small acidic protein (pI 4-4.5) expressed in skeletal and cardiac muscle. It is a single polypeptide of 159-162 residues in length (159 in rabbit skeletal troponin C, 161 in bovine cardiac troponin C, and 162 in turkey and chicken troponin C) (Collins *et al.*, 1973; Van Eerd & Takahashi, 1975; Van Eerd & Takahashi, 1976; Wilkinson, 1976; Reinach & Karlsson, 1988; Golosinska *et al.*, 1991). The amino acid sequence of chicken skeletal troponin C is shown in Figure 4. The molecular weight of troponin C is approximately 18 kDa. Crystal structures of chicken and turkey skeletal troponin C were first determined in 1985 (Herzberg & James, 1985; Sundaralingam *et al.*, 1985) and later

refined at 2 Å resolution (Herzberg & James, 1988; Satyshur *et al.*, 1988). In these crystal structures there are two globular domains, each containing two hlh calcium binding sites, connected by a nine-turn α-helix, three turns of which are fully exposed to solvent. The crystals were obtained at pH ~5, and the two sites in the C-terminal domain are calcium bound while the N-terminal sites are calcium free. This structure is similar to that of CaM except that the central helix of CaM is three residues shorter (5 Å shorter), and as a result, the orientation of the two globular domains is slightly different (reviewed in Strynadaka & James, 1989). The N-terminal domain has an additional helical structure, the N-helix, that is unique to troponin C. Several studies demonstrated that the two domains are closer together under physiological conditions than is observed in the crystal structures (Wang *et al.*, 1987; Hubbard *et al.*, 1988; Heidorn & Trewhella, 1988). The solution structures of the skeletal troponin C regulatory domain (N-terminal domain) in the apo and calcium-saturated states were determined recently (Gagné *et al.*, 1995). No change in secondary structure is observed upon calcium binding, but a change in tertiary structure occurs. The structural transition in the regulatory domain of troponin C upon calcium binding involves an opening of the structure through large changes in interhelical angles, which lead to an increased exposure of an extensive hydrophobic patch, an event that triggers skeletal muscle contraction (Gagné *et al.*, 1995).

The four calcium binding sites in skeletal troponin C are numbered I through IV. Sites I and II are located in the N-terminal domain, sites III and IV are located in the C-terminal domain. The calcium affinity of the N-terminal sites are approximately 2 orders of magnitude lower than that of the C-terminal sites (Table 1 and references therein). The low affinity N-terminal sites are calcium specific, whereas the high affinity C-terminal sites bind calcium and

magnesium competitively with a lower affinity for magnesium (K_d: 1 mM) (Potter & Gergely, 1975; Levine *et al.*, 1977; Potter *et al.*, 1976; Ogawa, 1985; Wang & Cheung, 1985). Under physiological conditions, the C-terminal domain is calcium- or magnesium-bound at all times and assumes a structural role, whereas the N-terminal domain carries out the regulatory function (reviewed in Grabarek *et al.*, 1992).

Unlike skeletal troponin C, cardiac troponin C has three functional calcium binding sites, and mutations in the calcium binding loop of site I render this site nonfunctional (Potter *et al.*, 1977; Leavis & Kraft, 1978; Johnson *et al.*, 1980; Holroyde, *et al.*, 1980; Barskaya & Gusev, 1982; reviewed in Parmacek & Leiden, 1991). Site II in cardiac troponin C is the low affinity, calcium specific site, whereas sites III and IV in the C-terminal domain are the high affinity calcium/magnesium sites.

Troponin C is a component of the troponin complex consisting of troponin C, troponin I and troponin T (Greaser & Gergely, 1973). It is the molecular switch that triggers skeletal and cardiac muscle contraction in response to a calcium signal (reviewed in Leavis & Gergely, 1984; reviewed in Zot & Potter, 1987). Muscle contraction consists of a cascade of events involving several protein structural changes and protein-protein interactions. The basic building block of the contractile apparatus is the sarcomere. This multisubunit structure is composed of a precise geometric arrangement of myosin-containing thick filaments surrounded by an hexagonal array of thin filaments, each of which contains actin and the troponin/tropomyosin regulatory complex (reviewed in Leavis & Gergely, 1984; reviewed in Paracek & Leiden, 1991). For contraction to occur, the N-terminal domain of the myosin heavy chain (the globular head) must first bind to actin to form an active actomyosin complex (actomyosin Mg^{2+}-ATPase). This actin-myosin interaction is prevented by troponin I in

resting muscle. Upon release of calcium into cytoplasm of the muscle fiber, the N-terminal domain of troponin C binds two calcium ions and exposes its hydrophobic patch, which in turn interacts with the inhibitory and C-terminal regions of troponin I, allowing actin/myosin interactions and triggering muscle contraction (Gagné *et al.*, 1995).

1.2.3. Parvalbumin

Parvalbumins are a subfamily of hlh calcium binding proteins found in high concentrations in the sarcoplasm of skeletal muscles of fish, amphibians, and mammals (Baron *et al.*, 1975). Members of this family vary in their molecular weight (10 to 13 kDa) and isoelectric points (pI). The parvalbumin family encompasses two sub-lineages: α-parvalbumins (pI > 5.0) and β-parvalbumins (pI <5.0) (Goodman *et al.*, 1979). X-ray data for one of the carp parvalbumins (carp parvalbumin 4.25, 108 residues in length and sequence in Figure 7) show that the molecule contains six helical regions designated A-F (Kretsinger & Nockolds, 1973). Two pairs of the helical regions (CD and EF), together with connecting loops, form a pair of functional hlh calcium binding sites (CD and EF sites) similar to those found in the N- or C-terminal domain of troponin C and CaM. Unlike the dumbbell-shaped troponin C and CaM, parvalbumin is a globular molecule that can be described as an ellipsoid with dimensions of 36 × 30 × 30 Å (Kretsinger & Nockolds, 1973; Moews & Kretsinger, 1975). Helices A and B flank an 8-residue loop, constituting a nonfunctional calcium binding site. Unlike troponin C and CaM, whose N- and C-terminal domains are linked by a long central helix, the N-terminal part (residues 1-39) of parvalbumin folds over, packing its hydrophobic region into the hydrophobic patch formed by CD and EF sites. As a result,

parvalbumin has a buried central core of hydrophobic residues and an outer shell of hydrophilic residues (reviewed in Strynadka & James, 1989).

```
          1                   10                  20
Parv   Ac A F A G V L N D A D I A A A L E A C K A A D S F D H
Onco   Ac S I T D I L S A E D I A A A L Q E C Q D P D T F Q P

                30                  40                  50
Parv      K A F F A K V G L T S K S A D D V K K A F A I I
Onco      Q K F F Q T S G L S K M S A S Q V K D I F R F I

                            60                  70
Parv      D Q D K S G F I E E D E L K L F L Q N F K A D A R A
Onco      D N D Q S G Y L D G D E L K Y F L Q K F Q S D A R E

                80                  90                  100
Parv      L T D G E T K T F L K A G D S D G D G K I G V D E F
Onc       L T E S E T K S L M D A A D N D G D G K I G A D E F

                    108
Parv      T A L V K A
Onco      Q E M V H S
```

Figure 7. Amino acid sequences of carp parvalbumin 4.25 and rat oncomodulin. Parv, carp parvalbumin 4.25; Onco, rat oncomodulin. The calcium binding loops are underlined, and the chelating residues are in bold type. The sources of the sequences are: carp parvalbumin (Coffee & Bradshaw, 1973); rat oncomodulin (MacManus *et al.*, 1983).

Parvalbumin CD and EF sites bind calcium with the highest affinity (K_d: 1 nM) among the hlh calcium binding proteins studied so far (reviewed in Linse & Forsén, 1995; Table 1 and references therein). Magnesium competes with calcium for the two sites with a K_d ranging from 2.5 μM to 10.5 μM (Haiech *et al.*, 1979; Cave *et al.*, 1979; Moeschler *et al.*, 1980). As a result, the apparent calcium dissociation constants of the two sites are significantly lower in the presence of magnesium (0.1-1 μM) than in the absence of magnesium (1-10 nM) (Table 1 and references therein). Sodium and potassium ions bind to parvalbumin only at high concentrations possibly due to non specific electrostatic interactions (Pechère, 1977; Grandjean *et al.*, 1977; Permyakov *et al.*, 1983).

The unique structure of parvalbumin confers upon it a function as a calcium buffer, not an enzyme regulator (reviewed in Wnuk *et al.*, 1982; reviewed in Gillis, 1985). It is believed that parvalbumin is usually in the magnesium-bound form in resting muscle. At physiological levels of magnesium (~1 mM), potassium (~100 mM), and calcium (~ 0.1 μM) in the resting muscle, parvalbumin binds two magnesium ions. When calcium concentration is increased in the cell following a stimulus, troponin C and CaM bind calcium first, presumably due to the very slow off rate of magnesium from parvalbumin. Upon muscle relaxation, parvalbumin takes up the calcium ions released from troponin C and CaM, thereby quickly reducing the calcium concentration so contraction is not reinitiated. The fact that parvalbumins are found in greatest quantities in fast twitch muscles may support this hypothesis. It should be noted that parvalbumins are essentially skeletal muscle proteins. They are usually not found in cardiac or smooth muscle and therefore are not essential components of the contractile mechanism (reviewed in Strynadaka & James, 1989).

A special member of the parvalbumin family is oncomodulin. It was first discovered in extracts of rat hepatoma (MacManus, 1979). The amino acid sequence of rat oncomodulin is shown in Figure 7 (MacManus *et al.*, 1983). The amino acid sequences of oncomodulin and parvalbumin from rat are identical at 55 of 108 positions (Berchtold *et al.*, 1982; MacManus *et al.*, 1983; Epstein *et al.*, 1986; Gillen *et al.*, 1987; MacManus *et al.*, 1989). Compared to the CD and EF sites of rat parvalbumin, the CD site of oncomodulin displays 390 fold lower affinity for calcium, whereas the EF site has 21 fold lower calcium affinity (Rinaldi *et al.*, 1982; Hapak *et al.*, 1989; Table 1). The magnesium dissociation constants of CD and EF sites of oncomodulin are 3 and 0.18 mM, respectively (Hapak *et al.*, 1989). The normal expression of oncomodulin is confined to the fetal placenta. This protein frequently reappears upon neoplastic transformation and is detectable in a variety of mammalian tumors (MacManus & Whitfield, 1983). The exact function of oncomodulin is unknown, and the three-dimensional structure of oncomodulin has not been determined.

1.2.4. Calbindin$_{9K}$

Calbindin$_{9K}$, also known as the vitamin D dependent intestinal calcium binding protein, contains two calcium binding sites. It is the smallest of the known hlh calcium binding proteins and located primarily in the cytoplasm of the absorptive cells of mammalian small intestine (Taylor, 1983). It is a 75 residue protein with a molecular weight of approximately 9 kDa (Figure 8). The crystal structure of calbindin$_{9K}$ with two bound calcium ions shows that it contains four helices designated I (residues 3-14), II (residues 25-35), III (residues 46-53), and IV (residues 62-75) (Szebenyi, *et al.*, 1981; Szebenyi & Moffat, 1986). Calcium

```
                                1                   10
CaD9K                           K S P E E L K G I F E K Y
Calcy           M A S P L D Q A I G L L I G I F H K Y
                1                   10

                        20                      30                      40
CaD9K   A A K E G D P N Q L S K E E L K L L L Q T E F P S L L
Calcy   S G K E G D K H T L S K K E L K E L I Q K E L T I G S
        20                      30                      40

                                50                      60
CaD9K   K G P S T L D E L F E E L - D K N G D G E V S F E E
Calcy   K L Q D A E I V K L M D D L D R N K D Q E V N F Q E
                50                      60                      70

                        70          75
CaD9K   F Q V L V K K I S Q
Calcy   Y I T F L G A L A M I Y N E A L K G
                        80                      90
```

Figure 8. Amino acid sequences of bovine calbindin$_{9K}$ and rabbit calcyclin. The calcium binding loops are underlined, and the chelating residues are in bold type. CaD$_{9K}$, bovine calbindin$_{9K}$. Calcy, rabbit calcyclin. '-' represents a deletion. The sources of the sequences are: bovine calbindin$_{9K}$ (Fullmer & Wasserman, 1981); rabbit calcyclin (Ando *et al.*, 1992).

binding loops are observed between helices I and II and between helices III and IV. The C-terminal site (site II) is a normal EF-hand, whereas the N-terminal site (site I) is a pseudo-EF hand with a 14 residue loop which chelates calcium with four backbone peptide carbonyls (residues 14, 17, 19, and 22) and a single side chain carboxyl oxygens (Glu27). A water molecule is also involved in direct chelation of the calcium ion at the -X position in site I. The overall structure has an ellipsoidal shape with dimensions of 30 Å long and 25 Å in

diameter. Unlike the paired hlh calcium binding sites in CaM, troponin C and parvalbumin, which usually have a 4-5 residue linker between the two sites, the two sites in calbindin$_{9K}$ have a 10 residue linker (residues 36-45). This extended linker has hydrophobic residues interacting with the hydrophobic patch formed by the inner surfaces of helices A to D. Like parvalbumin, calbindin$_{9K}$ has no significant hydrophobic patches on the surface that might serve as interaction sites for target molecules.

The solution structures of Ca^{2+}-bound and apo-calbindin$_{9K}$ were determined using ^{1}H-NMR spectroscopy (Kördel *et al.*, 1993; Skelton *et al.*, 1990a; Skelton *et al.*, 1994; Skelton *et al.*, 1995). The distribution of secondary structure and the global folding patterns of apo and calcium-bound calbindin$_{9K}$ are virtually identical (Skelton *et al.*, 1990b). The similarity of three dimensional structures of calbindin$_{9K}$ in the apo and calcium bound states in solution is clearly demonstrated from the overlay of the two average structures (Skelton *et al.*, 1994). The fact that calcium binding to calibindin$_{9K}$ does not induce a structural change in the protein suggests that calcium binding domains comprised of paired hlh motifs can be adjusted to remain essentially intact or respond strongly to calcium binding. It is speculated that this fine tuning of the response to calcium binding has evolved so that activation of calcium-dependent pathways and control of calcium concentrations within cellular compartments can be regulated independently (Skelton *et al.*, 1994).

The two sites of calbindin$_{9K}$ have a moderate affinity for calcium with a K_d of approximately 1 μM under near physiological salt concentrations and pH (Table 1 and references therein). The calcium affinity of the sites is significantly higher in the absence than in the presence of salts (Kesvatera *et al.*, 1994; Table 1 and references therein). The exact function of calbindin$_{9K}$ is unclear, but it has been proposed that it acts as a calcium buffer in

calcium translocation or absorption at the intestinal wall (Levine & Williams, 1982; Wasserman & Fullmer, 1982; Wasserman *et al.*, 1983).

1.2.5. Calcyclin

Calcyclin is a member of the S100 protein subfamily. It has been found in the form of homodimer (Ando *et al.*, 1992), and the monomer is a 90 residue peptide (Figure 8, page 33). The three-dimensional solution structure of rabbit apo-calcyclin has been determined using ^{1}H-NMR spectroscopy (Potts *et al.*, 1995). This solution structure reveals a symmetric homodimeric fold that is unique among hlh calcium binding proteins of known three-dimensional structure. The structure of each subunit is comprised of a single globular domain consisting of a pair of hlh motifs that are joined by an ill-defined linker loop. Similar to calbindin$_{9K}$, each monomer of calcyclin has a pseudo EF hand (site I) and a normal EF hand (site II). A short antiparallel β-sheet is found between the two binding loops, similar to the globular domains of hlh calcium binding proteins described earlier. The distribution of the elements of secondary strucutre is found to be very similar to that of apo calbindin$_{9K}$ (Skelton *et al.*, 1990b) and apo S100β (Kilby *et al.*, 1995). However, the three-dimensional structure of calcyclin is different from that of calbindin$_{9K}$ in terms of the interhelical angles (Potts *et al.*, 1995). Dimerization is mediated primarily by hydrophobic contacts from several highly conserved residues, and approximately 1200 Å^2 of solvent-accessible surface area becomes buried upon dimerization. The dimer has a dimension of ~38 × 33 × 31 Å, and a wide cleft, a possible binding surface for target protein, is created upon formation of the dimer. Compared with the amino acid sequence of calbindin$_{9K}$, it is found that the highly conserved

hydrophobic residues which initiate dimerization in calcyclin are lacking in calbindin$_{9K}$. This may explain why dimerization occurs in calcyclin but not in calbindin$_{9K}$.

Calcium binding affinity of calcylin has not been determined. Other S100 proteins show moderate affinity for calcium (Table 1 and references therein). S100 proteins also bind zinc, and zinc binding to S100 proteins increases the affinity for calcium (Baudier *et al.*, 1985; Baudier *et al.*, 1986).

The exact function of calcyclin and other S100 proteins is still unknown. They may be involved in cell growth and differentiation, cell cycle regulation, and metabolic control (Donato, 1991; Hilt & Kligman, 1991).

1.3. VU-1 CALMODULIN

VU-1 CaM is a recombinant CaM encoded by a synthetic CaM gene (Roberts *et al.*, 1985). The calcium dissociation constants of VU-1 CaM range from 0.7 to 3 μM (Haiech *et al*, 1991), which are similar to those of tissue-isolated CaM (Table 1 and reference therein). The phosphodiesterase regulatory activity of VU-1 CaM is also similar to that obtained with spinach and gizzard calmodulins, however, VU-1 CaM activates NAD kinase to a maximal level which is 3.2 fold higher than that obtained with spinach CaM and 6 fold higher than that obtained with gizzard CaM (Roberts *et al.*, 1985).

1.3.1. The synthetic CaM gene and the pVUCH-1 CaM expression vector

The synthetic CaM gene was prepared from 61 deoxyoligonucleotides and first cloned in the plasmid pKK223-3 expression vector (Roberts *et al.*, 1985). This CaM expression

vector is named pVUC-1. The synthetic CaM gene is 455 base-pairs (bp) in length, and contains 26 restriction endonuclease sites designed for the introduction of specific modifications in the coding sequence (Figure 9). It provides a system for generating calmodulins with specific modifications for studies on structure/function relationships. Another CaM expression vector, pVUCH-1, that allows mutagenesis, amplificaton, characterization and expression of the mutant calmodulin gene in *E. coli*. has been constructed from pVUC-1 and pUC8 (Lukas *et al.*, 1987). The CaM gene is expressed under the control of the tac promotor, and the ampicillin resistant gene in the plasmid permits screening for *E. coli* clones containing plasmids by culturing on ampicillin media. In pVUCH-1, the CaM gene contains 18 unique restriction endonuclease sites that are not found in the other regions of the plasmid. A simplified restriction map of pVUCH-1 is shown in Figure 10.

1.3.2. The amino acid sequence of VU-1 CaM

The amino acid sequence of VU-1 CaM is shown in Figure 11. This protein is a hybrid of vertebrate and plant calmodulins. The bacterially expressed protein lacks the two posttranslational modifications. N-terminal Ala is not acetylated and Lys115 is not trimethylated. Except for the lack of acetylation, the changes in VU-1 CaM have been observed in both mammalian and plant calmodulins (Lukas *et al.*, 1987).

```
1 Eco RI      10  Bcl I  Pvu II 20          30          40    Aha III    50
AATTCATGGC TGATCAGCTG ACTGACGAGC AGATCGCTGA ATTTAAAGAG
    GTACCG ACTAGTCGAC TGACTGCTCG TCTAGCGACT TAAATTTCTC

           60          70          80  Rsa I/Kpn I  90          100
GCTTTCTCTC TGTTTGACAA AGACGGTGAC GGTACCATCA CTACCAAAGA
CGAAAGAGAG ACAAACTGTT TCTGCCACTG CCATGGTAGT GATGGTTTCT

Sac I/Hgi AI 110    Mst I   120      Bal I  130 Bbv I      140         150
GCTCGGCACC GTTATGCGCA GCCTTGGCCA GAACCCGACT GAAGCTGAAC
CGAGCCGTGG CAATACGCGT CGGAACCGGT CTTGGGCTGA CTTCGACTTG

Pst I        160          170  Sal I      180  Hga I      190      Cla I  200
TGCAGGACAT GATTAACGAA GTCGACGCTG ACGGTAACGG CACCATCGAT
ACGTCCTGTA CTAATTGCTT CAGCTGCGAC TGCCATTGCC GTGGTAGCTA

   Hpa II  210          220      Bss HII 230          240          250
TTTCCGGAAT TTCTGAACCT GATGGCGCGC AAGATGAAAG ACACTGACTC
AAAGGCCTTA AAGACTTGGA CTACCGCGCG TTCTACTTTC TGTGACTGAG

           260          270 Stu I       280          290          300
TGAAGAGGAA CTGAAAGAGG CCTTCCGTGT TTTCGACAAA GACGGTAACG
ACTTCTCCTT GACTTTCTCC GGAAGGCACA AAAGCTGTTT CTGCCATTGC

           310 Xma III  320          330          340          350
GTTTCATCTC GGCCGCTGAA CTGCGTCACG TTATGACTAA CCTGGGTGAA
CAAAGTAGAG CCGGCGACTT GACGCAGTGC AATACTGATT GGACCCACTT

Hind III     360          370      Xmn I  380    Nru I  390    Aat II   400
AAGCTTACTG ACGAAGAAGT TGACGAAATG ATTCGCGAAG CTGACGTCGA
TTCGAATGAC TGCTTCTTCA ACTGCTTTAC TAAGCGCTTC GACTGCAGCT

           410    Hpa I  420          430          440      Dde I  450
TGGTGACGGC CAGGTTAACT ACGAAGAGTT CGTTCAGGTT ATGATGGCTA
ACCACTGCCG GTCCAATTGA TGCTTCTCAA GCAAGTCCAA TACTACCGAT

    455 Bam HI
AGTAG
TCATCCTAG
```

Figure 9. Sequence of the synthetic CaM gene. The restriction endonuclease sites are underlined and labeled. The start codon ATG and stop codon TAG are boxed.

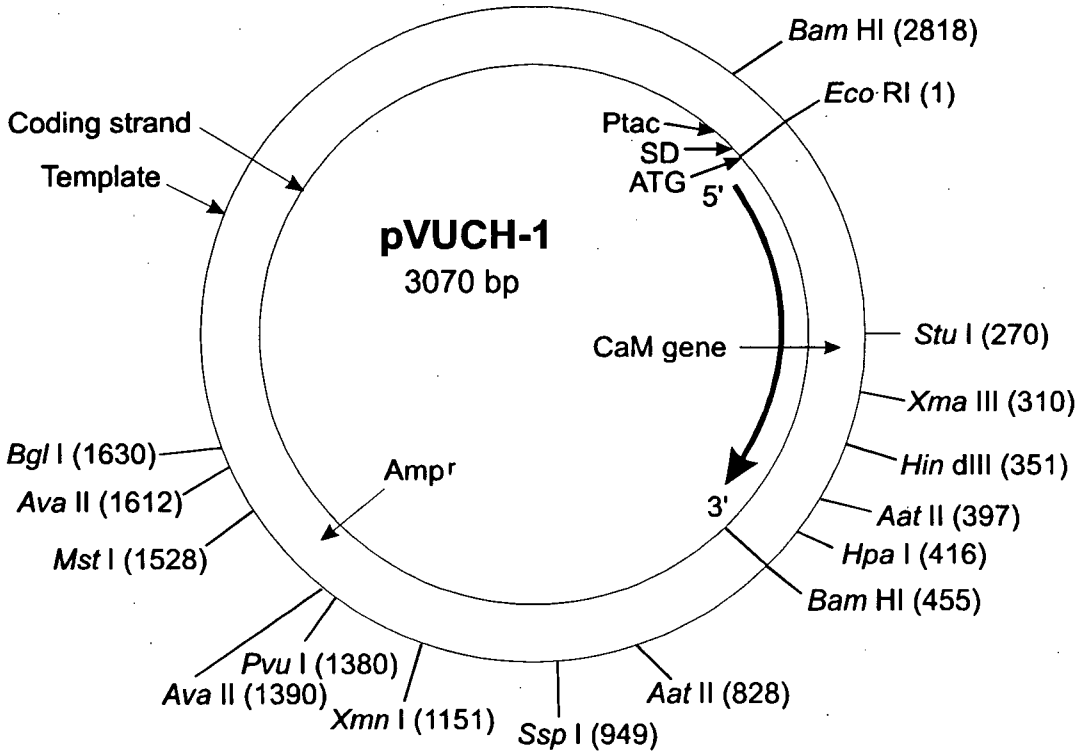

Figure 10. Structure of pVUCH-1 CaM expression vector. The synthetic CaM gene (455 bp) and the ampicillin resistance gene (Amp^r) are labeled. Some restriction endonucelase sites are marked. 'Ptac' refers to the hybrid trp-lac promotor, and 'SD' refers to the Shine-Dalgarno sequence. The positions of Ptac and SD relative to the initiation codon ATG of the CaM gene are indicated.

```
         1                   10                  20
VU-1     A D Q L T D E Q I A E F K E A F S L F D K D G D G T I
BCaM Ac  - - - - - E - - - - - - - - - - - - - - - - - - - - -

             30                  40                  50
VU-1     T T K E L G T V M R S L G Q N P T E A E L Q D M I N E
BCaM     - - - - - - - - - - - - - - - - - - - - - - - - - - -

                 60                  70                  80
VU-1     V D A D G N G T I D F P E F L N L M A R K M K D T D S
BCaM     - - - - - - - - - - - - - - - T M - - - - - - - - - -

                         90                  100
VU-1     E E E L K E A F R V F D K D G N G F I S A A E L R H V
BCaM     - - - I R - - - - - - - - - - - - Y - - - - - - - - -

           110                 120                 130
VU-1     M T N L G E K L T D E E V D E M I R E A D V D G D G Q
BCaM     - - - - - - - - - - - - - - - - - - - - - I - - - - -

                 140                 148
VU-1     V N Y E E F V Q V M M A K
BCaM     - - - - - - - - M - T - -
```

Figure 11. Amino acid sequences of VU-1 CaM and bovine brain CaM. '-' represents an identical amino acid residue in the position. 'VU-1' represents VU-1 CaM. 'BCaM' represents bovine brain CaM. K115 in bovine brain CaM is trimethylated.

1.4. STUDIES ON STRUCTURE/CALCIUM AFFINITY RELATIONSHIPS USING ENGINEERED PROTEINS

Site-directed mutagenesis is a powerful tool to prepare proteins with pre-designed amino acid residues at specific positions. As a result, a large number of studies on structure/calcium affinity relationships in hlh calcium binding proteins have been carried out using engineered proteins. The effect of the nature of the chelating residues on calcium affinity of the site or the paired sites has been a natural starting point for many mutagenesis studies. The effect of non-chelating residues in the loop and in the helices of the hlh calcium binding motif on calcium affinity has also been examined.

1.4.1. Mutation at the invariable +X and -Z positions

Mutation of the highly conserved residue at either the +X (Asp) or the -Z (Glu) position always causes a reduction in calcium affinity by 2 to 3 orders of magnitude or a loss in calcium binding (Babu *et al.*, 1992; Negele *et al.*, 1992; Putkey *et al.*, 1989; Beckingham, 1991; Maune *et al.*, 1992). Point mutation of Asp to either Glu or Asn at the +X position in site II of rabbit skeletal troponin C inactivated this site in calcium binding at pCa 3.5 (Babu *et al.*, 1992). Similarly, when E/D or E/Q mutations were made at the -Z position in site I, the proteins were able to bind only three calcium ions per molecule at pCa 3.5 (Babu *et al.*, 1992). When Asp was replaced by Ala at the +X position in either site II, site III, or site IV of chicken cardiac troponin C (D65A, D105A, or D141A), the mutated sites did not bind calcium at pCa 4 (Negele *et al.* 1992; Putkey *et al.*, 1989). Point mutations of Glu to Ala at the -Z position in site II (E67A) and site IV (E140A) of VU-1 CaM reduced the calcium affinity of the mutated site by 100-300 fold (Haiech *et al.*, 1991). Point mutations of Glu to

either Gln or Lys at the -Z position in each of the loops in *Drosophila melanogaster* CaM also significantly affected the calcium affinity of the mutated sites (Maune *et al.*, 1992). Calcium binding at the mutated sites was undetectable in most of the CaM mutants, E31Q, E67Q, E67K, E104Q, E104K, E140Q, and E140K, in the presence of 1 mM magnesium. However, in the absence of magnesium, E104Q (mutation in site III) and E140Q (mutation in site IV) gave calcium dissociation constants of 1250 and 200 μM for the mutated sites, respectively (Maune *et al.*, 1992).

1.4.2. Mutation at the +Y position

Substitution at the +Y position in different sites can have different effects on calcium binding properties. D58N mutation at the +Y position in site II of CaM led to a slight increase in calcium affinity of the N-terminal domain and a substantial increase in cooperativity in this domain, however, D95N mutation at the +Y position in site III decreased the calcium affinity of the C-terminal domain and also reduced the positive cooperativity between the two sites in the C-terminal domain (Waltersson *et al.*, 1993). While point mutation of Asp to either Glu or Ala at the +Y position in site II and point mutation of Asn to Ala at the +Y position in site III of rabbit skeletal troponin C inactivated the mutated sites with respect to calcium binding, respectively, point mutation of Asp to Asn in the same position in site II had no significant effect on calcium affinity (Babu *et al.*, 1992; Dotson *et al.*, 1993). N56A mutation at the +Y position in site II of calbindin$_{9K}$ also significantly decreased the calcium affinity of site II (Linse *et al.*, 1995).

1.4.3. Mutation at the -Y position

Substitution of Phe for Tyr at the -Y position of the CD site of rat oncomodulin (Y57F) did not affect calcium binding in either the CD or EF site (Palmisano *et al.*, 1990). This is in agreement with the fact that the -Y position is occupied by a variety of amino acids with different size, charge or hydrophobicity (Marsden *et al.*, 1990; Falke *et al.*, 1994; Figure 2). It is not the side chain but the backbone carbonyl oxygen that chelates the calcium ion, as a result, the nature of the side chain of the residue at this position appears not to be critical in calcium binding. Interestingly, the mutation of E60Q at the -Y position of site II of calbindin$_{9K}$ caused a very small reduction in overall calcium affinity and reduced cooperativity between sites I and II (Linse *et al.*, 1991b). Mutation of E60D at the identical position in calbindin$_{9K}$ led to a significant decrease in overall calcium affinity by a factor of 38 and an enhanced cooperativity between the two sites (Linse *et al.*, 1994). Unlike the -Y residue in oncomodulin, Glu60 at the -Y position in calbindin$_{9K}$ chelates the calcium ion through its backbone carbonyl oxygen in site II. Concurrently, the carboxylate group of the same residue forms a hydrogen bond to a water molecule that constitutes a calcium ligand in site I. As a result, the -Y position in site II of calbindin$_{9K}$ is not as variable as that in other hlh calcium binding proteins.

1.4.4. Mutation at the -X position

A D59E mutation at the -X position in the CD site of oncomodulin was designed to make the CD site more like the same site in parvalbumin (MacManus *et al.*, 1989; Hapak *et al.*, 1989; Golden *et al.*, 1989). Flow dialysis showed that the mutation only slightly increased the calcium affinity of the CD site by 1.4 fold and magnesium affinity of this site by

3 fold (Hapak *et al.*, 1989). The calcium and magnesium affinities of the EF site were not affected by the D59E mutation (Hapak *et al.*, 1989). Fluorescence and NMR studies demonstrated that this substitution of Glu for Asp increased the affinity of the CD site for magnesium and lutetium (which has a smaller ionic radius and higher charge density than calcium). Meanwhile, the affinity of the EF site for magnesium and lutetium was also increased by a factor of approximately 5 (Golden *et al.*, 1989).

The effect of mutation of Gln at the -X position to seven different residues commonly observed in natural EF-hands on the calcium affinity of the single calcium binding site in *E. coli* D-galactose binding protein was determined recently (Drake *et al.*, 1996). Although the bidentate Glu is from a region that is distant in sequence from the rest of the chelating residues, all the ligands in the protein are arranged in a way that is virtually identical to that of an EF-hand (Vyas *et al.*, 1989). Neutral residues of different size at the -X position [Gln (wild type), Asn, Thr, Ser, Ala, and Gly] were found to yield similar calcium affinities. Change in the charge of the residue by the Q142E or Q142D mutation was observed to reduce calcium affinity by at least 357 fold for Q142E and approximately 16 fold for Q142D (Falke *et al.*, 1991; Drake *et al.*, 1996). These results indicate that while the neutral residue of different size in the -X position does not alter the calcium affinity of the site, changes in the charge of this position can alter calcium affinity (Drake *et al.*, 1996).

1.4.5. Mutation of charged residues on the surface

Effect of charged residues on the surface of the protein on calcium binding properties has also been examined in calbindin$_{9K}$ (Martin *et al.*, 1990; Linse *et al.*, 1991b). Removal of three negative surface charges by the triple mutation of E17Q/D19N/E26Q caused a 45-fold

decrease in average calcium affinity (per site) at low ionic strength and a 5-fold reduction at 150 mM KCl (Linse *et al.*, 1991). The reduction in calcium affinity was mainly caused by a reduction in the calcium on-rate (Martin *et al.*, 1990).

1.4.6. Mutation of non-chelating residues in the loop

Substitution of Glu for Ala at position 2 between the +X and the +Y positions in site II of rabbit skeletal troponin C did not affect calcium binding to this site (Babu *et al.*, 1992). A single substitution of Lys for Gln at position 4 between the +Y and the +Z positions in the CD site of oncomodulin (Q54K) did not alter calcium affinity of the site, however, mutation of N52K at position 2 in this site slightly decreased calcium affinity of the site by 1.6 fold, and mutation of G60E at position 10 slightly increased calcium affinity of the site by 1.5 fold (Palmisano *et al.*, 1990). Substitution of Val for Thr at position 8 between the -Y and the -X positions in site IV of CaM caused 3 fold decrease in the overall calcium affinity (Han & Roberts, 1997). It appears that the non-chelating residues in the loop are not as critical as the chelating residues, however, they can affect calcium affinity of the site through interactions with the chelating residues.

1.4.7. Mutation of non-polar residues that become more solvent-exposed upon calcium binding

As proposed and observed in the three dimensional structures of apo and calcium-loaded troponin C and CaM, calcium binding causes the exposure of a number of hydrophobic residues to produce a hydrophobic patch (Babu *et al.*, 1985;1988; Herzberg & James, 1985; 1988; Herzberg *et al.*, 1986; Sundaralingam *et al.*, 1985; Satyshur *et al.*, 1988;

Zhang *et al.*, 1995; Kuboniwa *et al.*, 1995; Finn *et al.*, 1995; Gagne *et al.*, 1995). The unfavorable energy requirement for the exposure of hydrophobic residues to solvent is presumed to be compensated for by the binding of calcium. Point mutations of V45T, M46Q, L49T, M48A, and M82Q increased the calcium affinity of sites I and II in the N-terminal domain of troponin C by 1.3 to 2.7 fold (Pearlstone *et al.*, 1992). Similar results were also reported for V45T and M48A troponin C mutants (Da Silva *et al.*, 1993). In the later study, the V45T and M48A troponin C mutants had a 5.1 and 2.6 fold increase in calcium affinity, respectively. Residues 45, 46, 48, 49 are located in the C-terminal α-helix of site I, and residue 82 is located in the C-terminal α-helix of site II (the N-terminal part of the central helix). These positions are observed to be more solvent-exposed upon calcium binding (Gagne *et al.*, 1995). All these point mutations increase the hydrophilic property of the mutated residues thereby reducing the energy required for the residues to become more solvent-accessible leading to an increase in calcium affinity of the respective sites.

1.4.8. Mutation of Gly92 at the center of the central helix of skeletal troponin C

Point mutations of G92A and G92P at the center of the central helix of chicken skeletal troponin C did not affect calcium affinities of the N- and C-terminal domains nor the in vitro regulation of actin-activated ATPase of myosin (Reinach & Karlsson, 1988). These results suggest that Gly92 is not essential for the proper interaction of the calcium regulatory sites with the other components of the thin filament, and therefore exclude a large rotation around Gly92 as the mechanism of information transfer between the two domains of troponin C postulated by Herzberg & James (1986).

1.4.9. Mutation of the entire calcium binding loop or the entire hlh motif

It is found that the calcium binding capacity of an EF-hand is retained when the entire loop or the entire EF-hand is removed from its natural location to another EF-hand or another protein (Brodin *et al.*, 1990; Matsuura *et al.*, 1991; George *et al.*, 1993; George *et al.*, 1996; Matsuura *et al.*, 1993; Persechini *et al.*, 1996). The engineered site always has a different calcium affinity in the new environment, and in most cases, the calcium affinity is lower than in the natural location. When site I and site II were exchanged in calbindin$_{9K}$, or site II was replaced by site I, or site I was replaced by site II, the two sites in the new environments were still able to bind calcium, however, the calcium affinity of each site was 12.5 to 160 fold lower in the new environments than in the natural locations (Brodin *et al.*, 1990). When the loop and the C-terminal helix of the non-functional site IV of yeast CaM was engineered to replace a similar region in chicken CaM, the chimeric site IV was still unable to bind calcium, however, the functional site IV of chicken CaM was able to bind calcium when the loop and the C-terminal helix of this site was engineered into yeast CaM (Matsuura *et al.*, 1993). When site II of CaM was replaced by site IV, the I-IV pair in the N-terminal domain of the mutant protein has a calcium affinity similar to the native I-II pair in the native protein. However, when site I of CaM was replaced by site III, the III-II pair in the N-terminal domain is intermediate in calcium affinity to the native III-IV and I-II pairs (Persechini *et al.*, 1996).

Recently, George *et al.* (1993; 1996) have examined the calcium binding properties of a number of CaM-cardiac troponin C chimeras in which either site III, site IV, both site III and site IV, loop IV, loop III and loop IV, the N-terminal helix of site IV, or the C-terminal helix of site IV of cardiac troponin C were engineered to replace the respective region in CaM.

Tyr fluorescence was used to monitor the calcium titration (Tyr5, Tyr111 at the -Y position in loop III, and Tyr150 at position 10 in loop IV in cardiac troponin C; Tyr99 at the -Y position in loop III and Tyr138 at position 10 in loop IV in CaM). It was observed that the chimera containing the N-terminal domain of CaM and the C-terminal domain of cardiac troponin C had an overall calcium affinity similar to that of cardiac troponin C, and that the chimera containing the N-terminal domain of cardiac troponin C and the C-terminal domain of CaM had an overall calcium affinity similar to that of CaM. The chimeras containing either the N- or the C-terminal helix of cardiac troponin C have 1.5 to 1.7 fold lower overall calcium affinity compared to CaM. However, in all other cases, the engineered chimeras had 2.4 to 10 fold lower calcium affinity compared to troponin C and 2 to 8 fold higher calcium affinity compared to CaM. It appears that the lower calcium affinity of CaM is dictated by site III (George *et al.*, 1993). A possible explanation is that three acidic chelating residues are located in site III of CaM, whereas there are four acidic chelating residues in sites III and IV of cardiac troponin C and site IV of CaM. Less negative charge in site III of CaM may cause the lower overall calcium affinity of the C-terminal domain of CaM than that of cardiac troponin C.

1.5. FLUORESCENCE LABELING OF HLH CALCIUM BINDING PROTEINS

Fluorescence labeling a protein can be done by introducing a fluorescent structure by either chemical reaction or site-directed mutagenesis. Large aromatic structures such as dansyl-cysteine and 5-iodoacetamidoeosin have been introduced into parvalbumin and troponin C, respectively through chemical reaction with the sulfhydral group of Cys residues in the proteins (Iio & Hoshihara, 1984; Wang & Cheung, 1985). With the development of

biotechnology, a fluorescent amino acid such as Trp is easily introduced into proteins using site-directed mutagenesis. Trp has been introduced into hlh calcium binding proteins, which are devoid of Trp residues in the native forms, as a unique fluorescent label (Kilhoffer *et al.*, 1988; 1992; Trigo-Gonzalez *et al.*, 1992; Pearlstone *et al.*, 1992; Hutnik *et al.*, 1990; Pauls, *et al.*, 1993).

1.5.1. T26W, T62W, F99W and Q135W calmodulins

Trp has been introduced into positions 26, 62, 99 and 135 of VU-1 CaM by point mutations of T26W, T62W, F99W, and Q135W, respectively (Kilhoffer *et al.*, 1988; 1992). These positions correspond to the -Y position in site I, II, III, and IV, respectively. It was observed that the fluorescence emission wavelengths of these Trp-labeled calmodulins were slightly different ranging from 343 to 350 nm when the excitation wavelength was set at 297 nm. Trp fluorescence polarization in these proteins monitored the local conformational changes in each globular domain where the Trp had been introduced. For proteins containing the Trp probe in either site III or site IV (F99W CaM and Q135W CaM), the fluorescence polarization changed when the first and second calcium were bound to the protein. For proteins containing the Trp probe in either site I or site II (T26W CaM and T62W CaM), the fluorescence polarization changed when the third and fourth calcium were bound to the protein. However, Trp fluorescence intensity in these proteins did not simply monitor local conformational changes induced by calcium binding to each globular domain where Trp was located. It appears that the fluorescence intensity of these proteins is affected by calcium binding to both the N- and the C-terminal domains. The overall calcium affinity of these

proteins is similar. The calcium dissociation constants of T26W, T62W, F99W, and Q135W calmodulins are 3.85, 2.5, 2.56, and 2.9 μM, respectively, as monitored by flow dialysis.

1.5.2. F102W parvalbumin and F102W oncomodulin

Trp has been introduced into position 102, a position one residue after the -Z position of the EF site in rat parvalbumin by the F102W mutation (Pauls *et al.*, 1993). Similar to the native protein, the Trp-labeled protein has two non-cooperative Ca^{2+}/Mg^{2+}-binding sites. The dissociation constants of the Trp-labeled protein for calcium and magnesium were found to be similar to those of the native protein (0.037 μM and 23 μM, respectively, for the Trp-labled protein, and 0.042 μM and 34.5 μM, respectively, for the native protein monitored by flow dialysis). The maximal emission wavelength of apo and calcium-bound protein was observed at 319 nm when the excitation wavelength was set at 295 nm. Based on the Trp fluorescence emission spectra, UV difference spectra and Tyr fluorescence spectra, it was concluded that Trp residue at position 102 was confined to a hydrophobic core and conformationally restricted. As a result, the fluorescence intensity was slightly affected by calcium or magnesium binding (the quantum yield for the apo and calcium-bound parvalbumin is 0.41 and 0.36, respectively).

Trp has also been introduced into position 102 in rat oncomodulin (Hutnik *et al.*, 1990). The engineered Trp was used as a spectral probe to monitor the local conformational changes around residue 102 upon calcium binding and decalcification. Based on the Trp fluorescent properties (emission spectra, quantum yield measurements, and time-resolved fluorescence) of F102W oncomodulin and cod III parvalbumin which has an intrinsic Trp at the identical position (position 102), it was found that oncomodulin was distinct from cod III

parvalbumin in terms of the electronic environment of the hydrophobic core around residue 102, the magnitude of the calcium induced conformational changes, and the number of calcium ions required to modulate the major conformational changes.

1.5.3. F29W or F105W troponin C

Chicken skeletal troponin C has been labeled with Trp by point mutations of F29W and F105 W (Trigo-Gonzalez *et al.*, 1992; Pearlstone *et al.*, 1992; Li *et al.*, 1994). Positions 29 and 105 correspond to the positions preceding the loop of sites I and III, respectively. It was found that Trp29 and Trp105 were successful probes for monitoring the calcium induced conformational changes of the corresponding globular domain where the probe was located. The Trp fluorescence intensity change of the F29W troponin C reflected calcium binding to the N- but not the C-terminal domain. Similarly, the Trp fluorescence intensity change of the F105 troponin C reflected calcium binding to the C- but not the N-terminal domain. The calcium dissociation constants of F29W and F105W troponin C mutants calculated from the Trp fluorescence-monitored calcium titration data were found to be similar to those of the low- and high-affinity sites of wild-type troponin C calculated from the CD-monitored calcium titration data.

1.6. OBJECTIVES

As discussed in the earlier sections, hlh calcium binding motifs in proteins are highly homologous, especially in the loop region. However, calcium affinity of hlh calcium binding proteins covers a range of at least 5 orders of magnitude (Table 1, page 7). To correlate the nature of the loop residues with calcium affinity of the hlh calcium binding motif, the Acid-

Pair Hypothesis was proposed among other theories (sections 1.1.4 and 1.1.5, pages 11-12). This hypothesis is supported by studies using synthetic single site peptide models of CaM site III (section 1.1.6, page 13). However, the Acid-Pair Hypothesis does not take into consideration cooperativity between paired sites, nor does it consider the non-chelating residues in the site or possible interactions with residues outside the site. Therefore, the relevance of the single site model and hence the Acid-Pair Hypothesis to calcium binding to hlh motifs in the natural protein remains unknown.

The overall objective of this study was to examine the applicability of the Acid-Pair Hypothesis to a hlh calcium binding motif in a whole protein model. In particular, this study was designed to examine the structure/calcium affinity relationships of the chelating amino acid residues in the loop of site III of CaM using CaM mutants.

To determine the calcium affinity of site III in the CaM model, we intended to introduce a strong fluorescent label into site III to monitor the calcium induced structural transition of the site. This specifically located fluorescent label is an attempt to reduce the ambiguity which is encountered when calcium binding parameters are obtained using such techniques as equilibrium or flow dialysis in assigning dissociation constants to specific sites. Since Trp at position 105 in chicken skeletal troponin C has been successfully used as a fluorescent label to monitor the calcium induced structural transition in the C-terminal domain of the protein (section 1.5.3, page 49), and CaM is very similar to troponin C in the overall three dimensional structure, it was anticipated that Trp substitution at position 92 in CaM, similar to Trp105 in chicken skeletal troponin C, would allow us to titrate the calcium induced conformational transition in the C-terminal domain, and calcium binding to the N-terminal domain would not affect the Trp fluorescence as in the case of F105W troponin C.

Since the structure/calcium affinity relationships in a multi-site protein such as CaM are complicated by cooperativity between the paired sites (reviewed in Strynadaka & James, 1989; Falke *et al.*, 1994; Linse & Forsén, 1995), we can not directly measure the calcium affinity of site III without the cooperative interference of site IV in CaM. Therefore, it is necessary to create a whole protein model in which site IV is inactivated with respect to calcium binding, and as a result, site III binds calcium independent of the cooperative interactions between sites III and IV. Since substitution of Glu for Asp at the +Z position in the synthetic single site peptide model caused the peptide model to lose all calcium and magnesium binding capacity (Reid & Procyshyn, 1995; section 1.1.6, page 13), it was hoped that the D133E mutation at the +Z position in site IV of CaM would have the same effect on calcium binding to the site.

The synthetic CaM gene encoding VU-1 CaM (section 1.3, page 36) was used to prepare the pre-designed CaM mutants. The objectives of this study were threefold:

1). **To introduce a strong fluorescent label into VU-1 CaM by F92W mutation;**

2). **To create a CaM model inactivated at site IV with respect to calcium binding by D133E mutation;**

3). **To examine the effect of the nature of the chelating residues on the calcium affinity of site III in the F92W/D133E VU-1 CaM model using CaM mutants.**

The studies which cover the first two objectives are presented in Chapter 2, and the studies which cover the third objective are presented in Chapter 3 in this thesis.

CHAPTER 2

INTRODUCING A FLUORESCENT LABEL INTO SITE III OF VU-1 CALMODULIN AND CREATING A CALMODULIN MUTANT INACTIVATED AT SITE IV WITH RESPECT TO CALCIUM BINDING CAPACITY

2.1. MATERIALS

Plasmid pVUCH-1 and *E. coli* K12 UT481 strain were provided by Dr. T. Lukas at Northwestern University, Chicago, USA. Restriction endonucleases, *Aat* II, *Bam* HI, *Eco* RI, *Hin* dIII, *Hpa* I, *Stu* I, and *Xma* III, alkaline phosphatase, polynucleotide kinase, T4 DNA ligase, DNase I, RNase A, lysozyme, 1,4-dithiothreitol (DTT), and DNA molecular weight marker (1 kb DNA) were purchased from Boehringer Mannheim, Germany. Calcium chloride standard solution (0.1 M) was obtained from Orion Research Inc., Boston, U.S.A. Bovine brain calmodulin, bovine heart 3',5'-cyclic nucleotide 5'-phosphodiesterase (PDE), lipid-free bovine serum albumin, adenosine 3',5'-cyclic monophosphate (cAMP), snake venom (*Crotalus atrox*), protein low range molecular weight marker, Commassie Brilliant Blue R250, phenylmethylsulfonylfluoride (PMSF), ampicillin, and agarose were obtained from Sigma Co., Missouri, USA. Acrylamide, N', N'-methylene-bisacrylamide and AG1-X2 anion exchange resin (200-400 mesh, hydroxide form) were obtained from Bio-Rad Laboratories, Hercules, California, USA. Agar, LB broth base, M9 minimal salts, NZCYM broth base, S.O.C. culture medium, and tris(hydroxymethyl)aminomethane (Tris) were purchased from Gibco BRL Life Technologies, Inc., Maryland, U.S.A.. Isopropyl-β-D-thioglactoside (IPTG) was purchased from Calbiochem, San Diego, U.S.A.. Petri dishes (100×15 mm) and Falcon culture tubes (2059, 17×100 mm polypropylene tubes) were obtained from Fisher Scientific Co., Ottawa, Canada. Phenyl Sepharose was obtained from Pharmacia Biotech Inc.,

Uppsala, Sweden. GeneClean II kit was obtained from BIO 101 Inc., Vista, California, U.S.A.. [2,8-^{3}H]cAMP and the scintillation fluid Cytoscint™ were obtained from ICN, California, U.S.A. Glass test tubes (12×75 mm) were purchased from VWR Scientific, Toronto, Canada. All other chemicals were obtained from either Sigma Co., Fisher Scientific Co., or BDH Inc..

Seven oligodeoxynucleotides (oligos), primer 1, aatII-1, aatII-2, hind-1, hpaI-1, stuI-1, and xma-1, were synthesized on a Perkin Elmer Applied Biosystems 391 DNA synthesizer in the Nucleic Acid and Protein Service (NAPS) Unit at the University of British Columbia. The sequences of the oligos are presented on pages xviii-xix.

PDE: 0.076 units/mg protein in the absence of CaM; 0.25 units/mg protein or 0.18 units/mg solid in the presence of CaM. One unit of this enzyme will hydrolyze 1.0 μmole of cAMP to 5'-AMP per min at pH 7.5 at 30°.

2.2. METHODS

2.2.1. Preparation of competent *E. coli* cells

Competent *E. coli* cells were prepared freshly according to the protocol from Sambrook *et al.* (1989). Briefly, an M9 agar plate (1% M9 salts; 1.5% agar; 25-30 mL/plate) was inoculated with an *E. coli* K12 UT481 glycerol culture and incubated at 37° for 2 days. A 3 mL LB broth (2% LB broth base) was inoculated with a single colony from the M9 plate and incubated overnight at 37° with shaking (260 rpm). A 50 mL LB broth was then inoculated with 1 mL of the overnight 3 mL culture and was incubated at 37° with shaking (260 rpm) until the optical density at 600 nm (OD_{600}) reached approximately 0.4. The 50 mL culture was then incubated on ice for 5 min and centrifuged at 3000 rpm for 10 min at 4°.

The cell pellet was re-suspended in approximately 15 mL of ice-cold $CaCl_2$ buffer containing 100 mM $CaCl_2$, 10 mM Tris-HCl, pH 8.0. The suspension was incubated on ice for 30 min and centrifuged again at 3000 rpm for 10 min at 4°. The cell pellet was gently re-suspended in approximately 5 mL of the $CaCl_2$ buffer. The competent cells were ready for transformation.

2.2.2. Transformation of *E. coli* cells with pVUCH-1

The VU-1 CaM expression vector, pVUCH-1, was introduced into *E. coli* cells using Ca^{2+}/heat shock method (Sambrook *et al.*, 1989). Competent *E. coli* cells (100 μl) were added to a pre-cooled (on ice) Falcon culture tube. Five microliters of plasmid pVUCH-1 (50 ng/μl) were added to the competent cells. The mixture was incubated for 30 min on ice, 60 sec in a 42° water bath, and then 2 min on ice followed by addition of 0.9 mL of S.O.C. culture medium. The mixture was incubated at 37° for 1-2 hrs with shaking (260 rpm) and diluted with S.O.C. culture medium (1:10 and 1:100 dilution, respectively). Then, the diluted cultures were plated separately on NZCYM/ampicillin selecting plates (2.2% NZCYM broth base, 100 μg/mL ampicillin) at 100 μl/plate. The plates were incubated overnight at 37°. A well-separated single colony on one of the plates was picked up with an inoculation needle for plasmid isolation.

2.2.3. Isolation of plasmid pVUCH-1

The method used here is a modification of the alkaline mini-preparation of plasmid (Sambrook *et al.*, 1989). A single colony on the NZCYM plate (see section 2.2.2) was picked up and used to inoculate a 3 mL LB broth containing ampicillin 100 μg/mL. The

inoculated LB broth was incubated overnight at 37° with shaking (260 rpm), and 1.5 mL of the overnight culture was transferred to a microcentrifuge tube and spun for 1 min in a microcentrifuge at 14000 rpm. The cell pellet was re-suspended by adding 200 μl of GTE buffer containing 50 mM glucose, 10 mM EDTA, 25 mM Tris-HCl, pH 8.0. The suspension was incubated for 5 min on ice followed by addition of 300 μl of 0.2 N NaOH/1% SDS (freshly made) and incubated on ice for another 5 min. Three hundred microliters of potassium acetate buffer containing 3 M potassium acetate, pH 4.8 with glacial acetic acid, were added, and the tube was inverted 5 times by hand followed by incubation on ice for 5 min. The mixture was spun for 10 min at 14000 rpm at room temperature, and the supernatant was transferred to a new microcentrifuge tube. RNase A was added to the supernatant to a final concentration of 20 μg/mL followed by incubation at 37° for at least 20 min. Then, the mixture was extracted twice with 400 μl of chloroform each time by vortexing 30 sec and spinning at 14000 rpm for 2 min to separate the organic and the aqueous phases. The plasmid DNA in the aqueous phase was precipitated by adding an equal volume of isopropanol, incubating on ice for 10 min and spinning at 14000 rpm at room temperature for 15 min. The plasmid DNA pellet was washed once with 1 mL of 70% ice-cold ethanol, dissolved in 30-50 μl of sterile water, and stored at -20° for later use.

2.2.4. Quantitation of plasmid DNA

Plasmid DNA in water was quantitated by UV-spectrophotometry. A microcuvette with a minimum volume of 50 μl was used for absorbance (A_{260}) measurement. The concentration was calculated using the following equation (Sambrook *et al.*, 1989):

$$C(mg / L) = 50 \times A_{260}$$

2.2.5. Sequencing the CaM gene in pVUCH-1

The plasmid pVUCH-1 isolated in this study as described in section 2.2.3 was verified by DNA sequencing as follows: the plasmid was analyzed by automated DNA sequencing using Taq DyeDeoxy™ Terminator Cycle sequencing chemistry on a Perkin Elmer Applied Biosystems (ABI) 373A DNA sequencer in the NAPS Unit at the University of British Columbia. The 18 mer oligodeoxynucleotide, primer 1, corresponding to the nucleotide positions 50 to 67 in the coding strand of the CaM gene, was used as the primer for DNA sequencing. The double-stranded circular plasmid DNA for sequencing was prepared using the alkaline-lysis method as described in section 2.2.3. and further purified by polyethylene glycol 8000 (PEG) precipitation described as follows: plasmid (20 μg) was dissolved in 32 μl of sterile water and precipitated by 8 μl of 4 M NaCl and 40 μl of 13% PEG on ice for 1 h. The DNA was recovered by spinning at 14000 rpm in a microcentrifuge for 15 min at 4 °C, and the DNA pellet was washed once with 1 mL of ice-cold 70% ethanol and dissolved in sterile water to give a concentration of approximately 0.5 to 1 μg/μl.

2.2.6. Construction of F92W CaM expression vector pf92w

A schematic construction diagram of the F92W CaM expression vector, pf92w, is shown in Figure 12, and the procedure is described in detail as follows:

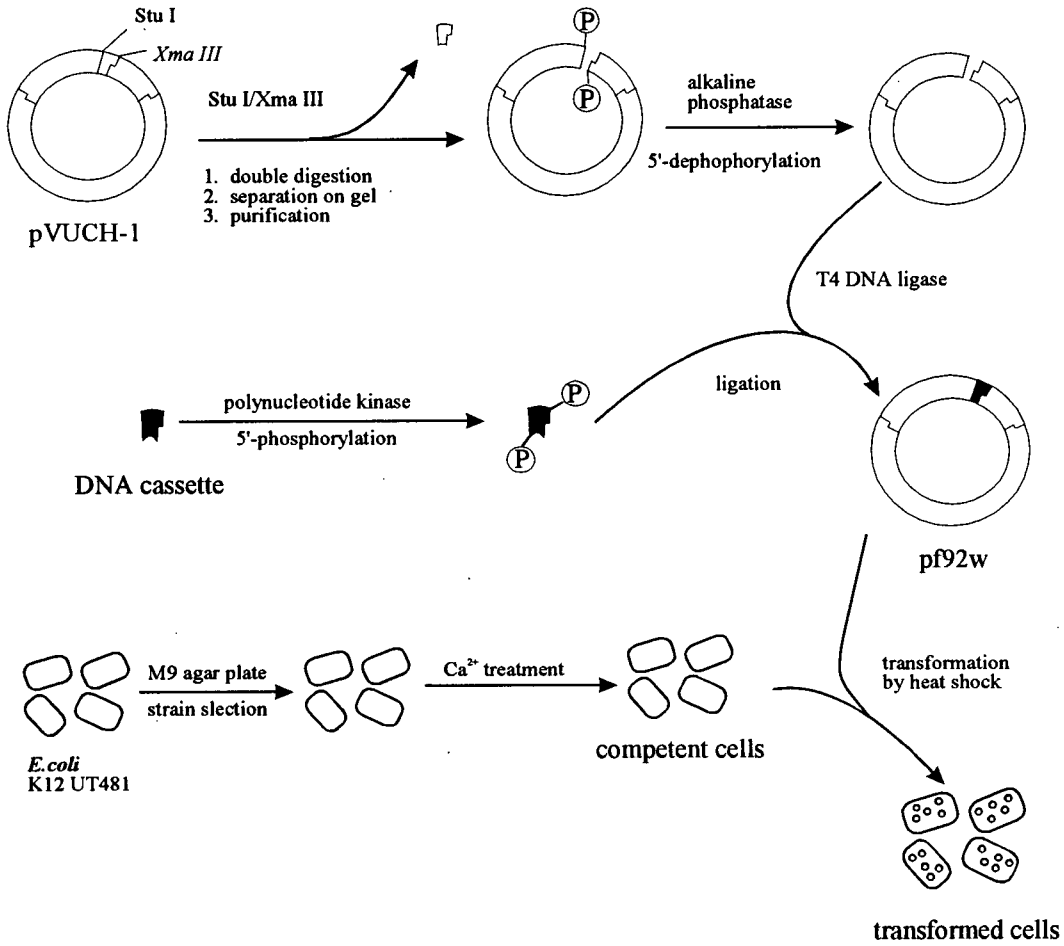

= 3'-GGAAGGCACAA**AAG**CTGTTTCTGCCATTGCCAAAGTAGAGCCGG-5'
5'-CCTTCCGTGTT**TTC**GACAAAGACGGTAACGGTTTCATCTC-3'
Phe

= 3'-GGAAGGCACAA**ACC**CTGTTTCTGCCATTGCCAAAGTAGAGCCGG-5'
5'-CCTTCCGTGTT**TGG**GACAAAGACGGTAACGGTTTCATCTC-3'
Trp

Figure 12. Schematic diagram for construction of pf92w. Plasmid pf92w was constructed from pVUCH-1 using site specific, cassette mediated mutagenesis. Codons for Phe92 and Trp92 are bold and boxed.

2.2.6.1. *Stu* I/*Xma* III digestion of pVUCH-1

Fifteen micrograms of pVUCH-1 were digested with 40 units of *Stu* I and 40 units of *Xma* III at 37° for 3 hrs in a buffer containing 100 mM NaCl, 5 mM $MgCl_2$, 1 mM 2-mercaptoethanol, 10 mM Tris-HCl, pH 8.0 (at 37°) in a total volume of 100 μl. Twenty microliters of 6× Stop/Load solution (50% glycerol, 100 mM EDTA, 1% SDS, 0.25% bromophenol blue) were added to the digestion mixture to stop the reaction.

2.2.6.2. Separation of digested fragments on agarose gel

Agarose gel (0.8%) was prepared using the protocol from Sambrook *et al.* (1989). Briefly, 0.62 g agarose was added to 77 mL of TAE buffer (40 mM Tris-acetate, 1 mM EDTA, pH 8.2-8.4), and the mixture was incubated in a microwave oven for 1-2 min. The melted agarose was cooled down to approximately 60° and poured into the electrophoresis tank with a size of 11x14 cm^2. The *Stu* I/*Xma* III double digestion mixture (approximately 120 μl from section 2.2.6.1) was loaded on the solidified agarose gel. The electrophoresis was carried out for approximately 3 hrs under constant voltage (100 volts) in a Horizon™ 11.14 electrophoresis apparatus from Gibcol BRL Life Technologies Inc., Maryland, USA. The TAE buffer was used as the electrophoresis buffer. The gel was stained in 1 μg/mL ethidium bromide solution for 15 min and destained in deionized water with 5 quick changes. DNA bands were visualized on a UV-translluminator (314 nm). The band at the position of 3 kb was excised for purification of the large fragment.

2.2.6.3. Purification of double-cut pVUCH-1 from agarose gel

The excised band from the agarose gel in section 2.2.6.2 was further cut into small pieces (approximately 2×2×2 mm^3), and the large fragment of the double-cut plasmid was purified using a GeneClean II Kit as described in the protocol provided by the manufacturer. The chopped gel slices were added to NaI (6 M) solution at 3 μl/μg gel and incubated at 55° for 5 min to dissolve the agarose. Glassmilk suspension was added to the mixture (5 μl for 5 μg or less of DNA and additional 1 μl for each 0.5 μg additional DNA above 5 μg) and incubated on ice for 5 min. The mixture was spun in a microcentrifuge at 14000 rpm for 5 sec to pellet the silica matrix with the bound DNA. The pellet was washed 3 times with NEW washing buffer provided by the manufacturer, 700 μl each time. Then, 5 μl of sterile water was added to the washed pellet, and the pellet was mixed by pipeting up and down several times. The mixture was spun in a microcentrifuge at 14,000 rpm for 1 min, and the supernatant was transferred to a new microcentrifuge tube for later use.

2.2.6.4. Dephosphorylation of double-cut pVUCH-1

The purified large fragment of *Stu* I/*Xma* III digested pVUCH-1 from the previous section was dephosphorylated at the 5'-end of each DNA strand. The reaction was carried out at 37° for 1 h in a buffer containing 0.1 mM EDTA, 0.5 units of alkaline phosphatase, 50 mM Tris-HCl, pH 8.5 in a total volume of 70 μl. The reaction was stopped by incubating at 65° for 10 min in the presence of 20 mM EGTA (pH 8.0 with NaOH). The dephosphorylated double-cut pVUCH-1 fragment was purified using a GeneClean II Kit as described in section 2.2.6.3. The amount of dephosphorylated double-cut DNA fragment was determined by semi-quantitative agarose gel electrophoresis as described in the following section.

2.2.6.5. Semi-quantitative agarose gel electrophoresis

Preparation of linearized pVUCH-1: Fifty micrograms of pVUCH-1 were incubated with 400 units *Eco* RI at 37° for 2 hrs in a buffer containing 100 mM NaCl, 10 mM $MgCl_2$, 1 mM dithioerythritol, 50 mM Tris-HCl, pH 7.5 in a total volume of 130 μl. The linearized plasmid was purified by extracting twice with 130 μl of chloroform. The plasmid in the aqueous phase was precipitated overnight at -20° with 2.5 volumes of absolute ethanol and 1/10 volume of 3 M sodium acetate (pH 5.2 with acetic acid). The plasmid pellet was washed once with 1 mL of 70% ice-cold ethanol and dissolved in 100 μl of sterile water. The purified linearized plasmid was then diluted to 0.5, 0.25, 0.125, 0.0625, and 0.03125 μg/μl with sterile water as standard solutions.

An agarose gel (0.8%) was prepared as described in section 2.2.6.2. One microliter of each linearized plasmid standard solution or 1 μl of the purified dephosphorylated double-cut pVUCH-1 fragment was loaded in each lane on the gel. The gel was electrophoresed and stained as described in section 2.2.6.2. The amount of the purified double-cut pVUCH-1 fragment in 1 μl was estimated by comparing the fluorescence intensity of its band to that of the linearized plasmid bands of known-amount.

2.2.6.6. Phosphorylation of DNA cassette

Oligos, stuI-1 and xma-1, were dissolved in sterile water and quantitated by UV-spectrophotometry as described in section 2.2.4. The concentration of each oligo was calculated using the following equation (Sambrook *et al.*, 1989):

$$C(mg / L) = 40 \times A_{260}$$

or

$$C(mM) = \frac{40 \times A_{260}}{MW}$$

The molecular weight (MW) of an oligo is estimated using the following equation:

$$MW(Dalton) = 330 \times Base\#$$

The DNA cassette containing the codon TGG for Trp at position 92 in VU-1 CaM was prepared from oligos stuI-1 and xma-1. Phosphorylation of stuI-1 and xma-1 oligos was carried out at 37° for 1 h in a reaction mixture containing 1 nmole of each oligo, 2 mM ATP, 40 units T4 polynucleotide kinase, 10 mM $MgCl_2$, 0.1 mM EDTA, 0.5 mM DTT, 0.1 mM spermidine, 50 mM Tris-HCl, pH 8.2 (at 25°), in a total volume of 100 μl. The reaction was terminated by incubating at 65° for 20 min. The reaction mixture was stored at -20° until ligation.

2.2.6.7. Ligation of DNA cassette with double-cut pVUCH-1

The DNA cassette was ligated with the *Stu* I/*Xma* III double-cut pVUCH-1 fragment by T4 DNA ligase. The ligation was carried out at room temperature for 3 hrs in a reaction mixture containing 0.065 pmoles of the double-cut, dephosphorylated pVUCH-1 fragment, 0.2 pmoles of the phosphorylated DNA cassette, 2 units T4 DNA ligase, 5 mM $MgCl_2$, 1 mM dithioerythritol, 1 mM ATP, 66 mM Tris-HCl, pH 7.5, in a total volume of 20 μl.

2.2.6.8. Introduction of ligated plasmid DNA into *E. coli* cells

The ligated plasmid DNA was introduced into *E. coli* UT K12 UT481 cells by transforming the competent *E. coli* cells with the ligation mixture from the previous section.

Competent cells were prepared as described in section 2.2.1. Five microliters of the ligation mixture from section 2.2.6.7 were used to transform 100 μl of the competent cells, and the transformed bacterial cells were plated on the NZCYM/ampicillin selecting plates as described in section 2.2.2.

2.2.6.9. Identification of the pf92w clone

Restriction enzyme mapping: Six colonies from the NZCYM/ampicillin selecting plates from the previous section were picked up for mini-preparation of plasmid DNA as described in section 2.2.3. All the plasmids were digested with *Stu* I and *Xma* III, respectively, at 37° for 2 hrs in a reaction mixture containing 2 μg of each plasmid, 10 units of either *Stu* I or *Xma* III, 100 mM NaCl, 5 mM $MgCl_2$, 1 mM 2-mercaptoethanol, 10 mM Tris-HCl, pH 8.0 (at 37°), in a total volume of 20 μl. Ten microliters of each digestion mixture plus 2 μl of the Stop/Load solution (section 2.2.6.1) was loaded on a 0.8% agarose gel. The gel was electrophoresed and stained as described in section 2.2.6.2.

A plasmid that was cut by both *Stu* I and *Xma* III, respectively, was further digested with *Eco* RI, *Bam* HI, *Hin* dIII, *Stu* I and *Xma* III, respectively. Digestion was carried out at 37 °C for 2 hrs in a reaction mixture containing 2 μg of pVUCH-1, 10 units of either *Bam* HI, *Hin* dIII, *Stu* I or *Xma* III, 100 mM NaCl, 5 mM $MgCl_2$, 1 mM 2-mercaptoethanol, 10 mM Tris-HCl, pH 8.0 (at 37°), in a total volume of 20 μl. Digestion with *Eco* RI was carried out in a reaction mixture containing 2 μg of the plasmid, 10 units *Eco* RI, 100 mM NaCl, 10 mM $MgCl_2$, 1 mM dithioerythritol, 50 mM Tris-HCl, pH 7.5 (at 37°), in a total volume of 20 μl. Ten microliters of each digestion mixture plus 2 μl of the Stop/Load solution were loaded on a 0.8% agarose gel. The gel was run and stained as described in section 2.2.6.2.

DNA bands were visualized on a UV-translluminator (256 nm), and a photograph of the gel was taken under the UV light.

DNA sequencing: After restriction enzyme mapping, the plasmid was further analyzed by automated DNA sequencing as described in section 2.2.5.

2.2.6.10. Storing the positive clones in glycerol culture

The identified positive clones were maintained in 15% glycerol LB cultures at -70°. *E. coli* cells that carry the pVUCH-1 plasmid or the pf92w plasmid, were cultured at 37° for 8-10 hrs with shaking (180 rpm) in 30 mL LB broth in the presence of 100 μg/mL ampicillin. Sterile glycerol was added to the LB/ampicillin culture to a concentration of 15 %. Aliquots of 0.5 mL of the glycerol culture were dispensed into 2 mL cryogenic microcentrifuge tubes and stored at -70°.

2.2.7. Construction of F92W/D133E CaM expression vector pd133e

The F92W/D133E CaM expression vector, pd133e, was constructed from the plasmid pf92w and the DNA cassette containing the codon GAG for Glu at position 133 in F92W CaM molecule. A schematic construction diagram of pd133e is shown in Figure 13. The DNA cassette was prepared from oligoes hind-1, aatII-1, aatII-2 and hpaI-1. One nanomole of each oligo was added together and phosphorylated with 80 units of polynucleotide kinase as described in section 2.2.6.6. Fifteen micrograms of pf92w were double digested with 80 units of *Hind* III and 42 units of *Hpa* I at 37° for 1 h in a buffer containing 66 mM potassium acetate, 10 mM magnesium acetate, 0.5 mM DDT, 33 mM Tris-acetate, pH 7.5 (at 37°) , in a total volume of 100 μl. Twenty microliters of the Stop/Load solution was added to the

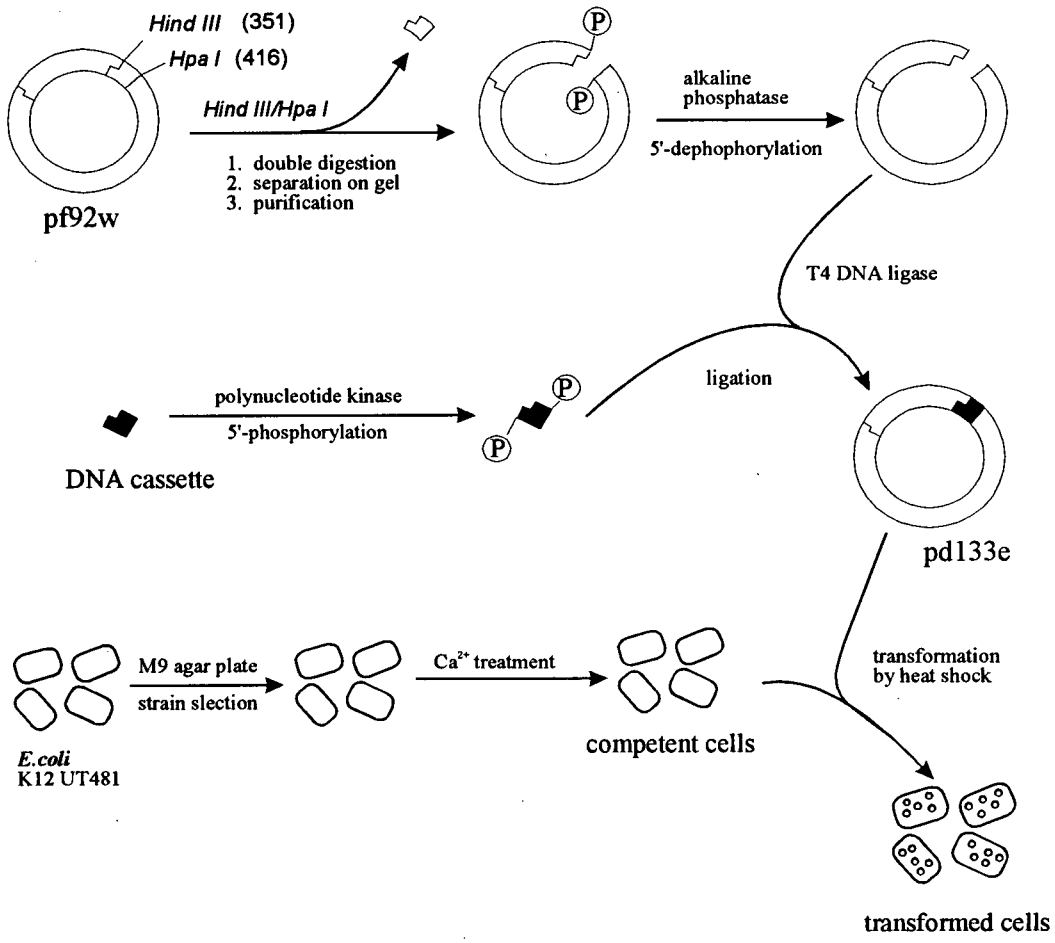

= 3'- ATGACTGCTTCTTCAACTGCTTTACTAAGCGCTTCGAC-5'
5'-AGCTTACTGACGAAGAAGTTGACGAAATGATTCGCGAAGCTGACGT-3'

3'-TGCAGCTACCA**CTG**CCGGTCCAA-5'
5'- CGATGGT**GAC**GGCCAGGTT-3'

= 3'- ATGACTGCTTCTTCAACTGCTTTACTAAGCGCTTCGAC-5'
5'-AGCTTACTGACGAAGAAGTTGACGAAATGATTCGCGAAGCTGACGT-3'

3'-TGCAGCTACCA**CTC**CCGGTCCAA-5'
5'- CGATGGT**GAG**GGCCAGGTT-3'

Figure 13. Schematic diagram for construction of pd133e. Plasmid pd133e was constructed from pf92w using site specific, cassette mediated mutagenesis. Codons for Asp133 and Glu133 are bold and boxed.

digestion mixture. The large fragment of the double-digested pf92w was separated on a 0.8 % agarose gel, purified using a GeneClean II kit, dephosphorylated with alkaline phosphatase, and ligated with the phosphorylated DNA cassette as described in sections 2.2.6.1, 2.2.6.2, 2.2.6.3, 2.2.6.4, 2.2.6.5, and 2.2.6.7. The ligated plasmid was introduced into competent *E. coli* K12 UT 481 cells as described in section 2.2.2. The positive clone of pd133e was identified by restriction enzyme mapping and automated DNA sequencing as follows:

Restriction enzyme mapping: A plasmid was isolated from a single colony growing on the LB/ampicillin agar plate as described in section 2.2.3. A half microgram of the plasmid was digested with 6 units of *Aat* II, 6 units of *Hpa* I, and 5 units of *Hin* dIII, respectively, at 37° for 1 h in the buffer used for *Hin* dIII /*Hpa* I digestion of pf92w in this section. The total volume of the reaction mixture was 20 μl. Ten microliters of each digestion mixture plus 2 μl of the Stop/Load solution were loaded on a 0.8% agarose gel. The gel was run and stained as described in section 2.2.6.2. DNA bands were visualized on a UV-translluminator (256 nm), and a photograph of the gel was taken under the UV light.

DNA sequencing: The sequence of the mutant gene in the plasmid was analyzed by automated DNA sequencing as described in section 2.2.5.

The pd133e clone was maintained in a 15% glycerol culture at -70° as described in section 2.2.6.10.

2.2.8. Expression of VU-1, F92W, and F92W/D133E calmodulins

All recombinant proteins were purified from 20 L cultures of positive clones by a modification of the method of Roberts, *et al.* (1985). An NZCYM/ampicillin (100 μg/mL)

agar plate was inoculated with either pVUCH-1 or pf92w or pd133e glycerol culture. The inoculated plate was incubated overnight at 37°. A well-separated single colony was picked up to inoculate a 30 mL NZCYM/ampicillin medium followed by incubation at 37° for 8-10 hrs with shaking (180 rpm). A 500 mL NZCYM/ampicillin medium was inoculated with 2-3 mL of the 30 mL culture and incubated at 37° overnight. Then, a 20 liter NZCYM/ampicillin medium was inoculated with 200-300 mL of the 500 mL culture and incubated at 37° in a 20 liter Chemap® fermentor (Volketswil, Switzerland) at an air flow rate of 10 liter/min with 10 % oxygen and agitation speed from 50 to 400 rpm. IPTG was added to the 20 L culture to a final concentration of 1 mM when OD_{600} reached 0.2. A second batch of ampicillin was added to the culture to 100 μg/mL when the culture was grown for 7-9 hrs, and the growth was continued until 20 to 22 hrs. *E. coli* cells were harvested using a Sharples centrifuge.

2.2.9. Purification of VU-1, F92W, and F92W/D133E calmodulins

The harvested *E. coli* cells were lysed with lysozyme on ice for 2-3 hrs in a buffer containing 1 mg lysozyme/g cell, 2 mM EDTA, 1 mM DTT, 50 mM Tris-HCl, pH 8.0, in a total volume of 200-300 mL. Ultra-sonication with 4×30 sec bursts on a Vibra Cell sonicator (Fisher Scientific Inc.) was carried out to further break the cells. DNase I and $MgCl_2$ were added to the lysate to final concentrations of 100 U/mL and 3 mM, respectively, and the mixture was incubated on ice for 30 min. The mixture was spun in a Beckman J2-21 centrifuge with a JA-17 rotor at 17,000 rpm (39812×g) at 4° for 30 min. The supernatant was transferred to a 300 mL glass beaker, and PMSF was added to the supernatant to a final concentration of 0.2 mM. The mixture was heated to 90-95° in a microwave oven followed by quick cooling in an ice/salt slurry. The mixture was spun again at 17,000 rpm at 4° for 30

min, and the supernatant was dialyzed at 4° for 3-4 hrs against 4 L of a buffer containing 0.5 mM EDTA, 0.5 mM DTT, 50 mM Tris-HCl, pH 7.5. $CaCl_2$ was added to the dialysate to a final concentration of 15 mM, and the calcified solution was incubated at 4° overnight. The expressed protein was purified from the calcified solution by affinity chromatography on a phenyl-Sepharose column with a bed volume of 10 mL described as follows:

For purification of VU-1 and F92W calmodulins, a phenyl-Sepharose column was first equilibrated with 50 mL washing buffer I containing 1 mM $CaCl_2$, 1 mM DTT, 50 mM Tris-HCl, pH 7.5, and the flow rate was set at 1 mL/min. The calcified solution was spun at 17,000 rpm for 30 min at 4°, and the supernatant was applied to the column at 15-20 mL/run. For each run, the column was washed with 50 mL of washing buffer I and 30 mL of washing buffer II (0.5 M NaCl, 1 mM $CaCl_2$, 1 mM DTT, 50 mM Tris-HCl, pH 7.5). VU-1 or F92W CaM was eluted from the column with 10 mL of the elution buffer containing 1 mM EGTA, 1 mM DTT, 50 mM Tris-HCl, pH 7.5. The eluant was dialyzed at 4° against 4 L of deionized water with 5-6 changes. The dialysate was lyophilized, and the lyophilized protein was stored at -20°.

For purification of F92W/D133E CaM, the affinity chromatography procedure was the same as that described for VU-1 CaM in the previous paragraph except that the concentration of $CaCl_2$ in the washing buffers I and II was 5 mM and the concentration of EGTA in the elution buffer was also 5 mM.

2.2.10. Preparation of the CaM-binding peptide W4I-M13

A 26 residue peptide analog (NH_2-KRRIKKNFIAVSAANRFKKISSSGAL-COOH) corresponding to the CaM-binding site of the skeletal muscle myosin light chain kinase (Ikura

et al., 1990) was synthesized on a 432A peptide synthesizer from Applied Biosystems/Perkin Elmer. The Trp residue in position 4 of the natural peptide fragment was replaced by Ile, a non-fluorescent residue, to eliminate interference with the Trp fluorescence of the Trp-labeled CaM. This peptide was purified by preparative reverse-phase HPLC on a C18 column using 0.1% TFA-acetonitrile (A)/0.1% TFA-water(B) as the mobile phase. The column was washed with a linear gradient from 0:100 (A:B) to 60:40 (A:B) over 40 min. The major peak monitored at 214 nm was collected, dialyzed against nanopure water (Barnstead Nanopure II) and lyophilized. The identity of W4I-M13 peptide was verified by amino acid composition analysis and mass spectrometry.

2.2.11. SDS-polyacrylamide gel electrophoresis of calmodulins

SDS-polyacrylamide gel electrophoresis was carried out using the buffer system of LaemmLi (1970). The discontinuous gel (stacking gel and resolving gel) and all buffers were prepared according to the protocols in Molecular Cloning (Sambrook *et al.*, 1989). The resolving gel was prepared by dissolving an acrylamide:bisacrylamide (29:1) mixture at 12% (g/mL) in a buffer containing 5% glycerol, 1% SDS, 375 mM Tris-HCl, pH 8.8. The stacking gel was prepared by dissolving an acrylamide:bisacrylamide (29:1) mixture at 5% (g/mL) in a buffer containing 1% SDS, 125 mM Tris-HCl, pH 6.8. Polymerization of the gels was initiated by adding $(NH_4)_2S_2O_8$ at 0.1% and a trace amount of TEMED (4 μl to 10 mL resolving gel mixture and 4 mL stacking gel mixture, respectively). Protein samples were prepared at 0.5-5 mg/mL in a buffer containing 2% SDS, 100 mM DTT, 12% glycerol, 0.1% bromophenol blue, 1 mM $CaCl_2$ or 1 mM EGTA, 50 mM Tris-HCl, pH 6.8. Fifteen microliters of each protein sample were loaded on the polymerized SDS-polyacrylamide mini-

gel (7×8 cm^2). The electrophoresis buffer (25 mM Tris base, 250 mM glycine, 1% SDS, pH 8.3) was used to run the gel in a Bio-Rad Mini-PROTEIN® II electrophoresis system under constant voltage: 60 volts for the stacking gel and 100 volts for the resolving gel. The gel was stained for 2 hrs with 0.25% Coomassie Brilliant Blue in methanol:water:acetic acid (40:50:10) and destained for 1 h in methanol:water:acetic acid (30:60:10). The stained gel was dried in a gel drier (model SE 540 from Hoefer Scientific Instruments, California, U.S.A.).

2.2.12. Amino acid composition analysis and determination of the extinction coefficient of F92W CaM

Each recombinant CaM was prepared in the EGTA buffer containing 100 mM KCl, 1 mM EGTA, 50 mM MOPS, pH 7.2 with NaOH. The amino acid composition analysis of each recombinant CaM was performed using a pre-column phenylisothiocyanate derivatization HPLC method on a 420A derivatizer, a 130A HPLC separation system and a 920A data analysis module from Applied Biosystems/Perkin Elmer. This work was done in the NAPS Laboratory at the University of British Columbia.

The extinction coefficient of F92W CaM was calculated as follows:

$$\mathrm{E}(cm^{-1} \cdot M^{-1}) = \frac{A_{280}}{C(mole / L)}$$

where C is the protein concentration determined by amino acid composition analysis, and A_{280} is the absorbance of the same protein solution at 280 nm measured on a Hewlett Packard 8152A Diode Array spectrophotometer.

2.2.13. Molecular weight determination by mass spectrometry

The molecular weight of each purified recombinant CaM and the CaM-binding peptide W4I-M13 was determined by electrospray mass spectrometry on a VG Quattro Quadrupol mass spectrometer (Fisons, Altrincham, England). Samples were prepared in 0.1 % formic acid in methanol : water (1:1).

2.2.14. Far-UV circular dichroism spectroscopy

Far-UV circular dichroism (CD) spectra [ellipticity (millidegree) as a function of wavelength] of VU-1, F92W, and F92W/D133E calmodulins were recorded on a Jasco J720 spectropolarimeter at ambient temperature. Each purified protein was dissolved in the EGTA buffer (100 mM KCl, 1 mM EGTA, 50 mM MOPS, pH 7.20) at concentrations of 15-30 μM, and 0.9 mL of the protein solution was used for each measurement. The light path of the quartz cuvette was 1 mm, and the maximal capacity was 1 mL. The protein concentrations were determined by amino acid composition analysis. The water used for preparing the buffers was nanopure water (Barnstead Nanopure II) treated with Chelex 100 resin (BioRad). For each protein sample, the ellipticity measurements were performed before and after addition of calcium chloride solution to saturation. Data were normalized by the molar concentration of the protein samples and the number of residues in the protein using the following equation:

$$[\theta] = \frac{mDeg \times 10^6}{residue\# \times C \times 1mm}$$

where [θ] is the molar ellipticity expressed as deg · cm^2/dmol; mDeg is the observed ellipticity value at a specific wavelength, and residue # is the number of residues in each protein; C is the μM concentration of the protein, and 1 mm is the light path of the cuvette.

2.2.15. Fluorescence spectroscopy and calcium titration

Fluorescence spectra were recorded on a Shimadzu RF540 Spectrofluorophotometer at ambient temperature. Spectra and titrations were performed on samples (2 mL) at concentrations of 40 μM for the VU-1 CaM and 15 μM for the F92W and F92W/D133E CaM mutants, in the same buffer used for the CD spectral measurements. The protein concentrations were determined by amino acid composition analysis. The emission spectra of VU-1 in the absence and presence of calcium were recorded at the excitation wavelength of 278 nm, and the emission spectra of F92W and F92W/D133E calmodulins were recorded at the excitation wavelength of 282 nm. Calcium titration of VU-1 CaM was monitored by following the tyrosine fluorescence at the excitation wavelength of 278 nm and the emission wavelength of 309 nm. The slit width for both excitation and emission was 5 nm. Calcium titrations of F92W and F92W/D133E calmodulins were monitored by following the tryptophan fluorescence at the excitation wavelength of 282 nm and the emission wavelength of 340 nm. The slit width for excitation was 5 nm and that for emission was 2 nm.

2.2.16. Effect of W4I-M13 CaM-binding peptide on calcium affinity of calmodulins.

Fluorescence emission spectral measurements and calcium titrations of VU-1, F92W and F92W/D133E calmodulins were carried out in the presence of the CaM-binding peptide,

W4I-M13 as described in section 2. 2.15. The protein concentrations were 30 μM for VU-1 and 10 μM for both F92W and F92W/D133E mutants, respectively, in the same buffer used for CD spectral measurements. Protein concentrations were determined by UV-spectrophotometry using the extinction coefficients: E_{278} = 1500 ($M^{-1}\cdot cm^{-1}$) for VU-1 CaM from Klee and Vanaman (1982) and E_{280} = 8223 ($M^{-1}\cdot cm^{-1}$) for F92W and F92W/D133E calmodulins determined in this study as described in section 2.2.12. The peptide concentration was determined by weight. The protein to peptide ratios were 1:1.5, 1:4 and 1:4 for VU-1, F92W and F92W/D133E calmodulins, respectively.

2.2.17. Calcium titration data analysis

Free Ca^{2+} concentrations were calculated from total Ca^{2+} concentrations in the EGTA buffer using the EQCAL program from Biosoft. The logarithmic binding constants ($Log_{10}K$) for proton and calcium ion to EGTA, used to calculate free calcium concentrations, were as follows: H^+ to $EGTA^{4-}$, 9.53; H^+ to $HEGTA^{3-}$, 8.88; H^+ to H_2EGTA^{2-}, 2.65; H^+ to H_3EGTA^-, 2.0; Ca^{2+} to $EGTA^{4-}$, 10.89; Ca^{2+} to $HEGTA^{3-}$, 5.30. Each set of the fluorescence titration data was fitted to the one-site, two-site, three-site and four-site models (equations 1 to 4, respectively) (Fletcher *et al.*, 1970) using the programs SigmaPlot® for Windows and SlideWrite® for Windows.

$$f = \frac{[Ca^{2+}]^n}{K^n + [Ca^{2+}]^n} \quad \text{(1)}$$

$$f = f_1 \cdot \frac{[Ca^{2+}]^{n_1}}{K_1^{n_1} + [Ca^{2+}]^{n_1}} + (1 - f_1) \cdot \frac{[Ca^{2+}]^{n_2}}{K_2^{n_2} + [Ca^{2+}]^{n_2}} \quad \text{(2)}$$

$$f = f_1 \cdot \frac{[Ca^{2+}]}{K_1 + [Ca^{2+}]} + f_2 \cdot \frac{[Ca^{2+}]}{K_2 + [Ca^{2+}]} + (1 - f_1 - f_2) \cdot \frac{[Ca^{2+}]}{K_3 + [Ca^{2+}]} \quad \text{.....} (3)$$

$$f = f_1 \cdot \frac{[Ca^{2+}]}{K_1 + [Ca^{2+}]} + f_2 \cdot \frac{[Ca^{2+}]}{K_2 + [Ca^{2+}]} + f_3 \cdot \frac{[Ca^{2+}]}{K_3 + [Ca^{2+}]} + (1 - f_1 - f_2 - f_3) \cdot \frac{[Ca^{2+}]}{K_4 + [Ca^{2+}]}$$

..... (4)

where f is the fraction of the fluorescence intensity change expressed as the fluorescence intensity change at a given free Ca^{2+} concentration from that of apo-CaM over the maximal change during the titration. K is the apparent calcium dissociation constant, and n is the slope factor of the titration curve. Subscripts refer to the potential calcium binding sites.

The Hill coefficient (n_H) was obtained from the following equation (Dahlquist, 1978):

$$\log \frac{f}{1-f} = b + n_H \cdot \log[Ca^{2+}]$$

where f is the parameter as defined in the previous paragraph, and *b* is a constant. This equation was obtained from the central linear part of the Hill plot {log[Ca^{2+}] versus log(f/(1-f))}, which covers a region where log (f/(1-f)) goes from negative to positive.

Statistical analysis was carried out by un-paired Student's t-test. A probability, p, of less than 0.05 was considered significant.

2.2.18. Phosphodiesterase stimulation assay

Bovine brain CaM and the recombinant calmodulins were examined for their regulation of CaM-dependent PDE activity in the presence of calcium using the method of Wallace et. al. (1983). cAMP was used as a substrate. Calmodulins were dissolved in 10 mM Tris-HCl buffer (pH 7.5). Protein concentrations in the stock solutions were determined by UV

spectrophotometry using the extinction coefficients: E_{278} =1500 ($M^{-1}\cdot cm^{-1}$) for VU-1 CaM and E_{280} = 8223 ($M^{-1}\cdot cm^{-1}$) for F92W and F92W/D133E calmodulins. The concentration of bovine brain CaM was calculated based on the claimed weight on the label. A series of CaM solutions was prepared by diluting each CaM stock solution with 0.1 % lipid-free bovine serum albumin to prevent the loss of CaM to the wall of the test tube.

The PDE assay was first performed in which the initial cAMP hydrolysis rate was determined as a function of time. The assay was carried out at 30° for either 1, 2, 3, 5, 7, 10, 13, 17, or 20 min in a reaction mixture containing 10 mM [2,8-^{3}H] cAMP (8 μCi/mL), 0.2 units/mL of PDE, 0 or 10 nM F92W CaM, 3 mM $MgSO_4$, 15 mM $CaCl_2$, 100 mM KCl, 40 mM Tris-HCl, pH 7.5 in a volume of 100 μl in a glass test tube (12 × 75 mm). The reaction was terminated by incubating the reaction mixture in a boiling water bath for 1 min. After incubation at 30° for 5 min, 20 μl of 1 mg/mL snake venom, as a source of nucleotidase, was added to a final concentration of 167 μg/mL to convert 5'-AMP into adenosine, and the reaction mixture was incubated at 30° for another 15 min. One milliliter of the 33 % (g/mL) AG1-X2 anion exchange resin slurry was added to the reaction mixture to adsorb the un-hydrolyzed cAMP, and the mixture was vortexed briefly. The resin was sedimented by centrifuging on a Jouan CR3000 centrifuge at 3000 rpm for 10 min. Four hundred milliliters of the supernatant were added to 5 mL scintillation fluid (Cytoscint™), and the mixture was counted on a Beckman LS 6000TA liquid scintillation counter. PDE stimulation activity was expressed as pmole of cAMP hydrolyzed per unit of PDE per min (pmol/U/min).

The PDE assay was then performed in which the initial cAMP hydrolysis rate was determined as a function of CaM concentration. The assay was carried out for 10 min in the presence of 0-800 nM CaM at either 50 μM or 15 mM $CaCl_2$ under the same conditions

described in the previous paragraph. Data were fitted to the following Hill equation using SigmaPlot® for Windows.

$$v = \frac{V_{max} \cdot C}{K_{50} + C}$$

where v is the stimulated PDE activity at a given concentration, C, of CaM; V_{max} is the maximal stimulated PDE activity; K_{50} is the concentration of CaM that is able to produce one-half of the maximal stimulated PDE activity.

Statistical analysis was carried out by un-paired Student's t-test. A probability, p, of less than 0.05 was considered significant.

2.3. RESULTS

2.3.1. Confirming the DNA sequence of the CaM gene in pVUCH-1

The DNA sequence corresponding to the nucleotide positions 86 to 460 of the synthetic CaM gene (Figure 9, page 37) in pVUCH-1 was confirmed by automated DNA sequencing. Since the primer used for DNA sequencing was an 18 mer oligodeoxynucleotide corresponding to the positions 50 to 67 of the synthetic CaM gene, the upstream sequence (positions 1-67) and a short region of the immediate downstream sequence (the length varies between experiments) were not checked in this study.

2.3.2. Identification of the pf92w clone

To identify the pf92w clone, a plasmid that was cut by both *Stu I* and *Xma* III, respectively, was further digested with *Eco* RI, *Hin* dIII, *Stu* I, and *Xma* III. The digestion

mixtures were analyzed by agarose gel electrophoresis (Figure 14). One DNA band at a position of 3 kb was seen when the plasmid was digested with either *Hin* dIII, *Eco* RI, *Xma* III, or *Stu* I, indicating that the plasmid was linearized by these enzymes as expected (Figure 14, lanes 2, 4, 5, and 6). Two bands at positions of approximately 2.4 kb and 0.6 kb, respectively, were seen when the plasmid was digested with *Bam* HI, indicating that two DNA fragments of the expected sizes were generated by *Bam* HI digestion (Figure 14, lane 3). Multiple bands were seen when the plasmid was undigested, however, no band was seen at the position of 3 kb (Figure 14, lane 1). The band at the position close to 2 kb was most likely the monomer of the undigested circular plasmid DNA, and the bands at positions of more than 3 kb were polymers of the undigested plasmid. These results indicate that this plasmid contains the restriction enzyme sites for *Bam* HI, *Eco* RI, *Hin* dIII, *Stu* I, and *Xma* III as expected.

The DNA sequence corresponding to the nucleotide positions 86 to 460 of the synthetic CaM gene was confirmed except that T283 was changed to G283 and C284 was changed to G284 as expected. These changes reflect the change of the codon TTC for Phe92 to codon TGG for Trp92 in the protein sequence. These data, together with the restriction enzyme mapping data, confirm the identity of the pf92w clone.

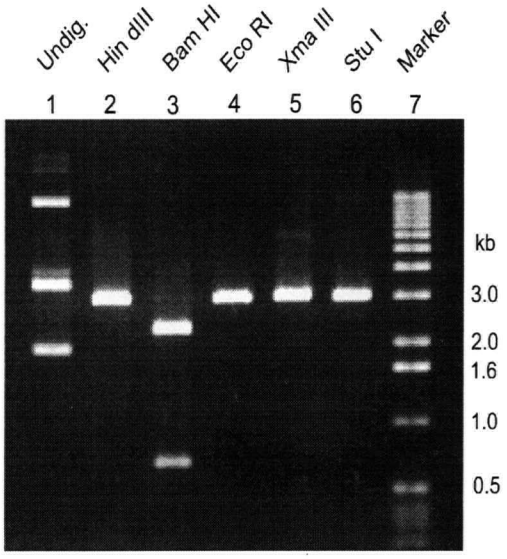

Figure 14. Agarose gel electrophoresis of restriction enzyme digested pf92W. Plasmid pf92w was digested with either *Bam* HI, *Eco* RI, *Hind* III, *Stu* I, or *Xma* III. Each digestion mixture was loaded on the gel (0.8%) as indicated by the enzyme used. Undig. means the plasmid was undigested. The gel was run in TAE buffer (40 mM Tris-acetate, 1 mM EDTA, pH 8.3) and stained with ethidium bromide (1 μg/mL). The photo was taken under UV (254 nm) light.

2.3.3. Identification of the pd133e clone

To identify the pd133e clone, a plasmid was first analyzed for the unique restriction enzyme sites for *Aat* II, Hpa I, and *Hin* dIII. The plasmid was digested with *Aat* II, Hpa I, and *Hin* dIII, respectively. The digestion mixtures were analyzed by agarose gel electrophoresis (Figure 15). One band at a position of 3 kb was seen when the plasmid was digested with either *Aat* II, *Hpa* I, or *Hin* dIII, indicating that the plasmid was linearized by these enzymes as expected (Figure 15, lanes 2, 3, and 5). One clear band at a position of approximately 2.9 kb and another very faint band at a position of less than 0.5 kb (hardly seen on the photocopy shown in this manuscript but can be seen on the original photo) were seen when the plasmid was digested with both *Hin* dIII and *Hpa* I, indicating that two DNA fragments of the expected sizes were generated by *Hin* dIII/*Hpa* I digestion (Figure 15, lane 4). One band at a position close to 2 kb was seen when the plasmid was undigested (Figure 15, lane 6) because the undigested circular plasmid migrated faster than a linearized plasmid of the same size. These results indicate that the this plasmid retains the unique restriction enzyme sites for *Hin* dIII, *Aat* II and *Hpa* I as expected.

The DNA sequence corresponding to the nucleotide positions 113 to 460 of the synthetic CaM gene was confirmed except that T283 was changed to G283, C284 was changed to G284, and C407 was changed to G407. These changes reflect the change of the codon TTC for Phe92 to the codon TGG for Trp92 and the change of the codon GAC for Asp133 to the codon GAG for Glu133 in the protein sequence. These data, together with the restriction enzyme mapping data, confirm the identity of the pd133e clone.

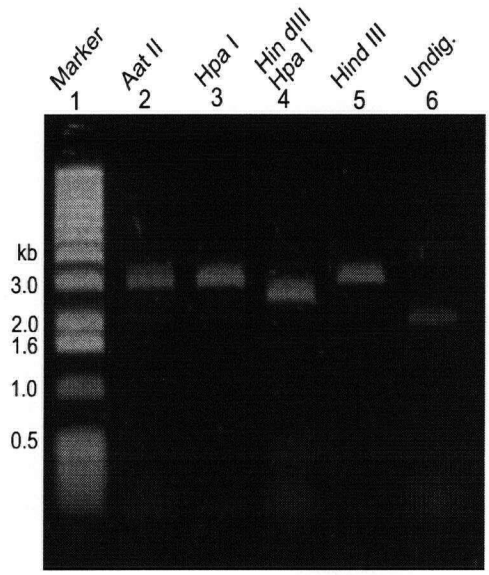

Figure 15. Agarose gel electrophoresis of restriction enzyme digested pd133e. Plasmid pd133e was digested with either *Aat* II, *Hpa* I, *Hind* III, or *Hpa* I/*Hind* III. Each digestion mixture was loaded on the gel (0.8%) as indicated by the enzyme used. Undig. means the plasmid was undigested. The gel was run in the TAE buffer (40 mM Tris-acetate, 1 mM EDTA, pH 8.3) and stained with ethidium bromide (1 μg/mL). The photo was taken under UV (254 nm) light.

2.3.4. Identification of VU-1, F92W and F92W/D133E calmodulins

The homogeneity of the protein preparations were evaluated by SDS-polyacrylamide gel electrophoresis (Figure 16). First, a single band at the position similar to that of bovine brain CaM was observed in the lanes loaded with the purified proteins, indicating that the protein preparations were fairly pure and had similar molecular weight to that of commercially obtained bovine brain CaM (16.7 kDa). Secondly, VU-1, F92W, and F92W/D133E calmodulins exhibited a Ca^{2+}-dependent migration shift on the gel as did bovine brain CaM, although the band shift of F92W/D133E was not as obvious as that of bovine brain CaM.

The amino acid compositions of VU-1, F92W, and F92W/D133E calmodulins are shown in Table 3. Since analysis of the Trp residue required a different hydrolysis method (alkaline hydrolysis), Trp was not analyzed in this study. Compared to the predicted values based on the amino acid sequences, most of the observed values match the predicted values. However, some observed values are lower than the predicted values. For example, the observed values for Met are always lower than the predicted values due to oxidation of Met during the analysis. In some cases, the observed values for Asp plus Asn, Glu plus Gln, His, Arg, and Ile are also quite low possibly due to incomplete hydrolysis of protein samples.

Molecular weight of VU-1, F92W, and F92W/D133E calmodulins were determined by mass spectrometry (Table 4). The observed values match the predicted values very well. These results, together with the results from the SDS-polyacrylamide gel electrophoresis and the amino acid composition analysis, confirmed the identity of the protein preparations.

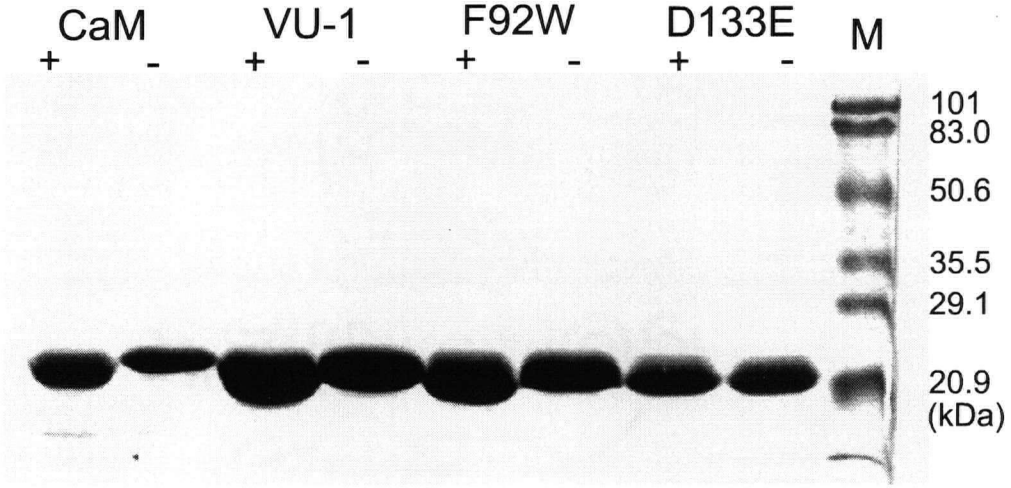

Figure 16. SDS-PAGE of VU-1, F92W, and F92W/D133E calmodulins. Protein samples were prepared in the presence of calcium (1 mM) or EGTA (1 mM). CaM: bovine brain CaM; VU-1: VU-1 CaM; F92W: F92W CaM; D133E: F92W/D133E CaM; M: a mixture of the pre-stained molecular weight standards; +: in the presence of calcium; -: in the presence of EGTA. The gel was run in Tris-glycine buffer (50 mM Tris, 250 mM glycine, 0.1 % SDS, pH 8.3) under constant voltage (60 volt for the stacking gel, 100 volts for the resolving gel). The gel was stained with Coomassie Brilliant Blue R250 (0.25 %) (Sambrook *et al.*, 1989).

Table 3. Amino Acid Compositions of VU-1, F92W and F92W/D133E Calmodulins

Amino acid	VU-1		F92W		F92W/D133E		
	P[a]	O[b] (120795[c])	P	O (120295)	P	O (112795)	O (052296)
Asp+Asn	25	22.47	25	21.86	24	26.13	24.74
Glu+Gln	26	24.90	26	23.74	27	26.85	27.33
Ser	4	3.97	4	4.54	4	4.15	4.06
Gly	11	11.29	11	11.68	11	11.86	11.60
His	1	0.77	1	0.64	1	0.84	0.92
Arg	5	3.82	5	3.59	5	4.56	5.33
Thr	10	10.82	10	10.65	10	9.76	9.40
Ala	11	11.00	11	11.00	11	11.00	11.00
Pro	2	2.02	2	2.09	2	1.68	1.41
Tyr	1	0.98	1	1.13	1	1.03	0.96
Val	9	8.42	9	7.41	9	8.24	8.17
Met	8	5.79	8	6.17	8	4.95	5.70
Ile	6	5.14	6	4.25	6	5.24	5.53
Leu	11	11.22	11	11.16	11	11.07	11.39
Phe	9	8.54	8	7.50	8	7.46	7.59
Lys	9	8.76	9	8.74	9	8.41	8.36
Trp	0	N/A[d]	1	N/A	1	N/A	N/A

[a] P means predicted values based on the amino acid sequence of each protein.
[b] O means observed values from two measurements by HPLC analysis.
[c] batch number of protein preparation.
[d] not available.

Table 4. Molecular Weight of VU-1, F92W and F92W/D133E Calmodulins

Protein	Predicted (Da)	Observed (Da) ± S.E.[b]
VU-1 CaM (120795[a])	16626.47	16626.95 ± 0.71
F92W CaM (120295)	16665.50	16666.35 ± 0.87
F92W/D133E (112795)	16679.53	16680.80 ± 1.35
F92W/D133E (052296)	16679.53	16679.00 ± 1.66

[a] batch number of protein preparation.

[b] S.E. is the standard error calculated from the different charge states of the protein molecule in one measurement.

2.3.5. Determination of the extinction coefficient of F92W CaM

The extinction coefficient for invertebrate and plant calmodulins was reported as E_{278} = 1500 ($cm^{-1}\cdot M^{-1}$) (Klee and Vanaman, 1982). Like *Drosophila* CaM and scallop CaM, VU-1 CaM has one Tyr residue and 9 phenylalanine residues in the same positions, the extinction coefficient [E_{278} = 1500 ($cm^{-1}\cdot M^{-1}$)] was used for VU-1 CaM in this study.

The UV spectra of F92W and F92W/D133E calmodulins are similar (data not shown). The maximal absorbance wavelength was observed at 280 nm between 240 and 400 nm for both proteins. The extinction coefficient of F92W CaM was determined as E_{280} = 8223 ($cm^{-1}\cdot M^{-1}$). Since F92W CaM and F92W/D133E CaM contain one Trp, one Tyr, and eight Phe residues at the identical positions, the extinction coefficient determined for F92W CaM [E_{280} = 8223 ($cm^{-1}\cdot M^{-1}$)] was also used for F92W/D133E CaM in this study.

2.3.6. Identification of W4I-M13 CaM-binding peptide

The amino acid composition analysis of the CaM-binding peptide, W4I-M13, was performed before the HPLC purification (Table 5). The molecular weight determined by mass spectrometry was 2891.20 ± 0.06 (mean ± S.E. of different charge states of the protein molecule in one measurement) which matches the calculated value of 2891.21. These results confirmed the identity of the peptide.

Table 5. Amino Acid Composition of W4I-M13 Peptide

Amino acid	Predicted	Observed[a]
Asn	2	1.40
Ser	4	3.75
Gly	1	1.17
Arg	3	2.46
Ala	4	4.00
Val	1	1.03
Ile	3	2.13
Leu	1	1.05
Phe	2	1.67
Lys	5	4.08

[a] Data from two measurements by HPLC analysis.

2.3.7. Far-UV CD spectra of VU-1, F92W, and F92W/D133E calmodulins

The normalized far-UV CD spectra of VU-1, F92W and F92W/D133E calmodulins in the absence and presence of calcium are shown in Figure 17. The corresponding molar ellipticity values and changes in ellipticity at 222 nm are presented in Table 6. Calcium was observed to induce an increase in the magnitude of the negative ellipticities of VU-1, F92W and F92W/D133E calmodulins. However, not only do the absolute ellipticities at 222 nm of each protein vary, but the relative changes from the Ca^{2+}-free state to the Ca^{2+}-bound state of these proteins are different as well (Table 6). It appears that Trp and Asp substitutions cause small difference in the overall structure of CaM.

Table 6. Molar Ellipticity of VU-1, F92W and F92W/D133E Calmodulins[a]

	$[\theta]_{222} \times 10^{-3}$ (deg · cm²/dmol) ± S.E.		
Protein	$-Ca^{2+}$	$+Ca^{2+}$	$\Delta[\theta]_{222}$
VU-1	14.31 ± 0.08	16.38 ± 0.06	2.07
F92W	13.76 ± 0.18	17.54 ± 0.03	3.78
F92W/D133E	12.20 ± 0.02	14.09 ± 0.04	1.89

[a] each value represents the mean ± S.E. of three separate measurements.

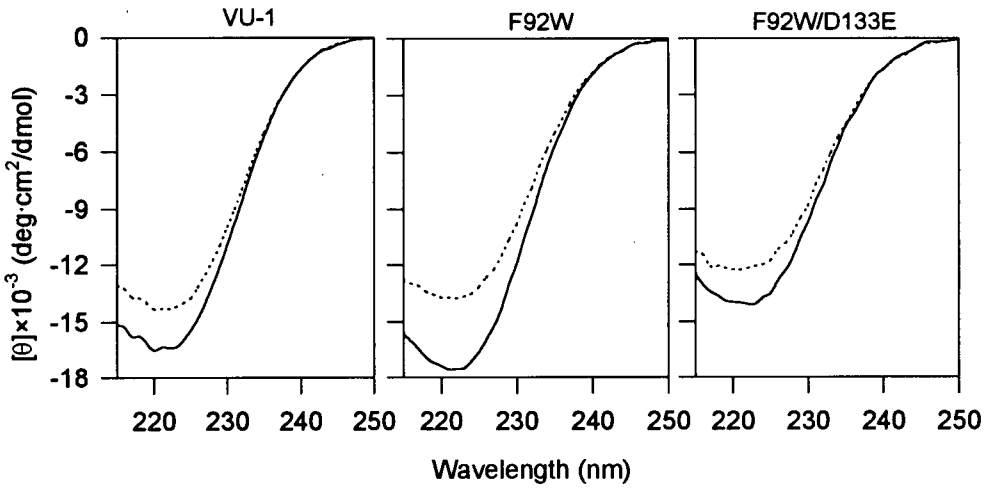

Figure 17. Far-UV CD spectra of VU-1, F92W and F92W/D133E calmodulins. Spectra were recorded at the protein concentrations of 28.5 μM VU-1, 24μM F92W and 15 μM F92W/D133E in the EGTA buffer (100 mM KCl, 1 mM EGTA, 50 mM MOPS, pH 7.20) before and after the addition of $CaCl_2$ to saturation (free calcium concentration: 7 mM for VU-1 and F92W, and 35 mM for F92W/D133E). Data were normalized by molar concentrations of the proteins using the equation in section 2.2.14, page 71. The solid lines represent the spectra in the presence of calcium and the dashed lines represent the spectra in the absence of calcium.

2.3.8. Fluorescence spectra of VU-1, F92W, and F92W/D133E calmodulins

The fluorescence excitation spectra of VU-1, F92W and F92W/D133E calmodulins were recorded at the emission wavelength of 309 nm (VU-1 CaM) and 340 nm (F92W and F92W/D133E), respectively (data not shown). The maximal excitation wavelength was observed at 278 nm for VU-1 and 282 nm for both F92W and F92W/D133E calmodulins. Therefore, calcium titrations of VU-1 CaM were performed at the excitation wavelength of 278 nm, and F92W and F92W/D133E mutants at 282 nm.

Fluorescence emission spectra of VU-1, F92W and F92W/D133E calmodulins were recorded before and after addition of calcium to saturation (Figure 18). Calcium was observed to induce a 3-fold increase in the fluorescence intensity of VU-1 CaM, a 2-fold increase in F92W CaM, and a 1.6-fold increase in F92W/D133E CaM at the corresponding maximal emission wavelength. There appears to be no shift in the maximal emission wavelength for VU-1 CaM in the absence and presence of calcium. Therefore the calcium titration of VU-1 CaM was monitored at the maximal emission wavelength of 309 nm. A small blue shift in the emission maximum from 342 nm in the absence of calcium to 340 nm in the presence of calcium for F92W CaM was observed. A blue shift in the emission maximum from 342 nm in the absence of calcium to 338 nm in the presence of calcium was observed for F92W/D133E CaM. Calcium titrations of F92W and F92W/D133E calmodulins were monitored at 340 nm where the largest difference in the fluorescence intensity between the apoprotein and Ca^{2+}-saturated protein occurred.

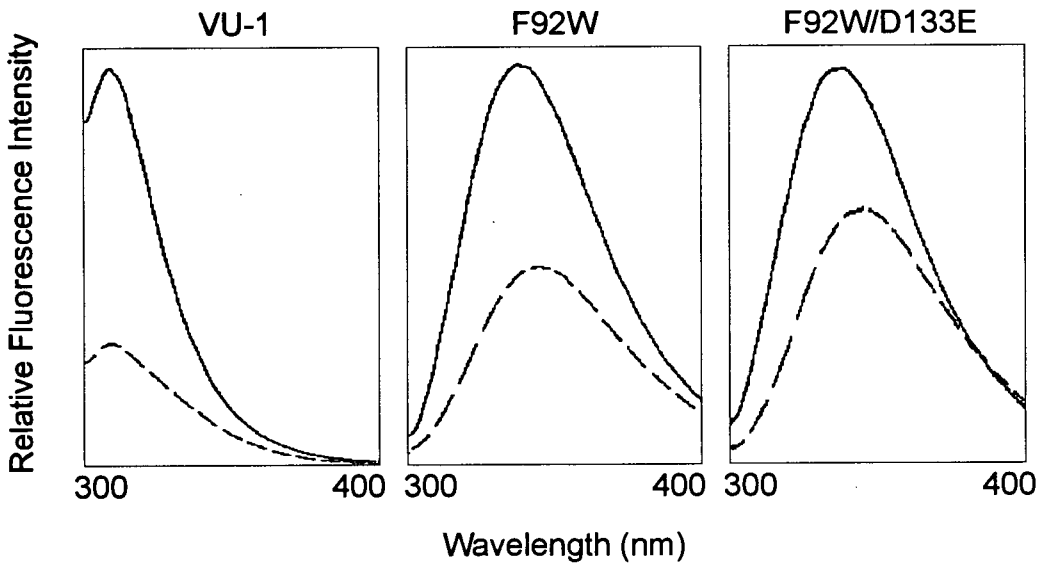

Figure 18. Fluorescence emission spectra of VU-1, F92W and F92W/D133E calmodulins. Spectra were recorded at the excitation wavelength of 278 nm for VU-1 (40 μM), and 282 nm for F92W (15 μM) and F92W/D133E (15 μM) calmodulins, respectively. The solid lines represent spectra in the presence of Ca^{2+} (free Ca^{2+} concentrations were 1 mM for VU-1 and F92W calmodulins and 8 mM for F92W/D133E CaM, respectively). The dashed lines represent the spectra in the absence of Ca^{2+} (1mM EGTA).

2.3.9. Calcium titration of VU-1, F92W, and F92W/D133E calmodulins

The calcium titration data of VU-1, F92W, and F92W/D133E calmodulins were fitted to the one-site, two-site, three-site, and four-site models (Tables 16, 18, 20, and 22 in the APPENDIX section). The parameters derived from the three-site and four-site models are not reliable as judged by the coefficient of variance (CV%), and the two models are over-parameterized to the data as judged by the dependency (Tables 20 and 22). The two-site model was more appropriate to the data than the one-site model as judged by the fitting coefficient (Tables 20 and 22). The calcium titration data and the fitted curves (by the two-site model) are shown in Figure 19. The two macroscopic calcium dissociation constants, K_1 and K_2, of the three calmodulins were calculated from each fitted two-site equation (Table 7). In all three calmodulins, K_1 is approximately 1 order of magnitude lower than K_2, indicating that one site has approximately 1 order of magnitude higher calcium affinity than the other in the C-terminal domains of these proteins. K_1 of F92W CaM is similar to that of VU-1 CaM, whereas K_2 of F92W CaM is significantly lower than that of VU-1 CaM (Table 7). These data indicate that the higher affinity site in the C-terminal domain of F92W CaM has similar calcium affinity to that of VU-1 CaM. However, the lower affinity site in the C-terminal domain of F92W CaM has approximately 2.3 fold higher calcium affinity than that of VU-1 CaM. The K_1 and K_2 of F92W/D133E CaM are significantly greater than those of F92W CaM (Table 7). These data indicate that the two sites in the C-terminal domain of F92W/D133E CaM have much lower binding affinities for calcium than those of F92W CaM.

The Hill coefficient (n_H) for VU-1 is not significantly different from 1 ($p>0.05$), F92W CaM has a n_H value of greater than 1 ($p<0.05$), and the n_H for F92W/D133E CaM is significantly less than 1 ($p<0.05$) (Table 7).

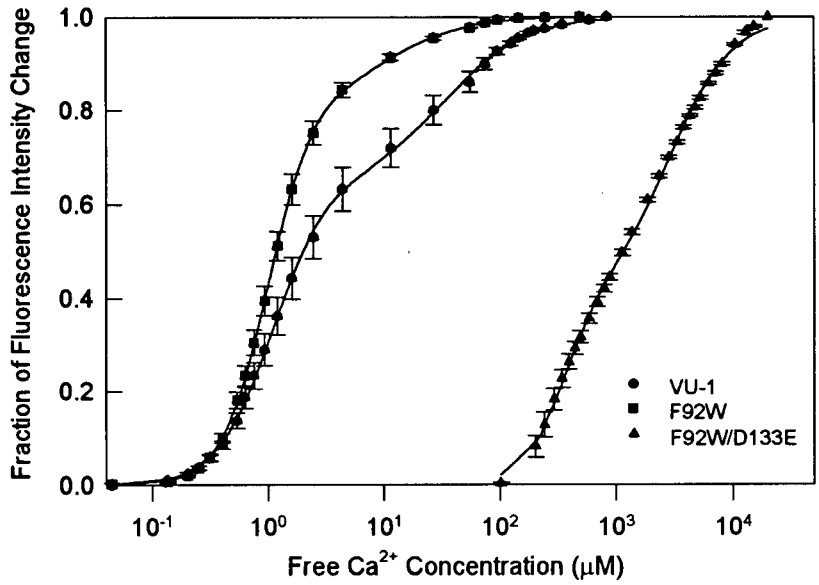

Figure 19. Calcium titration curves of VU-1, F92W, and F92W/D133E calmodulins. The fluorescence intensity changes were monitored at the emission wavelengths of 309 nm (tyrosine fluorescence) for VU-1 (40 μM) and 340 nm (tryptophan fluorescence) for both F92W (15 μM) and F92W/D133E CaM (15 μM) calmodulins, respectively. Each data point represents the average of six (VU-1 and F92W) or nine (F92W) separate titrations, and the standard error is shown as the error bar. The titration curves were obtained by fitting the data to the two-site model.

Table 7. Calcium Dissociation Constants of VU-1, F92W and F92W/D133E Calmodulins[a]

Protein	K_1 (μM)	K_2 (μM)	n_H
VU-1	1.1 ± 0.1	32 ± 5.7	1.10 ± 0.12
F92W	1.0 ± 0.1	14 ± 2.4	1.79 ± 0.06
F92W/D133E	335 ± 21	2760 ± 45	0.89 ± 0.02
TR_2C[b]	0.4	10	
F34[c]	0.6	18.4	
F34[d]	1	23.6	

[a] K is the calcium dissociation constant expressed as the mean ± S.E. of 6 (VU-1 and F92W calmodulins) and 9 (F92W/D133E CaM) separate titrations. Subscripts 1 and 2 refer to the high and low affinity sites in the C-terminal domain of each protein, respectively. n_H is the Hill coefficient.

[b] The calcium dissociation constants of the CaM fragment corresponding to the C-terminal domain of bovine CaM (residues 78-148) were obtained by calcium titration in the presence of a calcium chelator, 5,5'-Br_2BAPTA [5,5'-dibromo-1,2-bis(2-aminophenoxy)ethane-N.N,N',N'-tetraacetic acid]. Data from Linse *et al.*, 1991.

[c] The calcium dissociation constants of the CaM fragment corresponding to the C-terminal domain of scallop testis CaM (residues 78-148) were determined by flow dialysis. Data from Minowa & Yagi, 1984.

[d] The calcium dissociation constants of the CaM fragment corresponding to the C-terminal domain of scallop testis CaM (residues 78-148) were determined by equilibrium dialysis. Data from Minowa & Yagi, 1984.

2.3.10. Effect of W4I-M13 CaM-binding peptide on calcium affinity of VU-1, F92W, and F92W/D133E calmodulins

It was observed that W4I-M13 CaM-binding peptide did not affect the fluorescence emission spectra of the three calmodulins in the absence of calcium but caused a blue shift of the fluorescence emission spectra of F92W and F92W/D133E calmodulins in the presence of calcium (Figure 20). The maximal emission wavelength of VU-1 CaM was observed at 309 nm in the presence and absence of calcium. The maximal emission wavelength of F92W CaM was shifted from 342 nm in the absence of calcium to 326-328 nm in the presence of calcium. For F92W/D133E CaM, this shift occurred from 338 nm to 326-328 nm. Calcium titrations of F92W and F92W/D133E calmodulins were monitored at the emission wavelengths of 340 nm and 330 nm to examine the effect of wavelength on the fraction of fluorescence intensity change. It was observed that the fraction of fluorescence intensity change was not significantly affected by the two wavelengths (data not shown). Therefore, the titration data monitored at the two emission wavelengths are included in Figure 21.

Again, the calcium titration data did not fit to the three-site or four-site model as judged by the coefficient of variance (CV%) and the dependency (Tables 21 and 23 in the APPENDIX section). The two-site model was more appropriate than the one-site model as judged by the fitting coefficient (Tables 17 and 19 in the APPENDIX section). Accordingly the macroscopic calcium dissociation constants, K'_1 and K'_2, of the three calmodulins were calculated from each fitted two-site equation (Table 8). Compared to K_1 and K_2, K'_1 and K'_2 of the same protein are significantly lower ($p<0.05$), indicating that the calcium affinities of the calmodulins are higher in the presence of the CaM-binding peptide than in the absence of

the peptide. Unlike the n_H values obtained in the absence of the peptide, the n_H values of the three proteins obtained in the presence of the peptide are all greater than 1 (Table 8).

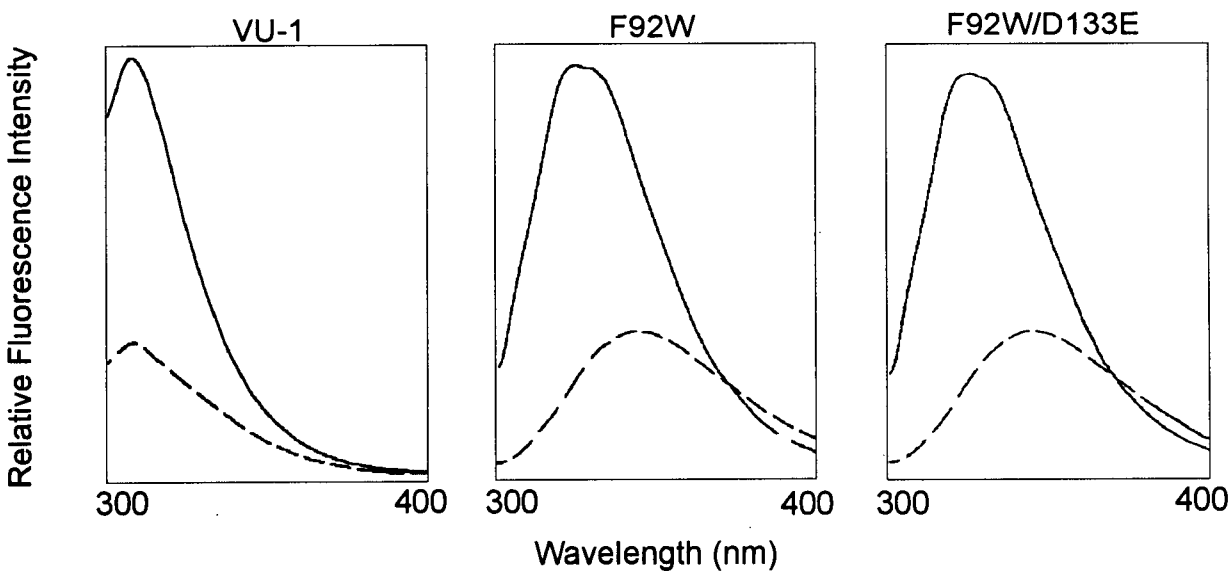

Figure 20. Fluorescence emission spectra of VU-1, F92W and F92W/D133E calmodulins in the presence of W4I-M13 CaM-binding peptide. The excitation wavelengths were 278 nm for VU-1 CaM and 282 nm for F92W and F92W/D133E calmodulins. The emission wavelengths were 309 nm for VU-1 CaM and 340 nm for F92W and F92W/D133E calmodulins. The protein concentrations were 30 μM for VU-1 and 10 μM for both F92W and F92W/D133E in the EGTA buffer (100 mM KCl, 1 mM EGTA, 50 mM MOPS, pH 7.20). Protein to peptide ratios were 1:1.5 for VU-1 and 1:4 for both F92W and F92W/D133E. The spectra were recorded before (dashed lines) and after (solid lines) the addition of $CaCl_2$ to saturation.

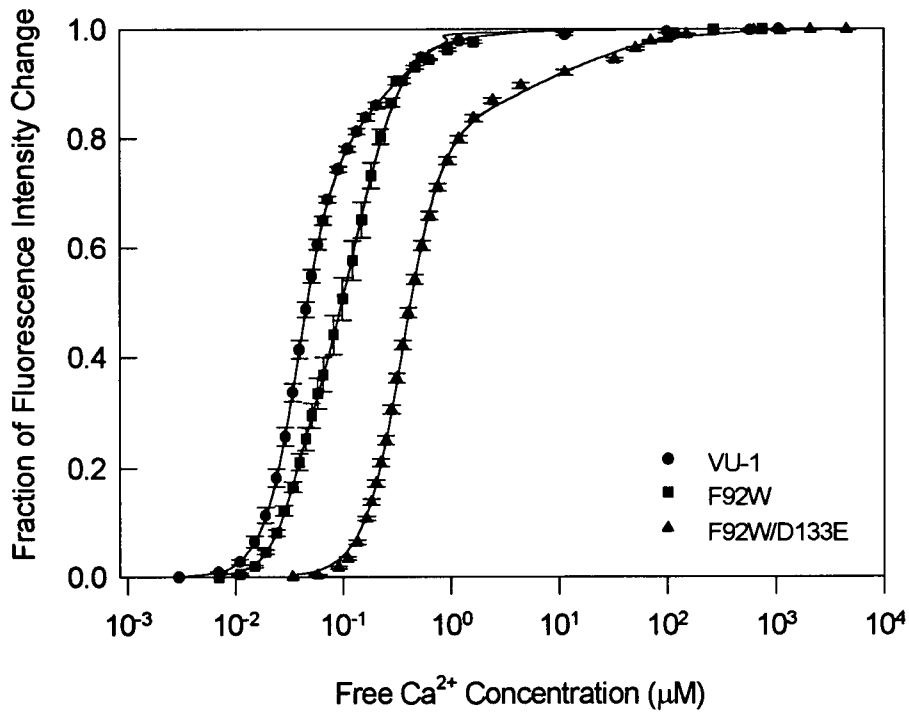

Figure 21. Calcium titration curves of VU-1, F92W, and F92W/D133E calmodulins in the presence of the CaM-binding peptide W4I-M13. The fraction change in tyrosine (VU-1) and tryptophan (F92W and F92W/D133E) fluorescence intensity is plotted as a function of free calcium concentration in the presence of W4I-M13 CaM-binding peptide. The protein concentrations were 30 μM for VU-1 and 10 μM for both F92W and F92W/D133E calmodulins, respectively. The protein to peptide ratios were 1:1.5 for VU-1 and 1:4 for both F92W and F92W/D133E calmodulins, respectively. Each data point represents the average of three (VU-1) or six (F92W and F92W/D133E) separate titrations, and the standard error is shown as the error bar. The titration curves were obtained by fitting the data to the two-site model.

Table 8. Calcium Dissociation Constants of VU-1, F92W, and F92W/D133E Calmodulins in the Presence of W4I-M13 CaM-Binding Peptide[a]

Calmodulin	K'_1 (μM)	K'_2 (μM)	n_H
VU-1	0.038 ± 0.002	0.250 ± 0.012	2.16 ± 0.08
F92W	0.037 ± 0.003	0.143 ± 0.003	1.48 ± 0.02
F92W/D133E	0.358 ± 0.005	8.13 ± 0.75	1.81 ± 0.02

[a] K'_1 and K'_2 are the apparent calcium dissociation constants of CaM in the presence of W4I-M13 CaM-binding peptide, which are expressed as the mean ± S.E. of three (VU-1) or six (F92W and F92W/D133E) separate titrations. n_H is the Hill coefficient.

2.3.11. Phosphodiesterase stimulation assay

To determine the linear range of the PDE-catalyzed cAMP hydrolysis rate, the amount of cAMP hydrolyzed by PDE was determined as a function of time in the absence and presence of 10 nM F92W CaM (Figure 22). The amount of cAMP hydrolyzed by PDE increased linearly with time up to 17 min in the absence and presence of F92W CaM. Data (except one point at 20 min) were fitted to a linear equation. The square of the coefficient is

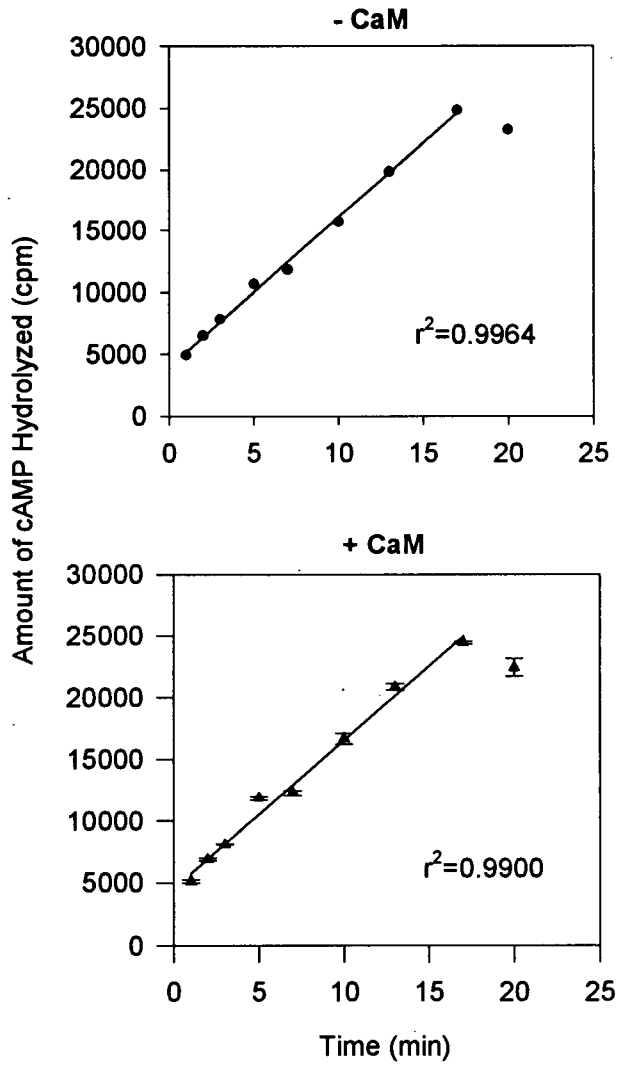

Figure 22. Time-course of hydrolysis of cAMP by PDE. The amount of cAMP (expressed as cpm) hydrolyzed by PDE was determined in a buffer containing 0.2 U/mL of PDE, 2 mM [^{3}H]cAMP, 15 mM $CaCl_2$, 3 mM $MgSO_4$, 100 mM KCl, 40 mM Tris-HCl, pH 7.5 in a volume of 100 μl at 30 ° in the absence (-CaM) or presence of 10 nM F92W CaM (+CaM). The time-course in the absence of CaM represents a single experiment. The time-course in the presence of CaM represents the average of three separate experiments, and the standard error is shown as the error bar for each data point.

0.9964 in the absence of F92W CaM and 0.9900 in the presence of F92W CaM. Therefore, the PDE stimulation assay was carried out for 10 min to determine the PDE stimulation activity of the calmodulins.

PDE stimulation parameters, V_{max} and K_{50}, of the bovine brain CaM and the three recombinant calmodulins are presented in Table 9. The PDE stimulation curves of bovine brain CaM and VU-1 CaM are shown in Figure 23, and the PDE stimulation curves of F92W and F92W/D133E calmodulins are depicted in Figure 24. At low calcium concentrations (50 μM), both VU-1 and F92W calmodulins stimulated PDE to a maximal level similar to that obtained with bovine brain CaM ($p>0.05$). While the K_{50} of VU-1 CaM is similar to that of bovine brain CaM ($p>0.05$), the K_{50} of F92W CaM is significantly lower than that of VU-1 CaM or bovine brain CaM (Table 9). These data indicate that VU-1 CaM and bovine brain CaM have similar affinity for the bovine heart PDE, whereas F92W CaM has a higher affinity for PDE than VU-1 CaM. The V_{max} of F92W/D133E CaM is approximately 3-fold lower than that of F92W CaM, and the K_{50} of F92W/D133E for PDE is 25-fold greater than that of F92W CaM in the presence of 50 μM calcium. These data indicate that F92W/D133E CaM has a significantly lower PDE stimulation activity with a significantly lower affinity for the enzyme than F92W CaM. However, the V_{max} and K_{50} of F92W/D133E CaM are similar to those of F92W CaM at higher calcium concentrations (15 mM) ($p>0.05$), indicating that the PDE regulatory activity of F92W/D133E CaM is restored to that of F92W CaM by high concentrations of calcium. The K_{50} of F92W for the enzyme is 6 fold larger at the higher calcium concentration which may indicate an ionic effect of the high calcium concentration on calmodulin interaction with the enzyme.

Table 9. Phosphodiesterase Stimulation Activity of Calmodulins[a]

	50 μM Ca^{2+}		15 mM Ca^{2+}	
Protein	V_{max} (pmol/U/min)	K_{50} (nM)	V_{max} (pmol/U/min)	K_{50} (nM)
CaM	177 ± 7.5	10.9 ± 0.9		
VU-1	172 ± 4.6	10.8 ± 1.0		
F92W	169 ± 4.8	7.4 ± 0.7	166 ± 8	43 ± 6
F92W/D133E	63.2 ± 2.5	185 ± 21.1	186 ± 9	41 ± 4

[a] Each value is presented as the mean ± S.E. of three separate experiments. V_{max} is the maximal stimulated PDE activity by CaM, and K_{50} is CaM concentration required for a half maximal stimulated PDE activity.

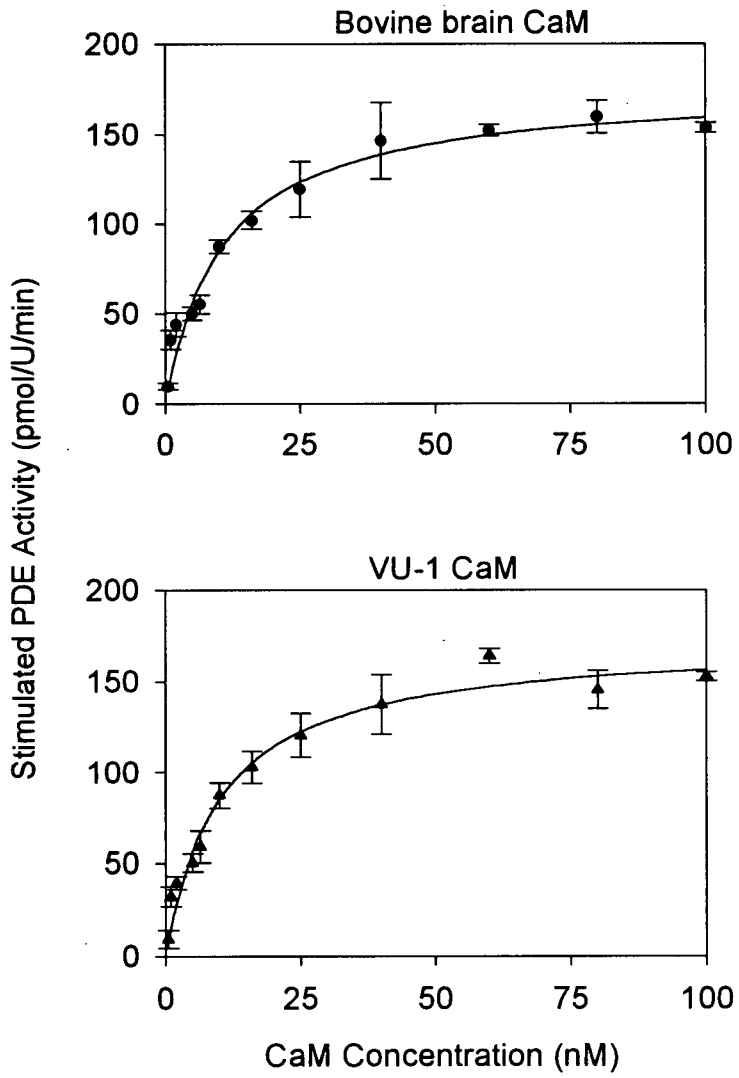

Figure 23. PDE stimulation curves of bovine brain CaM and VU-1 CaM. The assay was carried out in a buffer containing 0.2 U/mL of PDE, 2 mM [^{3}H]cAMP, 50 μM $CaCl_2$, 3 mM $MgSO_4$, 100 mM KCl, 40 mM Tris-HCl, pH 7.5 in a volume of 100 μl at 30 °. Each data point represents the average of three separate experiments, and the standard error is shown as the error bar.

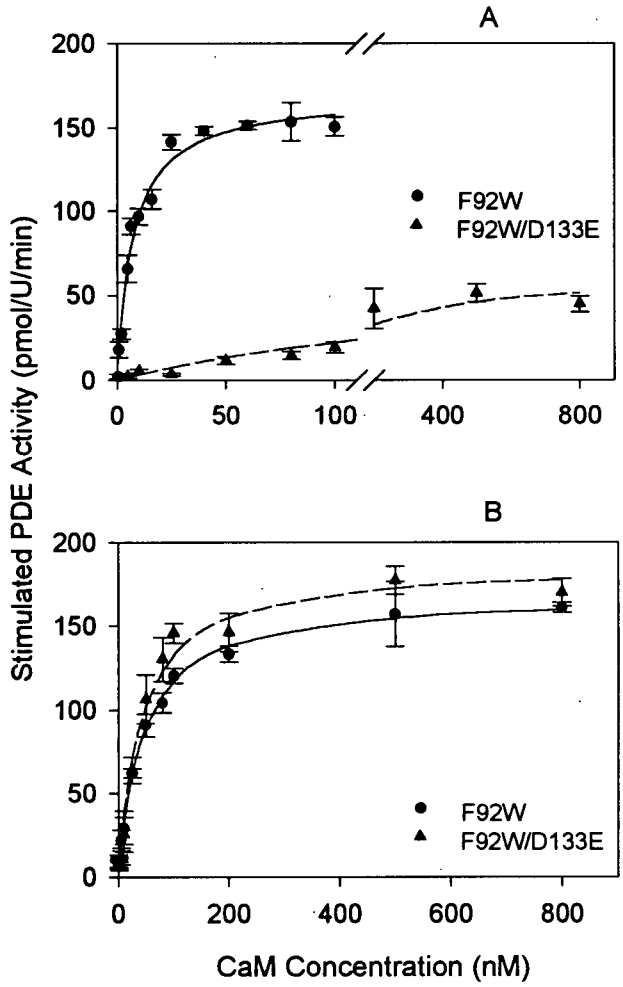

Figure 24. PDE stimulation curves of F92W and F92W/D133E calmodulins. The assay was carried out in a buffer containing 0.2 U/mL of PDE, 2 mM [^{3}H]cAMP, 50 μM $CaCl_2$ (A) or 15 mM $CaCl_2$ (B), 3 mM $MgSO_4$, 100 mM KCl, 40 mM Tris-HCl, pH 7.5 in a volume of 100 μl at 30°. Each data point represents the average of three separate experiments, and the standard error is shown as the error bar.

2.4. DISCUSSION

Binding constants for calcium in Ca^{2+}-binding peptides and proteins have been estimated by a variety of methods such as equilibrium and flow dialysis, CD-, NMR- and fluorescence-monitored calcium titration. The more direct techniques such as equilibrium and flow dialysis can not specify which site has which calcium binding affinity, however, the indirect techniques such as fluorescence-monitored calcium titration may be used to single out one site or one globular domain. Since this work focuses on site III of CaM, it is helpful to employ a method by which the calcium affinity of site III can be determined without interference of other sites. As an attempt to solve this problem, the calcium-dependent fluorescence monitoring of tryptophan located at the N-terminus of the loop region of site III is used to determine calcium binding affinity of CaM in the present study (Wu & Reid, 1997a). Although the only Tyr residue in site IV of VU-1 CaM allows us to titrate these proteins by monitoring the Tyr fluorescence intensity change, a Trp residue is introduced into site III of VU-1 CaM because we intend on having a spectral probe in site III at a position similar to that of F105W chicken troponin C (Trigo-Gonzalea *et al.*, 1992; Pearlstone *et al.*, 1992). It is anticipated that Trp substitution at this particular position will allow us to titrate the calcium induced conformational transition in the C-terminal domain, and calcium binding to the N-terminal domain will not affect the Trp fluorescence as in the case of F105W troponin C (Trigo-Gonzalea *et al.*, 1992; Pearlstone *et al.*, 1992).

The calcium dissociation constants of VU-1 CaM determined by flow dialysis range from 0.7 to 3 μM (Haiech *et al.*, 1991), which are comparable to the macroscopic calcium dissociation constants of VU-1 and F92W calmodulins obtained in the present study (Table

7). These data indicate that the Tyr fluorescence- and Trp fluorescence-monitored calcium titrations are valid methods for a calcium binding study.

The two macroscopic calcium dissociation constants, K_1 and K_2, are assumed to be the dissociation constants for site III and site IV in the C-terminal domain, although not necessarily in that order. The reason for this assumption is threefold. First, F29W and F105W point mutations in troponin C, a member of CaM superfamily, have been made, and Trp29 and Trp92 have been successfully used as spectral probes for monitoring the conformational transitions in the N- and C-terminal domains in the protein, respectively (Trigo-Gonzalea *et al.*, 1992; Pearlstone *et al.*, 1992). It has also been reported that changes in the environment of the only Tyr residue, Y138, analogous to Y138 in VU-1 CaM, reflect binding of calcium to the C-terminal domain of human calmodulin like protein (Durussel *et al.*, 1993). Second, studies of intact CaM and trypsin-digested fragments each containing two of the Ca^{2+}-binding sites suggest that calcium binding to one domain does not affect calcium binding to the other (Linse *et al.*, 1991; Minowa & Yagi, 1984). Although other studies suggest that interdomain interactions are evident (Seamon, 1980; Wang *et al.*, 1984; Kilhoffer *et al.*, 1992; Pedigo & Shea, 1995; Shea *et al.*, 1996), it is unknown to what extent these interactions may affect the calcium binding affinity of each domain. We assume these interdomain interactions do not significantly affect the calcium affinity of each domain. Third, the calcium dissociation constants of F92W CaM obtained in this study (1 and 14 μM) are similar to those obtained from the CaM C-terminal domain fragments (K_1 ranges from 0.4 to 1 μM, and K_2 ranges from 10 to 23.6 μM, Table 7). These data again suggest that the fluorescence changes in the whole CaM molecule reflect the calcium induced conformational changes of the C-terminal domain in CaM.

To determine any influence by the F/W substitution, F92W CaM was compared to VU-1 CaM in terms of CD spectra, calcium affinity and PDE stimulation activity. Although the overall pattern of the CD spectra of F92W CaM in the presence and absence of calcium is similar to that of VU-1 CaM, the calcium induced ellipticity change observed for F92W CaM at 222 nm is approximately 2 fold greater than that for VU-1 CaM (Table 6). Although the higher affinity site in the C-terminal domain of F92W CaM has similar calcium affinity to that of VU-1 CaM, the lower affinity site in the C-terminal domain of F92W CaM has an approximately 2.3 fold higher calcium affinity than that of VU-1 CaM (Table 7). Both F92W and VU-1 calmodulin stimulate the bovine heart PDE to a similar maximal level, however, F92W CaM has an approximately 1.5 fold higher affinity for PDE than VU-1 CaM (Table 9). Altogether, these data demonstrate that the F/W mutation affects the overall structure of CaM so that calcium affinity of the lower affinity site in the C-terminal domain increases, and as a result, the affinity for PDE increases. NMR studies have shown that Phe92 of CaM becomes more buried in the presence of calcium because this residue undergoes a net decrease in exposed surface upon calcium binding (Finn *et al.*, 1995). Substitution of a bulkier and more hydrophobic Trp residue for Phe at position 92 may alter the local structure of CaM in favor of the calcium bound state of the local site resulting in an increase in the calcium induced ellipticity change, calcium affinity, and overall affinity for PDE. It should be noted that this effect of the F92W mutation in the VU-1 CaM is contrary to the lack of effect observed for a similar mutation in troponin C (Trigo-Gonzalea *et al.*, 1992; Pearlstone *et al.*, 1992).

The fact that the F92W mutation in site III of F92W CaM caused a 2.3 fold increase in calcium affinity of the low affinity site in the C-terminal domain in this protein, whereas the

high affinity site is unaffected, indicate that site III is the low affinity site and site IV is the high affinity site in both VU-1 and F92W calmodulins. As a result, the calcium dissociation constant with a greater value (K_2) is tentatively assigned to site III and that with a lower value (K_1) to site IV. Site IV of F92W CaM is similar to site IV of VU-1 CaM in terms of calcium affinity. However, site III of F92W CaM has a higher calcium affinity than the same site in VU-1 CaM due to the Trp substitution for Phe in position 92 at the C-terminal end of the first helix in site III as discussed earlier.

Positive cooperativity is present between site III and site IV in F92W CaM as indicated by the n_H value of greater than 1, however, the n_H value of VU-1 CaM shows no cooperativity between sites III and IV in this protein (Table 7). Previous studies suggest that positive cooperativity is present between the two paired sites in each of the two globular domains as indicated by either a n_H value of greater than 1 or a positive value of free energy of interaction between two sites ($-\Delta\Delta G_{\eta=1}$) (Minowa & Yagi, 1984; Linse *et al.*, 1991). The n_H value for CaM (scallop testis CaM and bovine brain CaM) has been reported ranging from 1.25 to 1.33 (Minowa & Yagi, 1984; Crouch & Klee, 1980). The n_H values for the N- and C-terminal domains of scallop testis CaM are 1.14 and 1.84, respectively (Minowa & Yagi, 1984). We do not have any satisfactory explanation for the unusually low n_H value of VU-1 CaM at this moment. Unlike F92W CaM, F92W/D133E shows negative cooperativity between sites III and IV as indicated by the n_H value of less than 1 (Table 7). These data indicate that the very conservative D133E mutation has reversed the positive cooperativity between sites III and IV in F92W CaM to negative cooperativity between the same sites in F92W/D133E CaM.

In an attempt to eliminate the calcium binding affinity of site IV in CaM, the D133E CaM mutant is designed from the results of a study on a synthetic hlh peptide model of CaM site III in which the +Z residue was changed to a Glu to produce a Z axis Glu-Glu acid pair (Reid & Procyshyn, 1995). The D/E mutation in the + Z position caused the peptide to lose all calcium and magnesium binding capacity. Therefore, we expected that the D133E CaM mutant would have little or no calcium affinity in site IV. Since site III is unchanged, we assume that it would have a higher affinity for calcium than site IV in the F92W/D133E mutant. Therefore, K_1 is tentatively assigned to site III and K_2 to site IV in the F92W/D133E mutant (Table 7). The calcium dissociation constant of site IV in the F92W/D133E mutant is 2760-fold greater than the same site in F92W CaM. The dissociation constant of site III in the F92W/D133E mutant is 24-fold greater than that in F92W CaM. These results demonstrate that substitution of Glu for Asp at the +Z position in the loop region, a very conservative single residue change, induces a drastic reduction in calcium affinity of the corresponding site, and, at the same time, significantly decreases the calcium binding affinity of the paired, unmutated site in the same domain.

It is interesting to note that the Acid-Pair Hypothesis which correlates the nature of the chelating residues with calcium affinity of the hlh motif (section 1.1.5, page 12) would predict site IV of F92W/D133E CaM to be a high affinity calcium binding site because of the two acid pairs located on the X and Z axes. The fact that this site is a very low affinity site indicates that not only is location of acidic residues in the loop region critical to cation affinity but the type of acidic residues can greatly affect cation affinity.

Falke and his colleagues summarized the sequences of 567 hlh motifs using PROSITE sequence analysis software (Falke *et al.*, 1994; Figure 3). Among the 567 hlh motif

sequences, there are 295 Asp, 131 Ser, 123 Asn, 9 Thr, 8 Gly and only 1 Glu at the +Z position. This comparison suggests that the +Z position in the loop of an hlh motif is relatively variable among Asp, Ser and Asn but prefers Asp over Glu. Even though there is no charge change by substitution of Glu for Asp at the +Z position in F92W/D133E CaM, the larger Glu residue may cause unfavorable local interactions such as with Asp in the +Y position, or with Glu in the -Z position. Since Glu is longer than Asp by a methylene group, charge repulsion with Asp in the +Y position or with Glu in the -Z position may become significant enough to distort the calcium binding loop around the +Z position resulting in reduced calcium affinity. Alternatively, substitution of a larger Glu for Asp in the +Z position may simply cause a smaller binding cavity at the site resulting in a reduced calcium affinity. The reduction in calcium binding affinity in site IV results in a reverse of the cooperativity from positive to negative between sites III and IV in the C-terminal domain. The site IV change also results in a reduction in calcium affinity in site III although no mutation occurs in site III. Falke also found results supporting electrostatic repulsion between coordinating oxygens as a possible explanation for changes in ion selectivity in the *E. coli* galactose binding protein engineered with different residues in the -X position (Falk *et al.*, 1991; Drake & Falke, 1996; Drake *et al.*, 1996).

Previous studies have shown that point mutations of Glu to Ala at the highly conserved -Z position in site II (E67A) and site IV (E140A) of VU-1 CaM reduce the calcium binding affinity of the N- and C-terminal domains, respectively (Haiech *et al.*, 1991). The mutation of the invariable Glu in the -Z position to Ala reduces the calcium affinity by 100-300 fold, whereas our relatively conservative D/E mutation of the variable +Z position drops the calcium affinity for the site nearly 3000 fold. Beckingham, *et al.* have reported the effect of a

point mutation of Glu to either Gln or Lys at the -Z position in each of the loops in *Drosophila melanogaster* CaM on the calcium binding affinity (Maune *et al.*, 1992). Calcium binding at the mutated site was undetectable in most of the CaM mutants, E31Q, E67Q, E67K, E104Q, E104K, E140Q, and E140K, in the presence of 1 mM magnesium. However, in the absence of magnesium, E104Q (mutation in site III) and E140Q (mutation in site IV) gave calcium dissociation constants of 1250 and 200 μM for the mutated sites, respectively. And at the same time, the unmutated partner sites, site IV in E104Q and site III in E140Q, have values of 100 and 16.7 μM, respectively. Again the values reflect higher affinities for the drastically mutated invariable -Z position when compared to our less drastic mutation of a variable position in the loop region.

The CaM-binding peptide, W4I-M13, increases the macroscopic calcium affinity of all three calmodulins in the present study (Table 8). These results are consistent with a study in which the CaM-binding peptide, mastoparan, or the CaM-binding fragment of caldesmon increases the calcium affinity of scallop testis CaM (Yazawa *et al.*, 1987). Another study also shows that a CaM-binding peptide (RS20) corresponding to the CaM-binding site of smooth muscle myosin light chain kinase, increases the calcium affinity of VU-1 CaM, E67A CaM and E140A CaM in the presence of 5 mM $MgCl_2$ (Haiech *et al.*, 1991). Formation of a CaM-peptide complex stabilizes the Ca^{2+}-bound form of CaM thereby kinetically decreasing the dissociation rate constant (Brown *et al.*, 1997), and, at the same time, producing a positive cooperativity between the N- and C-terminal domains by bringing the two domains closer together (Yazawa *et al.*, 1987). As a result, the calcium binding affinity of CaM increases in the presence of the CaM-binding peptide. Unlike K_1 and K_2 (Table 7), K_1' and K_2' (Table 8) may not necessarily reflect the calcium affinities of the two sites in the C-

terminal domain because of the aforementioned positive cooperativity between the N- and C-terminal domains. Alternatively, they might reflect the macroscopic calcium affinities of the two domains in the protein.

F92W/D133E CaM has a reduced PDE regulatory activity when compared with F92W CaM in the presence of 50 μM calcium (Figure 24A and Table 9). However, the two calmodulins exhibit similar PDE regulatory activity when calcium concentration is increased to 15 mM (Figure 24B and Table 9). Since the calcium dissociation constants of sites III and IV of F92W/D133E CaM are 335 μM and 2.76 mM, respectively, the C-terminal domain of this protein is not saturated when the calcium concentration is 50 μM but saturated when the calcium concentration is 15 mM. These results indicate not only that the calcium bound form of CaM is essential for PDE regulation but that the D/E mutation alters calcium regulation of CaM mediated PDE activity without affecting CaM interaction with the enzyme. It is also obvious that the affinity of F92W for PDE is reduced 6 fold in the presence of 15 mM calcium which may indicate a detrimental ionic effect of the high calcium concentration on CaM/PDE interactions.

CHAPTER 3

TESTING THE ACID-PAIR HYPOTHESIS USING F92W/D133E CaM AS THE WHOLE PROTEIN MODEL

3.1. MATERIALS

Twelve oligos, stuI-2, stuI-3, stuI-4, stuI-5, stuI-6, stuI-7, stuI-8, stuI-9, xma-2, xma-3, hind-2, and hind-3, were synthesized on a Perkin Elmer Applied Biosystems 391 DNA synthesizer in the NAPS Unit at the University of British Columbia. The sequences of these oligos are presented on pages xviii-xix. All enzymes and chemicals used in this study were as the same as those described in section 2.1.

3.2. METHODS

3.2.1. Construction of the expression vectors for 3xCaM, 3zCaM, 4xCaM, 4zCaM, and 4xzCaM mutants

CaM mutants, 3xCaM, 3zCaM, 4xCaM, 4zCaM and 4xzCaM, were designed to have three or four acidic amino acid residues with acid-pairs on the X and/or the Z axes (see nomenclature for these mutants, page xxi). The amino acid sequences of the loop of site III of the CaM mutants are shown in Figure 25. The expression vectors for 3xCaM, 3zCaM, 4xCaM, 4zCaM, and 4xzCaM were constructed from the plasmid pd133e, the F92W/D133E CaM expression vector, using the procedure illustrated in Figure 13. For construction of the 3zCaM and 4zCaM expression vectors, p3zcam and p4zcam, the plasmid pd133e (15 μg) was digested with 40 units *Stu* I and 40 units *Xma* III as described in section 2.2.6.1. For construction of the 3xCaM, 4xCaM, and 4xzCaM expression vectors, p3xcam, p4xcam, and

	1	2	3	4	5	6	7	8	9	10	11	12
	+X		+Y		+Z		-Y		-X			-Z
F92/D133E	D	K	**D**	G	**N**	G	F	I	**S**	A	A	E
3xCaM	D	K	**N**	G	**N**	G	F	I	**D**	A	A	E
3zCaM	D	K	**N**	G	**D**	G	F	I	**S**	A	A	E
4xCaM	D	K	**D**	G	**N**	G	F	I	**D**	A	A	E
4zCaM	D	K	**D**	G	**D**	G	F	I	**S**	A	A	E
4xzCaM	D	K	**N**	G	**D**	G	F	I	**D**	A	A	E

Figure 25. The amino acid sequences of the calcium binding loop of site III of CaM mutants. The sequence positions in the loop are numbered 1 to 12, corresponding to positions 93 to 104 in VU-1 CaM (Figure 11). The positions of the chelating residues are denoted as the +X, +Y, +Z, -Y, -X, and -Z positions on the axes of a near octahedral coordination shell. Mutations are made at the +Y, +Z and -X, positions in addition to the F92W/D133E mutations, and the mutated residues are boldface and boxed.

p4xzcam, the plasmid pd133e (15 μg) was digested with 40 units *Stu* I and 40 units *Hin* dIII as described in section 2.2.6.1. The large fragments of the *Stu* I/*Xma* III double digested pd133e and the *Stu* I/*Hin* dIII double digested pd133e were separated, purified, dephosphorylated at 5' ends, and quantitated as described in sections 2.2.6.2 to 2.2.6.5.

A schematic diagram of the DNA cassettes used for constructing these five expression vectors are shown in Figure 26. For each DNA cassette, 1 nmole of each oligo was mixed together and phosphorylated with 40 units of polynucleotide kinase as described in section 2.2.6.6.

The dephosphorylated *Stu* I/*Xma* III double digested pd133e large fragment was ligated with the phosphorylated cassettes 3 and 4 for constructing the 3zCaM and 4zCaM expression

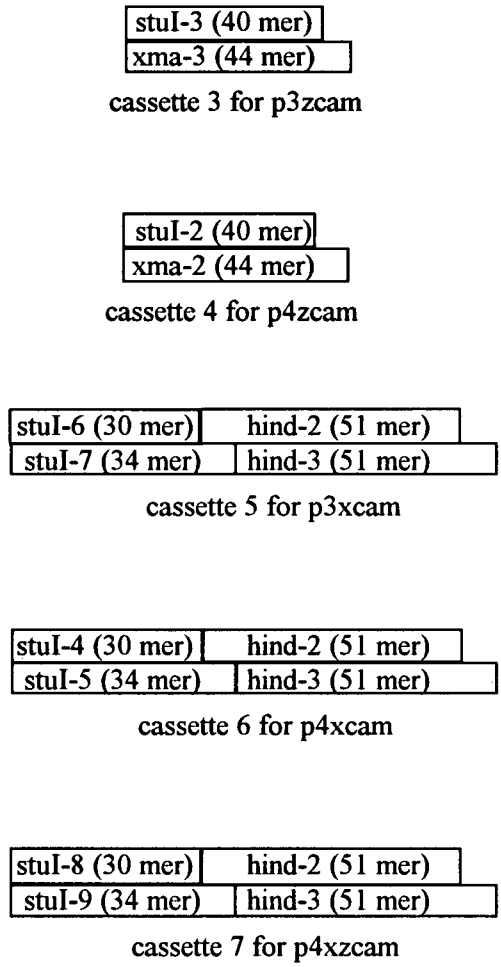

Figure 26. Schematic illustration of the DNA cassettes used for constructing p3xcam, p3zcam, p4xcam, p4zcam and p4xzcam. Each oligo is boxed. The size of each oligo is indicated in the brackets.

vectors, respectively. Similarly, the dephosphorylated *Stu* I/*Hin* dIII double digested pd133e large fragment was ligated with the phosphorylated cassettes 4, 5, and 6 for constructing the 3xCaM, 4xCaM, and 4xzCaM expression vectors, respectively. The ligation reactions were carried out as described in section 2.2.6.7, and the ligation mixtures were used to transform competent *E. coli* K12 UT 481 cells as described in section 2.2.2.

The p3zcam and p4zcam clones were identified by *Stu* I and *Xma* III digestion as described in section 2.2.6.9 and DNA sequencing as described in section 2.2.5. The p3xcam, p4xcam, and p4xzcam clones were identified by *Stu* I and *Hin* dIII digestion as described in section 2.2.6.9 and DNA sequencing as described in section 2.2.5. Each identified clone was stored in a 15% glycerol culture at -70° as described in section 2.2.6.10.

3.2.2. Expression and purification of CaM mutants

3xCaM, 3zCam, 4xCaM, 4zCaM, and 4xzCaM were expressed separately in a 20 L *E. coli* culture as described in section 2.2.8. Purification of these recombinant calmodulins was achieved essentially as described in section 2.2.9 ; however, the affinity chromatography procedure for these five CaM mutants were slightly different. Protein samples were applied to a phenyl-Sepharose column (10 mL bed volume) in the presence of 15 mM $CaCl_2$ and 0.5 M $(NH_4)_2SO_4$. The column was washed with 6 column volumes of the washing buffer consisting of 5 mM $CaCl_2$, 1 mM DTT, 50 mM Tris-HCl, pH 7.5. Each CaM mutant was eluted with 1 column volume of the elution buffer consisting of 5 mM EGTA, 1 mM DTT, 50 mM Tris-HCl, pH 7.5. The eluant was dialyzed at 4° against 4 L of deionized water with 6 changes. The dialysate was lyophilized, and the lyophilized protein was stored at -20°.

3.2.3. Characterization of CaM mutants

The homogeneity of the protein preparations was evaluated by SDS-polyacrylamide gel electrophoresis as described in section 2.2.11. The identity of each recombinant CaM mutant was confirmed by amino acid composition analysis as described in section 2.2.12 and mass spectrometry as described in section 2.2.13. The amino acid composition analysis of the CaM mutants was done in the Protein Service Laboratory at the University of Victoria. Far UV CD spectroscopy, fluorescence spectroscopy, calcium titration, calcium titration in the presence of W4I-M13 CaM binding peptide, and PDE stimulation assay of these five CaM mutants were carried out as described in sections 2.2.14 to 2.2.18.

3.3. RESULTS

3.3.1. Identification of the p3zcam and p4zcam clones

To identify the p3zcam and p4zcam clones, each plasmid sample was digested with *Stu* I and *Xma* III, respectively. The digested plasmid was analyzed by agarose gel electrophoresis (Figure 27). One band shown at a position of 3 kb in lanes 1, 2, 4, and 5 but not in lanes 3 and 6 indicates that the plasmids, p3zcam and 4zcam, were cut at one site by *Stu* I and *Xma* III, respectively. Another band shown at a position close to 2 kb in lanes 1, 2, 4, and 5 indicates that some plasmid DNA in the sample was undigested possibly due to insufficient enzyme or too high a concentration of plasmid in the digestion mixtures. The third band shown at a position between 6 and 7 kb in lane 4 also indicates the presence of undigested plasmid in the form of a polymer. The two bands shown in lanes 3 and 6 indicate the undigested plasmids in the forms of monomer and polymer, respectively. These results indicate that the two plasmids have one *Stu* I site and one *Xma* III site as expected.

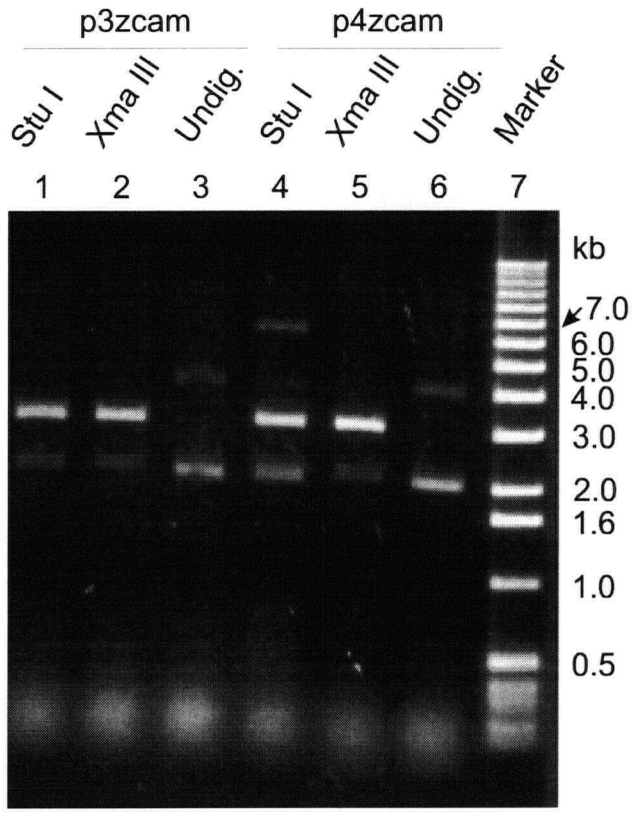

Figure 27. Agarose gel electrophoresis of restriction enzyme digested p3zcam and p4zcam. Plasmid p3zcam and p4zcam were digested with either *Stu* I or *Xma* III. Each digestion mixture was loaded on the gel (0.8%) as indicated by the enzyme used. Undig means the plasmid was undigested. The gel was run in TAE buffer (1 mM EDTA, 40 mM Tris-acetate, pH 8.3) and stained with ethidium bromide (1 μg/mL). The photo was taken under UV (254 nm) light.

The DNA sequencing of p3zcam was performed and the sequence corresponding to the nucleotide positions 102 to 460 of the synthetic CaM gene (460 bp) was confirmed except for the following expected changes: T283 to G283, C284 to G284, A290 to G290, G291 to A291, A297 to G297, and C407 to G407. These changes reflect the changes of the codon TTC for Phe92 to the codon TGG for Trp92, the codon AAA for Lys94 to the codon AAG for Lys94, the codon GAC for Asp95 to the codon AAC for Asn95, the codon AAC for Asn97 to the codon GAC for Asp97, and the codon GAC for Asp133 to the codon GAG for Glu133. The change of the codon AAA for Lys94 to the codon AAG for Lys94 was made to balance the GC and AT content in the sequence of the CaM gene. These results, together with the results from the restriction digestion of p3zcam, confirmed the identity of p3zcam.

The DNA sequencing of p4zcam was performed and the sequence corresponding to the nucleotide positions 102 to 460 of the synthetic CaM gene (460 bp) was confirmed except for the following expected changes: T283 to G283, C284 to G284, A290 to G290, A297 to G297, and C407 to G407. These changes reflect the changes of the codon TTC for Phe92 to the codon TGG for Trp92, the codon AAA for Lys94 to the codon AAG for Lys94, the codon AAC for Asn97 to the codon GAC for Asp97, and the codon GAC for Asp133 to the codon GAG for Glu133. Again, the change of the codon AAA for Lys94 to the codon AAG for Lys94 was made to balance the GC and AT contents in the sequence of the CaM gene. These results, together with the results from the restriction digestion of p4zcam, confirmed the identity of p4zcam.

3.3.2. Identification of the p3xcam, p4xcam, and p4xzcam clones

To identify the p3xcam, p4xcam, and p4xzcam clones, each plasmid sample was digested with *Stu* I and *Hin* dIII, respectively. The digested plasmid was analyzed by agarose gel electrophoresis (Figure 28). One band shown at a position of 3 kb in lanes 1, 2, 5, 6, 8, and 9 but not in lanes 3, 7, and 10 indicates that the plasmids, p4xzcam, p4xcam, and p3xcam, were cut at one site by *Stu* I and *Hin* dIII, respectively. Another band shown at a position close to 2 kb in lanes 1, 2, 5, 6, 8, and 9 indicates that some plasmid DNA in the samples was undigested as seen for p3zcam and p4zcam (Figure 27). The two bands shown in lanes 3, 7, and 10 indicate the undigested plasmids in the forms of monomer and polymer. These results indicate that the three plasmids, p3xcam, p4xcam, and p4xzcam, have one *Stu* I site and one *Hin* dIII site as expected.

The DNA sequencing of p3xcam was performed and the sequence corresponding to the nucleotide positions 75 to 460 of the synthetic CaM gene (460 bp) was confirmed except for the following expected changes: T283 to G283, C284 to G284, A290 to G290, G291 to A291, T309 to G309, C310 to A310, G311 to C311, and C407 to G407. These changes reflect the changes of the codon TTC for Phe92 to the codon TGG for Trp92, the codon AAA for Lys94 to the codon AAG for Lys94, the codon GAC for Asp95 to the codon AAC for Asn95, the codon TCG for Ser101 to the codon GAC for Asp101, and the codon GAC for Asp133 to the codon GAG for Glu133. Again, the change of the codon AAA for Lys94 to the codon AAG for Lys94 was made to balance the GC and AT content in the sequence of the CaM gene. These results, together with the results from the restriction digestion of p3xcam, confirmed the identity of p3xcam.

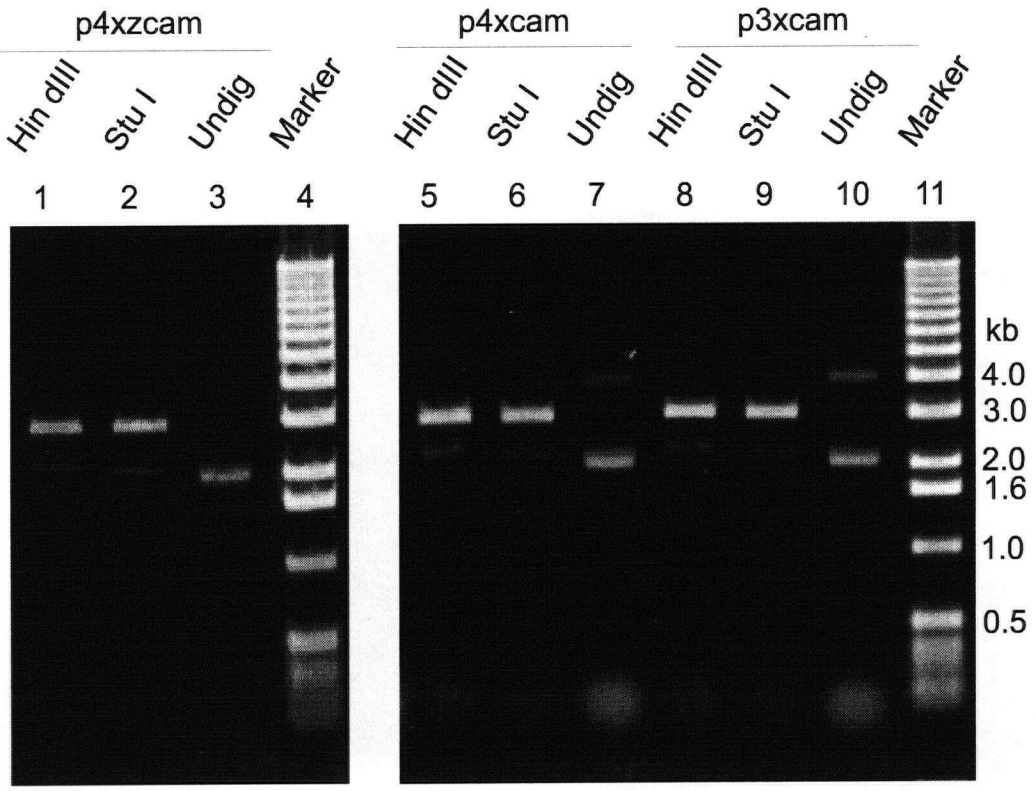

Figure 28. Agarose gel electrophoresis of restriction enzyme digested p3xcam, p4xcam, and p4xzcam. Plasmid p3xcam,p4xcam, and p4xzcam were digested with either *Stu* I or *Hinda* III. Each digestion mixture was loaded on the gel (0.8%) as indicated by the enzyme used. Undig means the plasmid was undigested. The gel was run in TAE buffer (1 mM EDTA, 40 mM Tris-acetate, pH 8.3) and stained with ethidium bromide (1 μg/mL). The photo was taken under UV (254 nm) light.

The DNA sequencing of p4xcam was performed and the sequence corresponding to the nucleotide positions 76 to 460 of the synthetic CaM gene (460 bp) was confirmed except for the following expected changes: T283 to G283, C284 to G284, A290 to G290, T309 to G309, C310 to A310, G311 to C311, and C407 to G407. These changes reflect the changes of the codon TTC for Phe92 to the codon TGG for Trp92, the codon AAA for Lys94 to the codon AAG for Lys94, the codon TCG for Ser101 to the codon GAC for Asp101, and the codon GAC for Asp133 to the codon GAG for Glu133. The change of the codon AAA for Lys94 to the codon AAG for Lys94 was due to the aforementioned reason. These results, together with the results from the restriction digestion of p4xcam, confirmed the identity of p4xcam.

The DNA sequencing of p4xzcam was performed and the sequence corresponding to the nucleotide positions 75 to 460 of the synthetic CaM gene (460 bp) was confirmed except for the following expected changes: T283 to G283, C284 to G284, A290 to G290, G291 to A291, A297 to G297, T309 to G309, C310 to A310, G311 to C311, and C407 to G407. These changes reflect the changes of the codon TTC for Phe92 to the codon TGG for Trp92, the codon AAA for Lys94 to the codon AAG for Lys94, the codon GAC for Asp95 to the codon AAC for Asn95, the codon AAC for Asn97 to the codon GAC for Asp97, the codon TCG for Ser101 to the codon GAC for Asp101, and the codon GAC for Asp133 to the codon GAG for Glu133. The change of the codon AAA for Lys94 to the codon AAG for Lys94 was due to the aforementioned reason. These results, together with the results from the restriction digestion of p4xzcam, confirmed the identity of p4xzcam.

3.3.3. Identification of 3xCaM, 3zCaM, 4xCaM, 4zCaM, and 4xzCaM

To evaluate the homogeneity of the recombinant calmodulin preparations, SDS-polyacrylamide gel electrophoresis of the purified protein samples was carried out in the presence and absence of calcium (Figure 29). First, single band at the position similar to that of bovine brain CaM was observed in the lanes loaded with the purified proteins, indicating that the protein preparations were fairly pure and had similar molecular weight as that of bovine brain CaM (16.7 kDa). Secondly, all CaM mutants exhibited a calcium-dependent migration shift on the gel as did bovine brain CaM. It was noticed that the calcium-dependent migration shift of all CaM mutants was not as large as that of commercially available bovine brain CaM. 3xCaM showed the smallest shift, whereas 4xzCaM exhibited the largest shift among the CaM mutants.

Amino acid compositions of the five purified recombinant proteins were analyzed (Table 10). Trp was not analyzed for these proteins (see section 2.3.4). Most of the observed values match the predicted values based on the amino acid sequences of the proteins. The fact that some observed values are lower than the predicted values may be due to oxidation (e.g., Met) or incomplete hydrolysis (e.g., Ile and Val) during the analysis.

The molecular weight of each CaM mutant was determined by mass spectrometry (Table 11). The observed values match the calculated values very well. These results, together with the results from the SDS polyacrylamide gel electrophoresis and the amino acid composition analysis, confirmed the identity of the five CaM mutants.

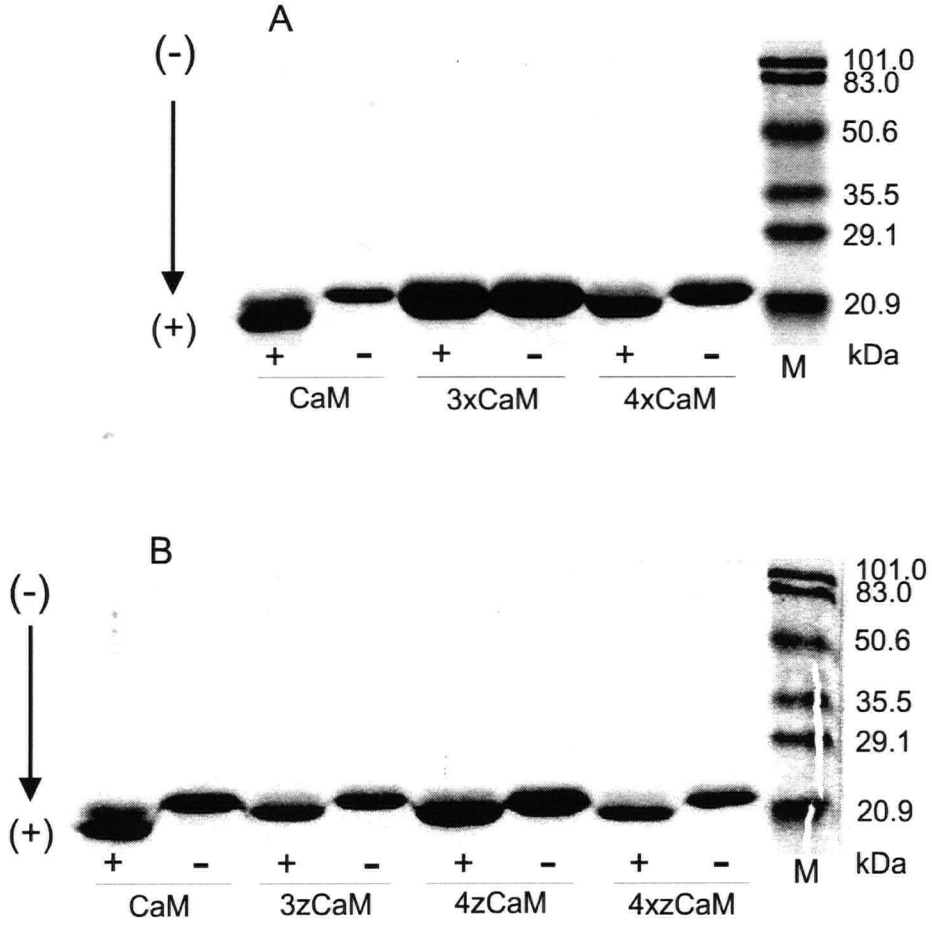

Figure 29. SDS-PAGE of 3xCaM, 3zCaM, 4xCaM, 4zCaM, and 4xzCaM. CaM: bovine brain CaM; M: a mixture of the pre-stained molecular weight standards; +: in the presence of 1 mM calcium; -: in the presence of 1 mM EGTA. The gels were run in Tris-glycine buffer (0.1% SDS, 50 mM Tris, 250 mM glycine, pH 8.3) under constant voltage (60 volts for the stacking gel, 100 volts for the resolving gel). The gels were stained with Coomassie Brilliant Blue R 250 (0.25%) (Sambrook *et al.*, 1989). See page xxi for nomenclature of the CaM mutants.

Table 10. Amino Acid Compositions of CaM Mutants[a]

Amino	3xCaM[b]		3zCaM		4xCaM		4zCaM		4xzCaM	
acid	P[c]	O[d]	P	O	P	O	P	O	P	O
Asp+Asn	25	24.96	24	24.21	25	24.76	24	24.00	25	24.89
Glu+Gln	27	27.58	27	28.61	27	27.38	27	28.69	27	28.31
Ser	3	3.00	4	3.68	3	3.31	4	3.78	3	3.36
Gly	11	10.61	11	10.43	11	11.18	11	10.89	11	12.01
His	1	0.93	1	0.90	1	0.87	1	0.93	1	1.12
Arg	5	5.11	5	5.48	5	5.50	5	5.38	5	5.49
Thr	10	9.13	10	9.09	10	9.18	10	9.17	10	9.26
Ala	11	11.00	11	11.00	11	11.00	11	11.00	11	11.00
Pro	2	1.31	2	1.29	2	1.38	2	1.39	2	1.83
Tyr	1	0.98	1	0.76	1	1.31	1	0.84	1	1.17
Val	9	8.46	9	8.42	9	8.83	9	8.53	9	7.77
Met	8	5.64	8	4.08	8	3.39	8	5.49	8	6.15
Ile	6	5.34	6	5.33	6	5.41	6	5.43	6	5.14
Leu	11	10.76	11	10.80	11	11.02	11	11.00	11	10.21
Phe	8	7.72	8	7.68	8	7.74	8	7.90	8	7.50
Lys	9	8.52	9	8.33	9	8.43	9	8.43	9	9.10
Trp	1	N/A[e]	1	N/A	1	N/A	1	N/A	1	N/A

[a] batch numbers are: 3xCaM, 032196; 3zCaM, 050696; 4xCaM, 040396; 4zCaM, 042196; 4xzCaM, 022896.

[b] see page xxi for nomenclature of the CaM mutants.

[c] P means predicted values based on the amino acid sequence of each protein.

[d] O means observed values from two measurements by HPLC analysis.

[e] not available.

Table 11. Molecular Weight of CaM Mutants

Protein	Predicted (Da)	Observed (Da) ± S.E.[b]
3xCaM (032196[a])	16706.56	16707.07 ± 0.36
3zCaM (050696[a])	16679.53	16679.81 ± 0.72
4xCaM (040396[a])	16707.54	16708.85 ± 1.02
4zCaM (042196[a])	16680.51	16680.31 ± 0.79
4xzCaM (022896[a])	16707.54	16707.89 ± 0.29

[a] batch number of the protein preparation. See page xxi for nomenclature of the CaM mutants.

[b] standard error calculated from the different charge states of the protein molecule in one measurement.

3.3.4. Far-UV CD spectra of CaM mutants

The normalized far-UV CD spectra of 3xCaM, 3zCaM, 4xCaM, 4zCaM and 4xzCaM in the absence and presence of calcium are presented in Figure 30. The overall shape of all the spectra are similar to each other and to those of VU-1 CaM (Figure 17). The corresponding molar ellipticity values and changes in ellipticity at 222 nm are presented in Table 12. Calcium was observed to induce an increase in the magnitude of the negative ellipticities of the five CaM mutants, indicating that calcium induces a change in the structures of the CaM mutants as it does to bovine brain CaM (Drabikowski *et al.*, 1982). The differences in the absolute molar ellipticities at 222 nm and the changes in ellipticities at 222 nm from the calcium-free state to calcium-bound state of the CaM mutants may indicate the effect of different mutations in the proteins.

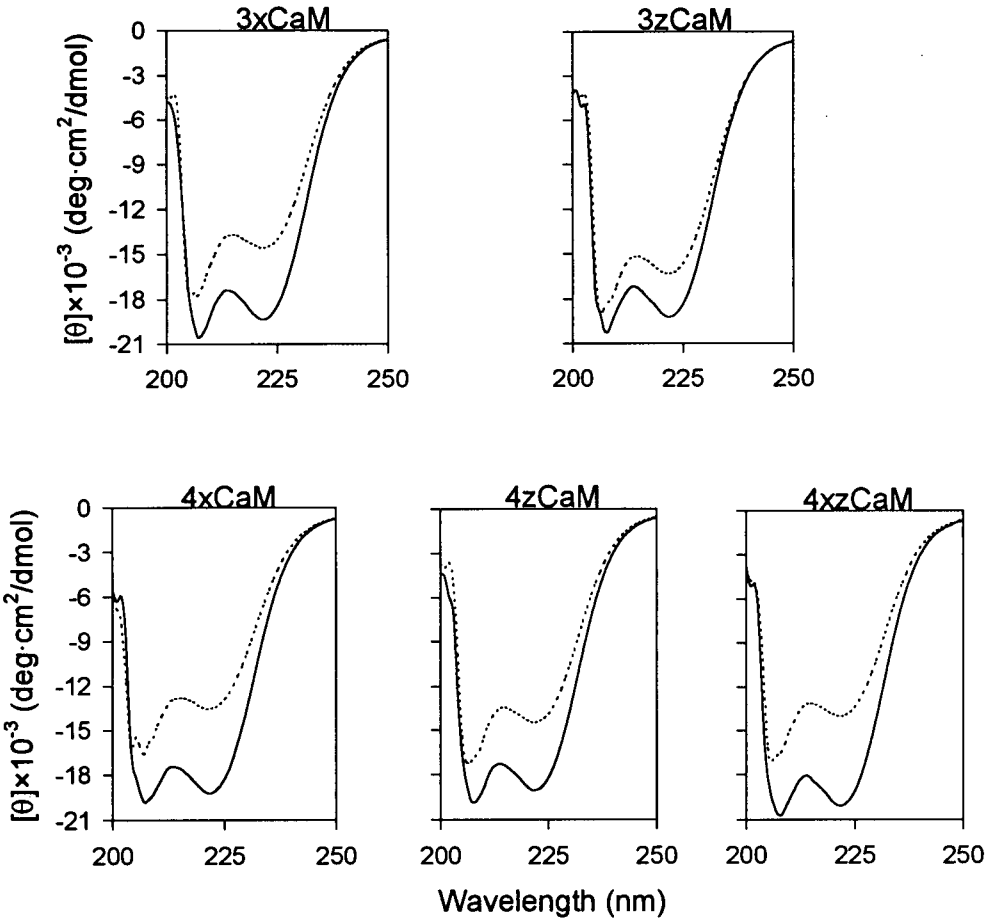

Figure 30. Far-UV CD spectra of 3xCaM, 3zCaM, 4xCaM, 4zCaM, and 4xzCaM. Spectra were recorded at the protein concentrations of 20-30 μM in the EGTA buffer (100 mM KCl, 1 mM EGTA, 50 mM MOPS, pH 7.20) before and after the addition of $CaCl_2$ to a final concentration of 40 mM. Data were normalized by molar concentrations of the proteins using the equation in section 2.2.14, page 71. The solid lines represent the spectra in the presence of calcium and the dashed lines represent the spectra in the absence of calcium. See page xxi for nomenclature of the CaM mutants.

Table 12. Molar Ellipticity of CaM Mutants[a]

CaM mutant	$[\theta]_{222} \times 10^{-3}$ (deg · cm^2/dmol) ± S.E.		
	- Ca^{2+}	+ Ca^{2+}	$\Delta[\theta]_{222}$
F92W/D133E[b]	12.20 ± 0.02	14.09 ± 0.04	1.89
3xCaM[c]	14.58 ± 0.30	19.35 ± 0.26	4.77
3zCaM	16.32 ± 0.16	19.22 ± 0.10	2.90
4xCaM	13.51 ± 0.07	19.22 ± 0.05	5.71
4zCaM	14.45 ± 0.11	19.05 ± 0.04	4.60
4xzCaM	14.01 ± 0.02	20.10 ± 0.03	6.09

[a] each value is presented as the mean ± S.E. of three separate measurements.
[b] data from Table 5.
[c] see page xxi for nomenclature of the CaM mutants.

3.3.5. Fluorescence emission spectra of CaM mutants

Fluorescence emission spectra of the five CaM mutants recorded in the absence and presence of calcium at the excitation wavelength of 282 nm are shown in Figure 31. A blue shift in the maximal emission wavelength was observed from 342 nm in the absence of calcium to 338 nm in the presence of calcium. Calcium was observed to induce a 1.5 to 2 fold increase in the tryptophan fluorescence intensity at 340 nm where the largest difference between the emission fluorescence intensity of the apoprotein and that of the Ca^{2+}-saturated protein occurred.

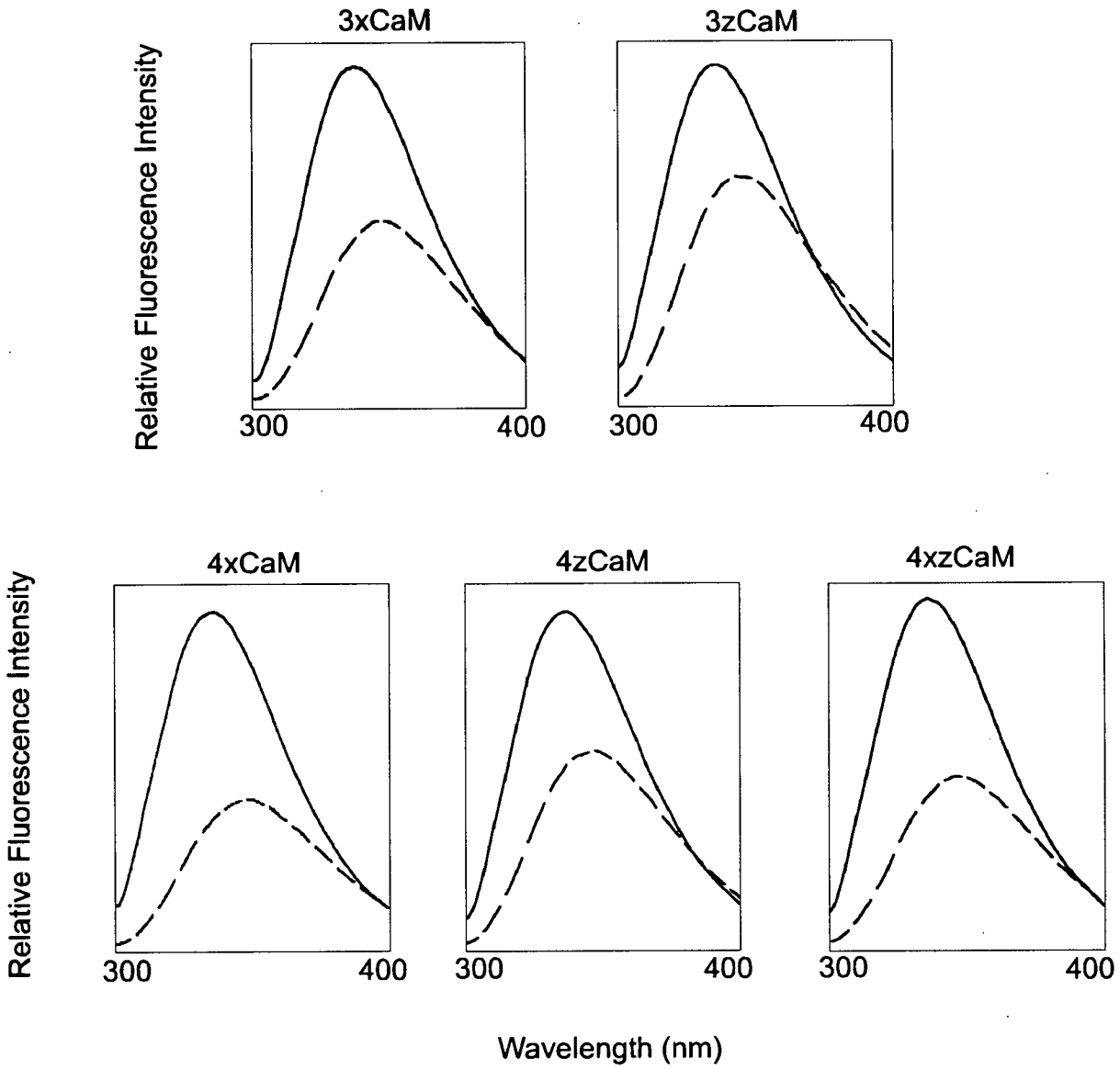

Figure 31. Fluorescence emission spectra of 3xCaM, 3zCaM, 4xCaM, 4zCaM, and 4xzCaM. Spectra were recorded at the excitation wavelength of 282 nm. The protein concentration was 10 μM in the EGTA buffer (100 mM KCl, 1 mM EGTA, 50 mM MOPS, pH 7.20) for each protein. The spectra were recorded before (dashed lines) and after (solid lines) the addition of $CaCl_2$ to a final concentrations of 16-18 mM. The slit width for excitation was 5 nm, and that for emission was 2 nm. See page xxi for nomenclature of the CaM mutants.

3.3.6. Calcium titration of CaM mutants

The calcium titration data did not fit to the three-site or four-site model as judged by the coefficient of variance (CV%) and the dependency (Tables 20 and 22 in the APPENDIX section). The two-site model was more appropriate to the data than the one-site model as judged by the fitting coefficients (Tables 16 and 18 in the APPENDIX section). Accordingly, the macroscopic calcium dissociation constants were calculated from each fitted two-site equation (Table 13). It was observed that biphasic patterns were more pronounced in the titration curves in an ascending order from 3xCaM, 3zCaM, 4xCaM, 4zCaM and 4xzCaM, indicating that the difference in calcium affinities between the two sites, sites III and IV, in the C-terminal domain of the proteins increases in the same order (Figure 32). Since D/E mutation at the +Z position of synthetic single site peptides caused either a drastic decrease or a complete loss in calcium binding capacity in the peptides (Reid & Procyshyn, 1995), and the same mutation in site IV of F92W/D133E CaM also decreased calcium affinity of site IV by 2760 fold (Table 7), we assumed that the D133E mutation would also cause a drastic decrease in calcium affinity in site IV of the five CaM mutants. Therefore, the smaller calcium dissociation constant was assigned to site III (K_{III}), and the greater value to site IV (K_{IV}) (Table 13). The K_{III} of these proteins changed significantly in a descending order from 3xCaM, 3zCaM, 4xCaM, 4zCaM to 4xzCaM, indicating an increase in the calcium affinity in site III in the same order (Table 13). These results demonstrate that the calcium affinity in site III increases with the increase in the number of acidic chelating residues from three to four, with the increase in the number of acid-pairs on the coordinating axes from zero to one and further to two, and with the change of location of the acid-pair from the X to Z axis. The K_{IV} values of the CaM mutants were also different from one another, indicating that

mutations in site III not only affect calcium affinity of this site but they have an effect on the partner site as well (Table 13).

The five CaM mutants have a n_H value of less than 1. These data indicate that a negative cooperativity is present between sites III and IV in these proteins, and the negativity increases as the calcium affinity of site III increases (Table 13).

Table 13. Calcium Dissociation Constants of CaM Mutants and Synthetic hlh Calcium Binding Peptides[a]

CaM Mutant	K_{III} (μM)	K_{IV} (μM)	n_H	Peptide[b]	K_d (μM)
F92W/D133E[c]	335±21	2760±45	0.89±0.02	3(DNS)	735±61[d]
3xCaM	237±7	3230±250	0.70±0.01	3x(NND)	524±16[d]
3zCaM	140±11	4461±69	0.56±0.02	3z(NDS)	58.8±0.1[d]
4xCaM	5.79±0.92	859±64	0.43±0.003	4x(DND)	42.1±1.2[e]
4zCaM	3.01±0.09	1846±24	0.23±0.003	4z(DDS)	29.2±1.0[e]
4xzCaM	2.09±0.14	1320±96	0.21±0.02	4xz(NDD)	19.1±0.2[d]

[a] Data are presented as the mean ± S.E. of six separate titrations. K is the calcium dissociation constant, and subscripts III and IV refer to sites III and IV, respectively. n_H is the Hill coefficient. See page xxi for nomenclature of the CaM mutants.

[b] Synthetic hlh calcium binding peptides derived from CaM site III encompassing residues 81-113. The number of acidic amino acid residues, the paired residues on either the X or Z axis or both axes, and the residues in positions +Y, +Z, and -X in the loop region are indicated in the peptide nomenclature. 3z(NDS), for example, indicates 3 acidic residues, two of them paired on the Z axis, and positions +Y, +Z, and -X occupied by N, D, and S, respectively.

[c] Data from Table 7.

[d] Data from Reid, 1990.

[e] Data from Procyshyn & Reid, 1993.

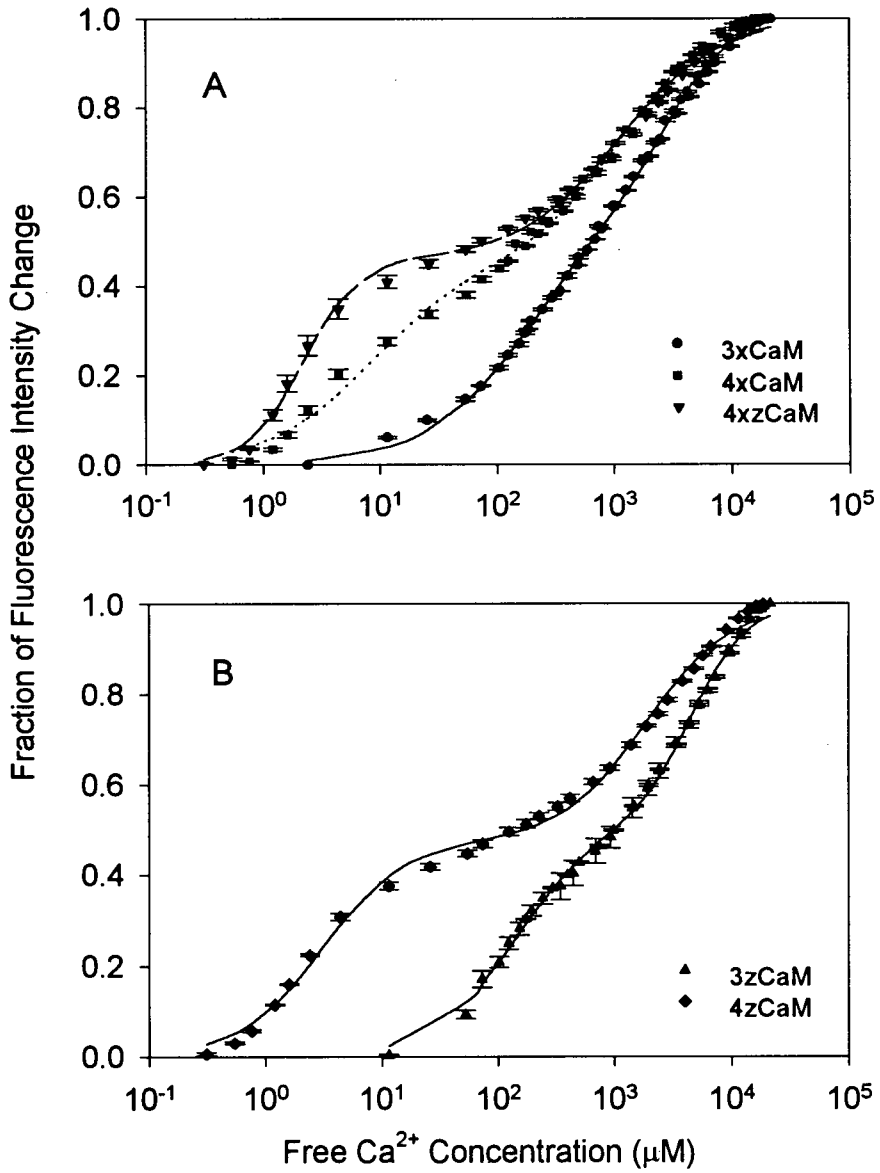

Figure 32. Calcium titration curves of 3xCaM, 3zCaM, 4xCaM, 4zCaM, and 4xzCaM. The protein concentration was 10 μM in the EGTA buffer (100 mM KCl, 1 mM EGTA, 50 mM MOPS, pH 7.20) for each CaM mutant. The fluorescence intensity changes were monitored at the excitation wavelength of 282 nm and the emission wavelength of 340 nm. Each data point represents the average of six separate titrations, and the standard error is shown as the error bar. Data were fitted to the two-site model. See page xxi for nomenclature of the CaM mutants.

3.3.7. Effect of W4I-M13 CaM-binding peptide on calcium affinity of CaM mutants

The fluorescence emission spectra of 3xCaM, 3zCaM, 4xCaM, 4zCaM, and 4xzCaM in the presence of W4I-M13 CaM-binding peptide are shown in Figure 33. A blue shift in the maximal emission wavelength was observed from 342 nm in the absence of calcium to 328 nm in the presence of calcium, which was more significant than the calcium-induced blue shift obtained in the absence of W4I-M13 peptide (342 to 338 nm, section 3.3.5.). The calcium-induced increase in the maximal fluorescence intensity in the presence of the peptide was also greater than that obtained in the absence of the peptide. These results suggest that the calcium-induced local environment change (to more hydrophobic) of Trp92 is greater in the presence of the peptide than in the absence of the peptide.

The calcium titration data obtained at the emission wavelength of 340 nm did not fit to the three-site or four-site model as judged by the coefficient of variance (CV%) and the dependency (Tables 21 and 23 in the APPENDIX section). The two-site model was more appropriate than the one-site model as judged by the fitting coefficient (Tables 17 and 19 in the APPENDIX section). The calcium titration data and the fitted curves are shown in Figure 34. The two macroscopic calcium dissociation constants calculated from each fitted two-site equation, K'_1 and K'_2, respectively, are presented in Table 14. Compared to K_{III} and K_{IV}, K'_1 and K'_2 of the same protein are significantly lower, indicating that the calcium affinities of the CaM mutants are significantly higher in the presence of the CaM-binding peptide than in the absence of the peptide (Tables 13 and 14). More interestingly, Hill coefficients of the CaM mutants are all greater than 1 in the presence of the peptide compared to n_H values less than 1 in the absence of the peptide (Tables 13 and 14).

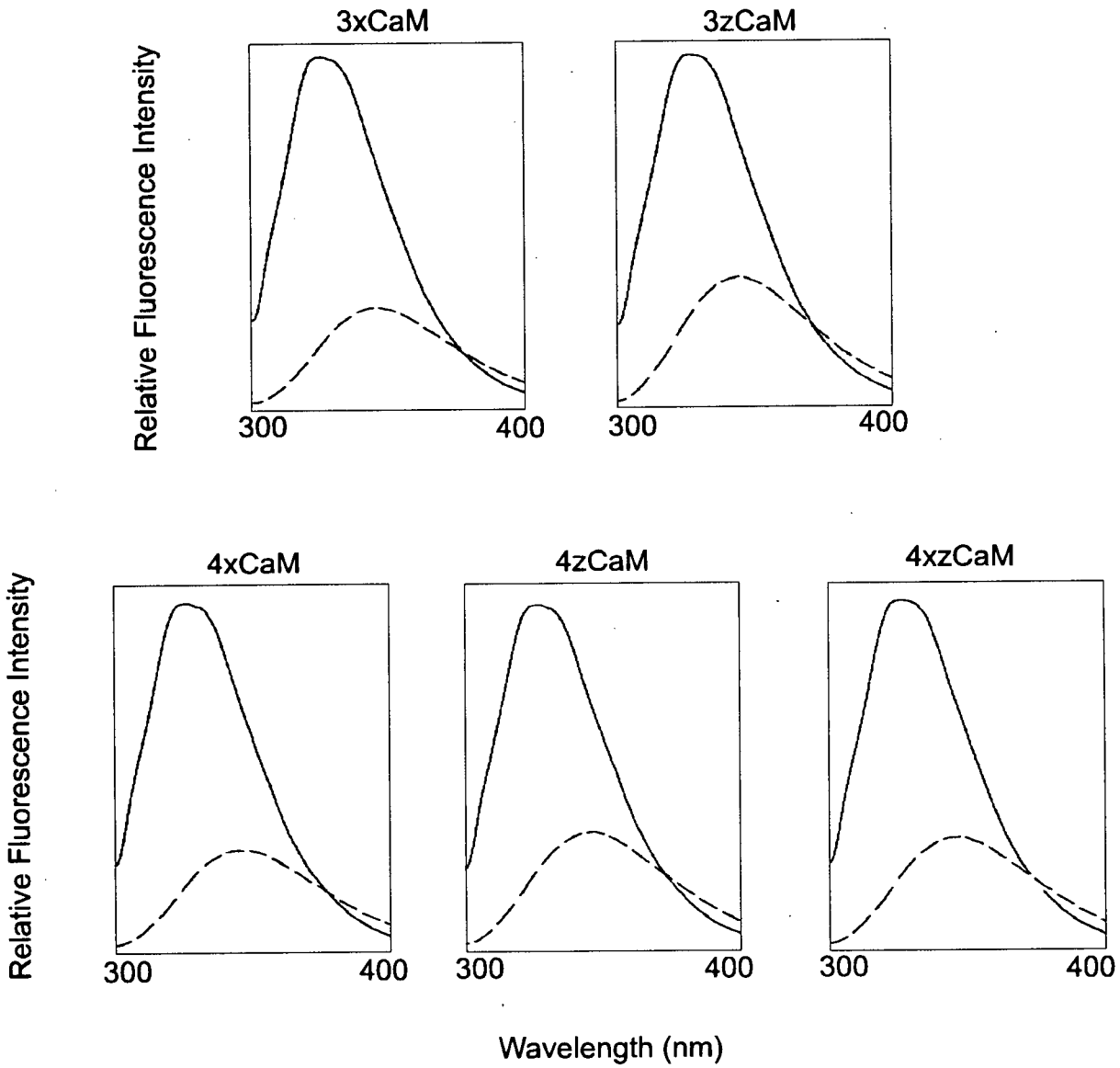

Figure 33. Fluorescence emission spectra of CaM mutants in the presence of W4I-M13 CaM-binding peptide. Spectra were recorded at the excitation wavelength of 282 nm. The protein concentrations were 10 μM in the EGTA buffer (100 mM KCl, 1 mM EGTA, 50 mM MOPS, pH 7.20), and protein to peptide ratios were 1:4 for all CaM mutants. The spectra were recorded before (dashed lines) and after (solid lines) the addition of $CaCl_2$ to saturation. The slit width for excitation was 5 nm, and that for emission was 2 nm. See page xxi for nomenclature of the CaM mutants.

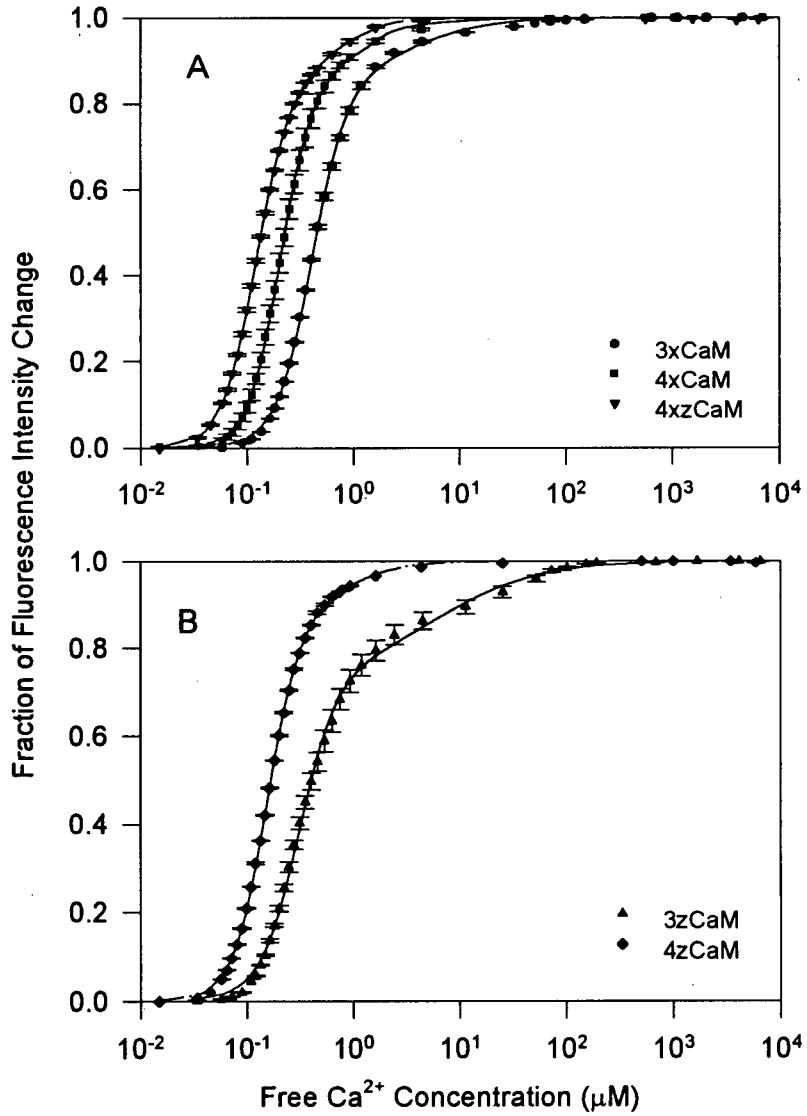

Figure 34. Calcium titration curves of CaM mutants in the presence of W4I-M13 CaM binding peptide. The protein concentrations were 10 μM, and the protein to peptide ratios were 1:4 for all mutants. Titrations were monitored at the excitation wavelength of 282 nm and the emission wavelength of 340 nm. Each data point represents the average of three separate titrations, and the standard error is shown as the error bar. Data were fitted to the two-site model. See page xxi for nomenclature of the CaM mutants.

Table 14. Calcium Dissociation Constants of CaM Mutants in the Presence of W4I-M13 CaM Binding Peptide[a]

CaM mutant	K'_1 (μM)	K'_2 (μM)	n_H
F92W/D133E[b]	0.358 ± 0.005	8.13 ± 0.75	1.81 ± 0.02
3xCaM	0.407 ± 0.001	2.75 ± 0.24	2.17 ± 0.05
3zCaM	0.310 ± 0.003	5.96 ± 0.79	1.41 ± 0.08
4xCaM	0.202 ± 0.003	0.977 ± 0.136	2.38 ± 0.01
4zCaM	0.155 ± 0.001	0.699 ± 0.071	2.33 ± 0.02
4xzCaM	0.122 ± 0.002	0.625 ± 0.030	2.26 ± 0.02

[a] data are expressed as the mean ± S.E. of three separate titrations. K'_1 and K'_2 are the apparent calcium dissociation constants of CaM, and n_H is the Hill coefficient. See page xxi for nomenclature of the CaM mutants.

[b] data from Table 8.

3.3.8. Phosphodiesterase regulation by CaM mutants

At low calcium concentrations (50 μM), each CaM mutant exhibited different PDE stimulation curve (Figure 35). The V_{max} values changed significantly in an ascending order from 3xCaM, 3zCaM, 4xCaM to 4zCaM, whereas the V_{max} value of 4xzCaM was not significantly different from that of 4zCaM (Table 15). The K_{50} values of the five CaM mutants ranged from 117 nM to 234 nM with no consistent pattern (Table 15). The V_{max} values obtained with the five CaM mutants, 3xCaM, 3zCaM, 4xCaM, 4zCaM, and 4xzCaM, were significantly lower than that obtained with F92W CaM, and the K_{50} values of the five CaM mutants were significantly greater than that of F92W CaM (Table 14). These results indicate that the five CaM mutants not only have different PDE stimulation activities with variable affinity for the enzyme among themselves but all of them have a lower PDE stimulation activity with a lower affinity for the enzyme than that of F92W CaM in the presence of 50 μM calcium.

At higher calcium concentrations (15 mM), the PDE stimulation curves of the five CaM mutants were superimposable (Figure 36). The V_{max} and K_{50} values of these CaM mutants were not significantly different from each other, or from that of F92W CaM (Table 15). These results indicate that the PDE regulatory activity of the five CaM mutants is restored to that of F92WCaM by high calcium concentrations.

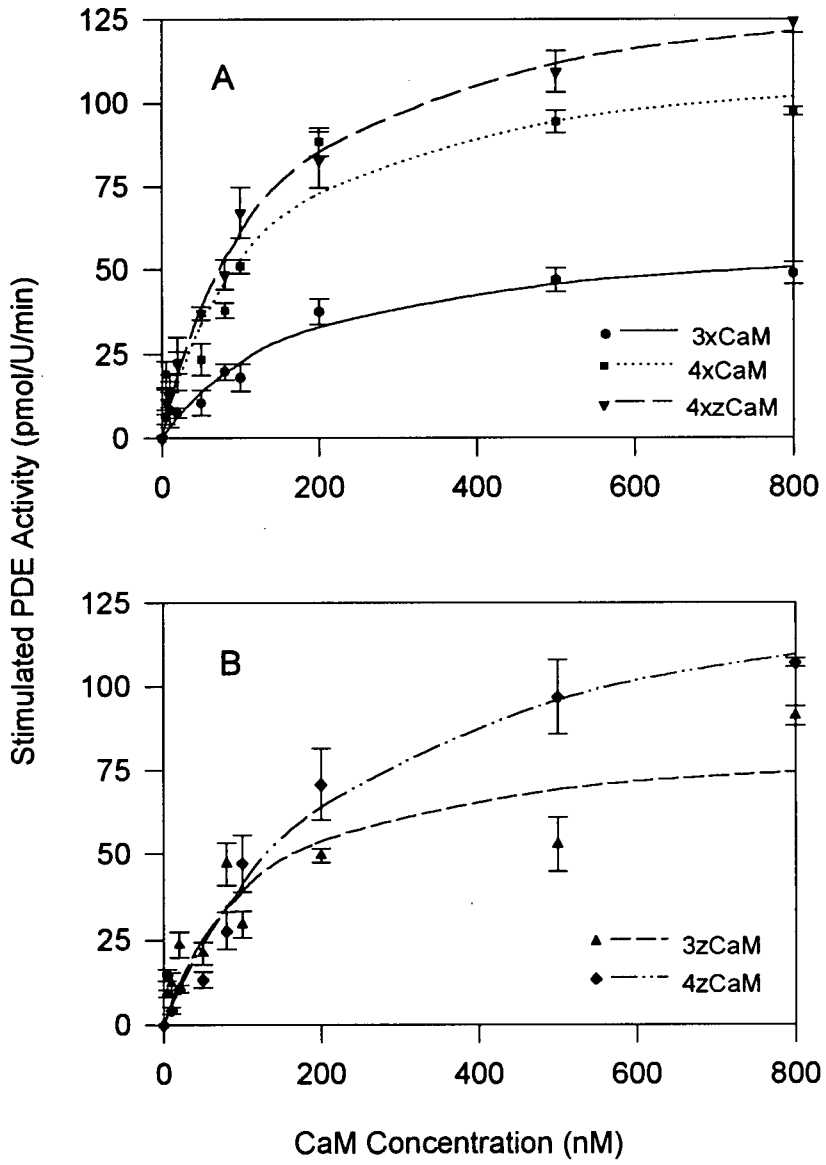

Figure 35. PDE stimulation curves of CaM mutants at low calcium concentration. Each assay was carried out in a buffer containing 0.2 U/mL of PDE, 2 mM [^{3}H]cAMP, 50 μM $CaCl_2$, 3 mM $MgSO_4$, 100 mM KCl, 40 mM Tris-HCl, pH 7.5 in a volume of 100 μl at 30 °C. Each data point represents the average of three separate measurements, and the standard error is shown as the error bar. See page xxi for nomenclature of the CaM mutants.

Table 15. Phosphodiesterase Stimulation Activity of CaM Mutants[a]

	50 μM Ca^{2+}		15 mM Ca^{2+}	
CaM mutant	V_{max} (pmol/U/min)	K_{50} (nM)	V_{max} (pmol/U/min)	K_{50} (nM)
F92W CaM[b]	169 ± 4.8	7.4 ± 0.7	166 ± 8	43 ± 6
F92W/D133E[b]	63.2 ± 2.5	185 ± 21	186 ± 9	41 ± 4
3xCaM	62.2 ± 1.4	186 ± 36	172 ±10	34 ± 2
3zCaM	85.3 ± 5.4	117 ± 16	171 ± 9	34 ± 2
4xCaM	118 ± 1	124 ± 11	190 ± 6	47 ± 12
4zCaM	141 ± 3	234 ± 39	175 ± 10	38 ± 2
4xzCaM	142 ± 6	134 ± 23	182 ± 12	44 ± 12

[a] Values are presented as the mean ± S.E. of three separate measurements. V_{max} is the maximal stimulated PDE activity by the CaM mutant, and K_{50} is the CaM concentration required for a half maximal stimulated PDE activity. See page xxi for nomenclature of the CaM mutants.

[b] Data from Table 9.

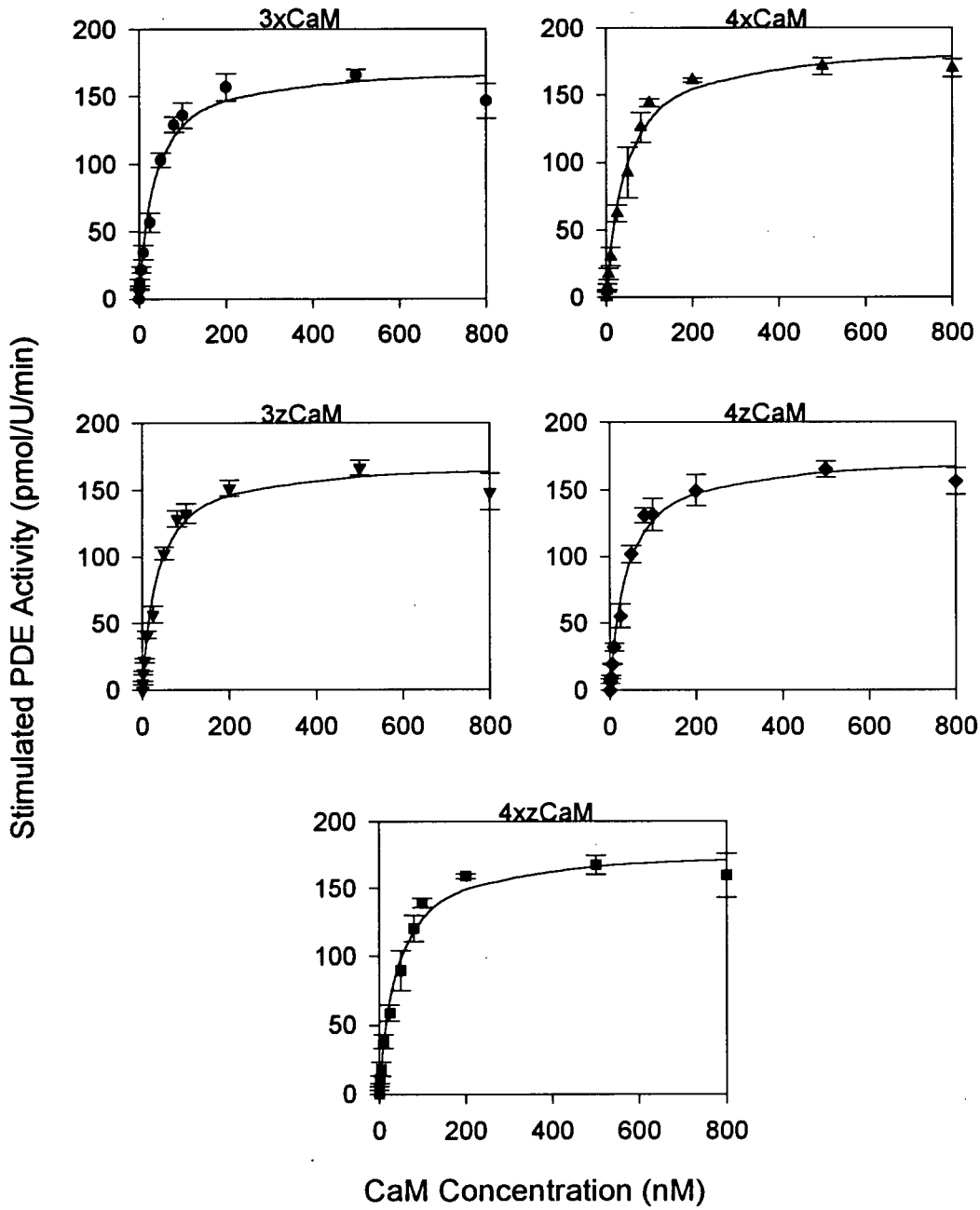

Figure 36. PDE stimulation curves of CaM mutants at high calcium concentration. Each assay was carried out in a buffer containing 0.2 U/mL of PDE, 2 mM [^{3}H]cAMP, 15 mM $CaCl_2$, 3 mM $MgSO_4$, 100 mM KCl, 40 mM Tris-HCl, pH 7.5 in a volume of 100 μl at 30 °C. Each data point represents the average of three separate measurements, and the standard error is shown as the error bar. See page xxi for nomenclature of the CaM mutants.

3.4. DISCUSSION

Five CaM mutants have been prepared to test the Acid Pair Hypothesis (APH, see section 1.1.5., page 12; Wu & Reid, 1997b). The mutants are altered in the +Y, +Z and –X chelating residue positions of site III to produce products that have either three or four acidic amino acid residues in chelating positions with the acidic residues paired on the X and/or Z axis (page xxi for nomenclature; Figure 25, page 111). Two other distinguishing features of the five mutants are relevant to their calcium binding characteristics. First, all mutants carry the D133E mutation that has been demonstrated to drastically reduce the calcium affinity of site IV (Table 7). Since site IV is cooperatively paired with site III in the C-terminal domain of calmodulin, this mutation was designed to eliminate cooperativity between these two sites. Second, Phe92 which immediately precedes the loop region of site III is replaced by a Trp residue to insert a fluorescent label to monitor the calcium induced conformational transitions in the C-terminal domain (Trigo-Gonzalez, *et al.*, 1992). An examination of the calcium dissociation constants of site III (K_{III}) in each of the mutants shows that the 4xz mutant has the highest calcium affinity followed by 4zCaM, 4xCaM, 3zCaM, 3xCaM and F92W/D133E. These results demonstrate that the number and location of the acidic residues in the chelating positions of site III significantly affect the calcium affinity of this site (Table 13).

The K_{III} values of the mutants with three acidic residues in chelating positions (see F92W/D133E CaM, 3xCaM and 3zCaM in Figure 25 and Table 13) are significantly higher when compared to the K_{III} values of those mutants with four acidic residues in chelating positions (see 4xCaM, 4zCaM and 4xzCaM in Figure 25 and Table 13). The data indicate that a hlh calcium-binding site with four acidic residues in the chelating positions has a higher

affinity for calcium than a site with three acidic chelating residues. This provides experimental support of the APH postulate that loops with four acidic chelating residues will have higher calcium affinity than those with three acidic chelating residues (Reid & Hodges, 1980).

Mutants with four acidic chelating residues in site III may have two acid-pairs with one on each of the X and Z axes (4xzCaM), one acid-pair on the Z axis (4zCaM) or one acid pair on the X axis (4xCaM) (Figure 25). The fact that the K_{III} for 4xzCaM is 1.4 and 2.8 fold lower than those of 4zCaM and 4xCaM, respectively, indicate that a hlh calcium-binding site with two acid-pairs on the X and Z axes has a higher calcium affinity than a site with one acid-pair on either the X or Z axis (Table 13). A possible interpretation of this data is that when four acidic residues are present in the ±X and ±Z positions (4xzCaM), the dentates are optimally separated and minimal electrostatic repulsion would result. When four acidic residues are present in the ±X, +Y and –Z positions (4xCaM) or in the +X, +Y, and ±Z positions (4xCaM), two dentates in the +X and +Y, or the +Y and +Z positions could possibly interact through electrostatic repulsion leading to a less stable inner sphere complex with the cation and a lower calcium affinity (Figure 25).

Among the CaM mutants which have three acidic chelating residues in site III, the K_{III} of F92W/D133E is 1.4 and 2.4 fold greater than those of 3xCaM and 3zCaM, respectively. This indicates that a hlh calcium-binding site with one-acid pair on either the X axis or Z axis has a higher affinity for calcium than a site with no acid-pairs at all (Table 13). This observation can also be explained as the unfavorable situation due to the dentate-dentate repulsion that may occur when two acidic residues are located at neighboring chelating positions in the sequence as in the case of F92W/D133E CaM (+X and +Y positions

occupied by Asp), whereas such electrostatic repulsion would not be predominant in 3xCaM and 3zCaM (Figure 25).

The demonstration that the K_{III} of 3zCaM is 1.7 fold lower than that of 3xCaM, and the K_{III} of 4zCaM is 1.9 fold lower than that of 4xCaM (Table 13) indicates that a hlh calcium-binding site with one acid-pair on the Z axis has a higher affinity for calcium than a site with one acid-pair on the X axis. This observation could be due to the fact that the residue in the –X position is indirectly involved in the chelation of calcium through a water molecule (reviewed in Strynadka & James, 1989; reviewed in McPhalen *et al.*, 1991; reviewed in Falke *et al.*, 1994; reviewed in Linse & Forsén, 1995). As a result, the X acid-pair contributes less negative charge in stabilizing the complex leading to a lower calcium affinity than the Z acid-pair.

To date, it would appear that the acid-pair is limited to Asp-Asp on the X axis and Asp-Glu on the Z axis. A Glu-Glu acid-pair on the Z axis has been shown to be detrimental to calcium affinity of the respective site in the CaM mutants in this study and in a previous study (Reid & Procyshyn, 1995). These results demonstrate that both the number and location of the acidic chelating residues as well as the type of acidic residue are critical to calcium affinity. Since the APH does not consider the type of acidic amino acid residue in the chelating positions, the result of reduction in calcium binding to hlh motifs with Glu in the +Z position is not predicted and appears to invalidate the hypothesis.

The K_{III} of the CaM mutants from the present study is compared to the calcium dissociation constant, K_d, of the synthetic single site calcium-binding peptides derived from CaM site III (Table 13). All the 33-residue single site peptides 3(DNS), 3x(NND), 3z(NDS), 4x(DND), 4z(DDS), and 4xz(NDD), have identical amino acid sequences in the loop to those

in site III of the CaM mutants, F92W/D133E, 3xCam, 3zCaM, 4xCaM, 4zCaM, and 4xzCaM, respectively, with the exception that the Tyr located in the –Y position in the peptides is replaced by a Phe in the proteins. By comparing the K_d of each single site peptide model with the K_{III} of the whole protein model [for example compare 3(DNS) with F92W/D133E] we find that the K_{III} of the whole protein model changes with the nature of the chelating residues in the site in a similar fashion to the changes in the K_d of the single site model These results demonstrate that the nature of the chelating residues, particularly the number and location of the acidic residues in the chelating positions, affect calcium affinity in the whole protein model in a manner similar to the isolated single site peptide model. The peptide model K_d values are greater than their respective protein model K_{III} values by a factor of 2.2 to 9.7 except for the 3z(NDS) and 3zCaM pair, indicating that there are still other interactions in the whole protein model that contribute to the increased calcium affinity of the site in the whole protein. The reason why the 3z(DNS) peptide has a 2.4 fold higher affinity for calcium than the 3zCaM protein is not clear at this moment but may possibly be a symptom of the reversal of cooperativity found in the mutants and discussed below. Although the whole protein model and the isolated single site model are not identical in terms of calcium affinity of the respective sites, the data from the present study and from the previous studies using the synthetic single site peptides demonstrate that the single hlh motif can be used as a valid model to study structure/calcium affinity relationships of the hlh motifs in calcium-binding proteins (Reid, 1990; Procyshyn & Reid, 1993).

Unlike K_{III}, K_{IV} did not show any consistent pattern in the different mutant proteins (Table 13). However, analysis of the Hill coefficients of the calcium titration of each mutant indicates that there is positive cooperativity in the F92W mutant that is lost in the

F92W/D133E mutant as a result of the D133E mutation. It is noteworthy that the subsequent mutants that have progressively increasing calcium affinities in site III also have a corresponding decrease in the Hill coefficient (Table 13). This is indicative of an increasing negative cooperativity as we increase the calcium affinity of site III. It would appear that the order of site filling in the natural protein (F92W and VU-1CaM) which is site IV → III is positively cooperative, however, reversing the order of filling of the sites (site III → site IV) produces negative cooperativity between the sites. Positive cooperativity is restored in all mutants when the sites are titrated in the presence of the CaM-binding fragment of myosin light chain kinase, W4I-M13 (Table 14). The full implication of these results for the biological role of calcium regulation of CaM and the erratic behavior of K_{IV} in these mutants is currently under investigation.

The macroscopic calcium binding affinity of the five CaM mutants is also increased in the presence of the CaM-binding peptide (Table 14). The reason for this fact has been discussed in section 2.4. We are not able to determine if the sequence of site filling reverts to the original IV → III sequence or remains as the III → IV sequence. It is also possible that the positive cooperativity indicated by the Hill coefficients is a result of the interaction between the N- and C-terminal domains (Table 14).

The PDE regulatory activity of the five CaM mutants were also examined in the presence of low (50 μM) and high (15 mM) calcium concentrations (Figures 35 and 36). At 50 μM calcium, 3xCaM, 3zCaM, 4xCaM, 4zCaM and 4xzCaM stimulate PDE to different maximal levels with different affinities for the enzyme (Table 15). The higher the calcium affinity of site III of the CaM mutant, the more efficient the protein is in PDE regulation. However, these CaM mutants are still less efficient in PDE regulation than F92W CaM in the

presence of 50 μM calcium. On the contrary, all five CaM mutants exhibit a similar PDE regulatory activity with a similar affinity for the enzyme to F92W CaM when the calcium concentration increases to 15 mM (Table 15). These results are consistent with those obtained with F92W/D133E CaM and demonstrate not only that the calcium bound form of CaM is essential for PDE regulation but that the multiple mutations alter calcium regulation of CaM mediated PDE activity without affecting CaM interaction with the enzyme.

CONCLUSIONS

Data from the present study demonstrate that Trp92 is a successful fluorescent label for monitoring the calcium induced conformational transition in the C-terminal domain of CaM. A novel CaM model (D133E CaM) has been prepared in which the mutated site IV has a 2760 fold lower calcium affinity, and at the same time, the unmutated site III has a 24 fold lower affinity for calcium. This is also a reverse in cooperativity from positive to negative between the two sites compared with the same sites in the unmutated CaM. This conservative D/E mutation at the relatively variable +Z chelating position causes greater changes in calcium affinity than the radical mutations which alter the highly conserved -Z position to uncharged Ala or Gln residues (Haiech *et al.*, 1991; Maune, *et al.*, 1992).

This study also demonstrates that the number, the location and the type of acidic chelating residues in the loop of the hlh calcium binding site affect calcium affinity of site III in the D133E CaM model. It appears that the number of acidic chelating residues dictates the calcium affinity of the site, while the location and the type of the acidic chelating residues fine-tune the calcium affinity. These results demonstrate the limited application of the APH to predicting the calcium affinities of a multi-site calcium binding protein. Conclusions drawn from studies on synthetic models of a single hlh calcium-binding site describing the effects of the number and location of acidic chelating residues on calcium affinity appear to be applicable to a multi-site protein. The fact that the D133E mutation drastically reduces the calcium affinity of site IV indicates that the type of acidic residue in chelating positions also plays a role in dictating calcium affinity of the hlh site. This mutation has also been useful in providing the opportunity for an interesting look at the possible relationship between the

sequence of filling the calcium binding sites and cooperative interactions between the sites. The IV → III sequence exhibits positive cooperativity while the III → IV sequence exhibits negative cooperativity. Although the calcium-binding loop provides primary control of the calcium binding parameters and the APH provides a basis to qualitatively predict the importance of particular loop residues for calcium affinity of the hlh calcium-binding motifs, evidence suggests that other regions of the hlh motifs also provide important control elements (Falke *et al.*, 1994; Linse & Forsén, 1995).

In addition, this study demonstrates that the CaM mutants which have reduced calcium affinity due to the D133E mutation have a less efficient phosphodiesterase (PDE) regulatory activity with a lower affinity for the enzyme than F92W CaM. The calcium-bound form of CaM is essential for PDE regulation, and the mutations alter calcium regulation of CaM-mediated PDE activity without affecting the interaction between CaM and the enzyme. Finally, this study shows W4I-M13, a 26 residue peptide analog derived from the CaM binding domain of skeletal muscle myosin light chain kinase, significantly increases the overall calcium affinity of VU-1 CaM and the CaM mutants.

FUTURE STUDIES

This study demonstrates that the number, the location, and the type of the acidic chelating residues significantly affect calcium affinity of a hlh calcium binding site in a CaM model. These parameters can be used to predict calcium affinity of single hlh calcium binding sites in calcium binding proteins. However, further studies are needed to gain more insight into the molecular mechanisms by which calcium binds to a multi-site calcium-binding protein.

1). The Acid-Pair Hypothesis (APH) states that a high affinity calcium binding site will have a maximum of two acid-pairs on both the X and Z axes (section 1.1.5, pages 11-12). Accordingly, a site with more than four or less than four acidic chelating residues should have lower calcium affinity than a site with four acidic chelating residues. This study clearly demonstrates that a site with three acidic chelating residues has a lower affinity for calcium than a site with four acidic chelating residues in the D133E CaM model, however, it is unknown whether it is true that a site with five or six acidic chelating residues has a lower affinity for calcium than a site with four acidic chelating residues.

2). According to the APH, site IV of F92W CaM and F92W/D133E CaM should have similar and very high affinity for calcium because of the two acid-pairs located on the X and Z axes in both proteins. The only difference between the two proteins is that the Z acid-pair in F92W CaM is an Asp-Glu pair, whereas the Z acid-pair in F92W/D133E CaM is a Glu-Glu pair. The fact that this site in F92W/D133E CaM has a very low affinity for calcium (2760 fold lower than that in F92W CaM) indicates that not only is the location of acidic chelating residues critical to calcium affinity but the type of acidic residues can greatly affect

calcium affinity. Accordingly, it is necessary to examine the effect of different combinations of acid-pairs on calcium affinity of the hlh calcium binding motif in the D133E CaM model.

3). The original APH does not consider the effect of the type of acidic residues nor the effect of non-chelating residues. Since non-chelating residues affect calcium affinity of the synthetic single site peptide model (Shaw *et al.*, 1991; Franchini & Reid, unpublished results) and hlh calcium binding sites in proteins (reviewed in Falke *et al.*, 1994; reviewed in Linse & Forsén, 1995), it would be interesting to test the results from the synthetic single site peptide mode in the D133E CaM model.

4). The D133E CaM model in which site IV is almost inactivated with respect to calcium binding capacity was used in this study. It would be interesting to examine the effect of the nature of the chelating residues on calcium affinity of site III in a CaM model in which site IV has a normal calcium affinity. By comparing the results from the present study with the results from this proposed study, we should be able to see the effect of the cooperative interactions between sites III and IV on calcium affinity of site III.

5). A change in calcium binding affinity can result from a change in the free energy of either the calcium-free state or the calcium-bound state, or both. Thermostability measurements by CD, fluorescence, or DSC on the CaM mutants may allow one to determine the free energy change of the mutants.

6). A change in calcium binding affinity can result from a change in either the on-rate or the off-rate, or both. Kinetic measurements of calcium binding to the CaM mutants by stop-flow fluorescence technique can be performed to determine the change in off and on rates.

7). Ion binding studies can be carried out to determine if the mutations in site III in the CaM mutants affect the selectivity of the site or the partner site for calcium relative to magnesium and other ions.

8). Isothermal titration calorimetry measurements of calcium binding to the CaM mutants can be performed to obtain more information such as $\Delta H°$ and $\Delta S°$ for each calcium binding event which may provide additional insight into the mechanism by which each mutation affects calcium binding.

9). The CD data presented in this thesis indicate that the mutations in site III do have some effects on the overall structures of the mutants. NMR measurements of the mutants may allow one to gain more information of structural changes of each mutant in more detail.

REFERENCES

Alexander, A., Cimler, B. M., Meier, K. E., & Storm, D. R. Regulation of calmodulin binding to P57, a neurospecific calmodulin binding protein. (1987) *J. Biol. Chem.* **262**, 6108-6113.

Alexander, A., Wakim, B. T., Doyle, G. S., Walsh, K.A.,& Storm, D. R. Identification and characterization of the calmodulin-binding domain of neuromodulin, a neurospecific calmodulin-binding protein. (1988) *J. Biol. Chem.* **263**, 7544-7549.

Anderson, J. M., Charbonneau, H., Jones, H. P., McCann, R. O., & Cormier, M. J. Characterization of plant nicotinamide adenine dinucleotide kinase activator protein and its identification as calmodulin. (1980) *Biochemistry* **19**, 3113-3120.

Ando, Y., Watanabe, M., Akatsuka, H., Tokumitsu, H., & Hidaka, H. Site-directed mutation makes rabbit calcyclin dimer. (1992) *FEBS Lett.* **314**, 109-113.

Babu, Y. S., Sack, J. S., Greenhough, T. J., Bugg, C. E., Means, A. R., & Cook, W. J. Three-dimensional structure of calmodulin. (1985) *Nature* **315**, 37-40.

Babu, Y. S., Bugg, C. E., & Cook, W. J. Structure of calmodulin refined at 2.2 Å resolution. (1988) *J. Mol. Biol.* **204**, 191-204.

Babu, A., Su., H., Ryu, Y., & Gulati, J. Determination of residue specificity in the EF-hand of troponin C for calcium coordination, by genetic engineering. (1992) *J. Biol. Chem.* **267**, 15469-15474.

Barbato, G., Ikura, M., Kay, L. E., Pastor, R. W., & Bax, A. Backbone dynamics of calmodulin studied by 15N relaxation using inverse detected two-dimensional NMR spectroscopy: the central helix is flexible. (1992) *Biochemistry* **31**, 5269-5278.

Baron, G., Demaille, J., & Dutruge, E. The distribution of parvalbumins in muscle and in other tissue. (1975) *FEBS Lett.* **56**, 156-160.

Barskaya, N.V., & Gusev, N.B. Biological activities of bovine cardiac-muscle troponin C C-terminal peptide (residues 84-161). (1982) *Biochem. J.* **207**, 185-192.

Baudier, J., Labourdette, G., & Gerard, D. Rat brain S100b protein: purification, characterization, and ion binding properties. A comparison with bovine S100b protein. (1985) *J. Neurochem.* **44**, 76-84.

Baudier, J., Glasser, N., & Gerard, D. Ion binding to S100 proteins: I. Calcium- and zinc-binding properties of bovine brain S100αα, S100a (αβ), and S100b (ββ) proteins: Zn^{2+} regulates Ca^{2+} binding on S100b protein. (1986) *J. Biol. Chem.* **261**, 8192-8201.

Beckingham, K. Use of site-directed mutations in the individual Ca^{2+}-binding sites of calmodulin to examine Ca^{2+}-induced conformational changes. (1991) *J. Biol. Chem.* **266**, 6027-6030.

Benzonana, G., Capony, J-P., & Pechere, J-F. The binding of calcium to muscular parvalbumins. (1972) *Biochim. Biophys. Acta* **278**, 110-116.

Berchtold, M. W., Heizmann, C. W., & Wilson, K. J. Primary structure of parvalbumin from rat skeletal muscle. (1982) *Eur. J. Biochem.* **127**, 381-389.

Bertrand, B., Wakabayashi, S., Ikeda, T., Pouysségur, J., & Shigekawa, M. The Na^+/H^+ exchanger isoform 1 (NHE1) is a novel member of the calmodulin-binding proteins: identification and characterization of calmodulin-binding sites. (1994) *J. Biol. Chem.* **269**, 13703-13709.

Blumenthal, D. K., & Stull, J. T. Activation of skeletal muscle myosin light chain kinase by calcium (2+) and calmodulin. (1980) *Biochemistry* **19**, 5608-5614.

Boguta, G., Stepkowski, D., & Bierzynski, A. Theoretical estimation of the calcium-binding constants for proteins from the troponin C superfamily based on a secondary structure prediction methods I. Estimation procedure. (1988) *J. Theor. Biol.* **135**, 41-61.

Bredderman, P. J., & Wasserman, R. H. Chemical compositions, affinity for calcium and some related properties of the vitamin D dependent calcium-binding protein. (1974) *Biochemistry.* **13**, 1687-1694.

Brodin, P., Johansson, C., Forsén, S., Drakenberg, T., & Grundström, T. Functional properties of calbindin D_{9K} mutants with exchanged Ca^{2+} binding sites. (1990) *J. Biol. Chem.* **265**, 11125-11130.

Brostrom, C O., Huang, Y. C., Breckenridge, B. M., & Wolff, D. J. Identification of a calcium binding protein as a calcium dependent regulator of brain adenylate cyclase. (1975) *Proc. Natl. Acad. Sci. USA* **72**, 64-68.

Brown, S. E., Martin, S. R., Bayley, P. M. Kinetic control of the dissociation pathway of calmodulin-peptide complexes. (1997) *J. Biol. Chem.* **272**, 3389-3397.

Burtnick, L. D., & Kay, C. M. The calcium-binding properties of bovine cardiac troponin C. (1977) *FEBS Lett.* **75**, 105-110

Callisano, P., Alema, S., & Fasella, P. Interaction of S-100 protein with cations and liposomes. (1974) *Biochemistry.* **13**, 4553-4560.

Carafoli, E., & Zurini, M. The Ca^{2+}-pumping ATPase of plasma membranes: purification, reconstitution and properties. (1982) *Biochim. Biophys. Acta* **683**, 279-301.

Cave, A., Parello, J., Drakenberg, T., Thulin, E., & Lindman, B. Mg^{2+} binding to parvalbumins studied by ^{25}Mg and ^{113}Cd NMR spectroscopy. (1979) *FEBS Lett.* **100**, 148-152.

Cheung, W. Y. Cyclic 3', 5'-nucleotide phosphodiesterase: demonstration of an activator. (1970) *Biochem. Biophys. Res. Commun.* **38**, 533-538.

Cheung, W. Y., Bradham, L. S., Lynch, T. J., Lin, Y. M., & Tallant, E. A. Protein activator of cyclic 3', 5'-nucleotide phosphodiesterase of bovine or rat brain also activates adenylate cyclase. (1975) *Biochem. Biophys. Res. Commun.* **66**, 1055-1062.

Clore, G. M., Bax, A., Ikura, M., & Gronenborn, A. M. Structure of calmodulin-target peptide complexes. (1993) *Current Opinion in Structural Biology* **3**, 838-845.

Coffee, C. J., & Bradshaw, R. A. Carp muscle calcium-binding protein. I. Characterization of the tryptic peptides and the complete amino acid sequence of component B. (1973) *J. Biol. Chem.* **248**, 3302-3312.

Cohen, A. I., Hall, I. A., & Ferrendelli, J. A. Calcium and cyclic nucleotide regulation in incubated mouse retina. (1978) *J. Gen. Physiol.* **71**, 595-612.

Cohen, P. The regulation of phosphorylase kinase activity by calmodulin and troponin. (1988) In *Calmodulin* (Cohen, P., & Klee, C. B. eds) pp123-144, Elsevier, Amsterdam, Netherlands.

Cohen, P. & Klee, C. B. eds. (1988) In *Calmodulin*. Elsevier, Amsterdam, Netherlands.

Cohen, P. The structure and regulation of protein phosphatases. (1989) *Annu. Rev. Biochem.* **58**, 453-508.

Colbran, R. J., Smith, M., Schworer, C. M., Fong, Y. L., Soderling, T. R. Regulatory domain of calcium/calmodulin-dependent protein kinase II. (1989) *J. Biol. Chem.* **264**, 4800-4804.

Collins, J. H., Potter, J. D., Horn, M. J., Wilshire, G., & Jackman, N. The amino acid sequence of rabbit skeletal muscle troponin C: gene replication and homology with calcium-binding proteins from carp and hake muscle. (1973) *FEBS Lett.* **36**, 268-272.

Corneliussen, B., Holm, M., Waltersson, Y., Onions, J., Hallberg, B., Thornell, A., & Grundstrom, T. Calcium/calmodulin inhibition of basic-helix-loop-helix transcription factor domains. (1994) *Nature* **368**, 760-764.

Cox, J. A., Wnuk, W., & Stein, E. A. Regulation of calcium-binding by magnesium. (1977) In *Calcium Binding Proteins and Calcium Function.* (Wasserman, R. H., Corradino, R. A., Carafoli, E., Kretsinger, R. H., MacLennan, D. H., & Siegel, F. L., eds.) pp266-269, Elsevier North-Holland, Inc., New York, New York.

Crivici, A., & Ikura, M. Molecular and structural basis of target recognition by calmodulin. (1995) *Annu. Rev. Biophys. Biomol. Struct.* **24**, 84-116.

Crouch, T. H., & Klee, C. B. Positive cooperative binding of calcium to bovine brain calmodulin. (1980) *Biochemistry.* **19**, 3692-3698.

Da Silva, A. C., De Araujo, A. H., Herzberg, O., Mout, J., Sorenson, M., & Reinach, F. C. Troponin C mutants with increased calcium affinity. (1993) *Eur. J. Biochem.* **213**, 599-604.

Dahlquist, F. W. The meaning of Scatchard and Hill plots. (1978) *Methods in Enzymology* **48**, 270-299.

Dasgupta, M., Honeycutt, T., & Blumenthal, D. K. The γ-subunit of skeletal muscle phosphorylase kinase contains two noncontiguous domains that act in concert to bind calmodulin. (1989) *J. Biol. Chem.* **264**, 17156-17163.

Donato, R. Perspectives in S-100 protein biology. (1991) *Cell Calc.* **12**, 713-726.

Dotson, D. G., & Putkey, J. A. Differential recovery of Ca^{2+} binding affinity in mutated EF-hands of cardiac troponin C. (1993) *J. Biol. Chem.* **268**,24067-24073.

Drabikowski, W., Brzeska, H., & Venyaminov, S. Y. Tryptic fragment of calmodulin: Ca^{2+}- and Mg^{2+}- induced conformational changes. (1982) *J. Biol. Chem.* **257**, 11584-11590.

Drake, S. K., Lee, K. L., & Falke, J. J. Tuning the equilibrium ion affinity and selectivity of the EF-hand calcium binding motif: substitutions at the gateway position. (1996) *Biochemistry* **35**, 6697-6705.

Durussel, I., Rhyner, J. A., Strehler, E. E., & Cox, J. A. Cation binding and conformation of human calmodulin-like protein. (1993) *Biochemistry.* **32**, 6089-6094.

Epel, D., Patton, C., Wallace, R. W., & Cheung, W. Y. Calmodulin activates NAD kinase of sea urchin eggs: an early event of fertilization. (1981) *Cell* **23**, 543-549.

Epstein, P., Means, A. R., & Berchtold, M. W. Isolation of a rat parvalbumin gene and full length cDNA. (1986) *J. Biol. Chem.* **261**, 5886-5891.

Falke, J. J., Snyder, E. E., Thatcher, K. C., & Voertler, C. S. Quantitating and engineering the ion specificity of an EF-hand-like Ca^{2+} binding site. (1991) *Biochemistry* **30**, 8690-8697.

Falke, J. J., Drake, S. K., Hazard, A. L., & Peersen, O. B. Molecular tuning of ion binding to calcium signaling proteins. (1994) *Quart. Rev. Biophys.* **27**, 219-290

Finn, B. E., Evenäs, J., Drakenberg, T., Waltho, J. P., Thulin, E., & Forsén, S. Calcium-induced structural changes and domain autonomy in calmodulin. (1995) *Nature Struct. Biol.* **2**, 777-783.

Fullmer, C. S., & Wasserman, R. H. Bovine intestinal calcium-binding protein: cation-binding properties, chemistry and trypsin resistance. (1977) In *Calcium Binding Proteins and Calcium Function*. (Wasserman, R. H., Corradino, R. A., Carafoli, E., Kretsinger, R. H., MacLennan, D. H., & Siegel, F. L., eds.) pp303-312, Elsevier North-Holland, Inc., New York, New York.

Fullmer, C. S., & Wasserman, R. H. The amino acid sequence of bovine intestinal calcium-binding protein. (1981) *J. Biol. Chem.* **256**, 5669-5674.

Gagné, S. M., Tsuda, S., Li, M. X., Smillie, L. B., & Sykes, B. D. Structures of the troponin C regulatory domains in the apo and calcium-saturated states. (1995) *Nature. Struct. Biol.* **2**, 784-789.

George, S. E., Su, Z., Fan, D., & Means, A. R. Calmodulin-cardiac troponin C chimeras. (1993) *J. Biol. Chem.* **268**, 25213-25220.

George, S. E., Su, Z., Fan, D., Wang, S., & Johnson, J. D. The fourth EF-hand of calmodulin and its helix-loop-helix components: impact on calcium binding and enzyme activation. (1996) *Biochemistry* **35**, 8307-8313.

Gillen, M. F., Banville, D., Rutledge, R. G., Narang, S., Seligy, V. L., Whitfield, J. F., & MacManus, J. P. A complete complementary DNA for the oncodevelopmental calcium-binding protein, oncomodulin. (1987) *J. Biol. Chem.* **262**, 5308-5312.

Gillis, J. M. Relaxation of vertebrate skeletal muscle. A synthesis of the biochemical and physiological approaches. (1985) *Biochim. Biophys. Acta* **811**, 97-145.

Golden, L. F., Corson, D. C., Sykes, B. D., Banville, D., & MacManus, J. P. Site-specific mutants of oncomodulin: ^{1}H NMR and optical stopped-flow studies of the effect on the metal binding properties of an $Asp^{59} \rightarrow Glu^{59}$ substitution in the calcium-specific site. (1989) *J. Biol. Chem.* **264**, 20314-20319.

Golosinska, K., Pearlstone, J. R., Borgford, T., Oikawa, K., Kay, C. M.,, Carpenter, M. R., & Smillie, L. B. Determination of and corrections to sequences of turkey and chicken troponin C: effects of Thr-130 to Ile mutation on Ca^{2+} affinity. (1991) *J. Biol. Chem.* **266**, 15797-15809.

Goodman, M., Pechere, J.-F., Haiech, J., & Demaille, J. G. Evolutionary diversification of structure and function in the family of intracellular calcium-binding proteins. (1979) *J. Mol. Evol.* **13**, 331-352.

Grabarek, Z., Tao, T., & Gergely, J. Molecular mechanism of troponin C function. (1992) *J. Muscle Res. Cell Motil.* **13**, 383-393.

Grandjean, J., Laszlo, P., & Gerday, C. Sodium complexation by the calcium binding site of parvalbumin. (1977) *FEBS Lett.* **81**, 376-80.

Greaser, M. L., & Gergely, J. Purification and properties of the components from troponin. (1973) *J. Biol. Chem.* **248**, 2125-2133.

Greenlee, D. V., Andreasen, T. J., & Storm, D. R. Calcium-independent stimulation of *Bordetella pertussis* adenylate cyclase by calmodulin. (1982) *Biochemistry* **21**, 2759-2764.

Guerrini, R., Menegazzi, P., Anacardio, R., Marastoni, M., Tomatis, R., Zorzato, F., & Treves, S. Calmodulin binding sites of the skeletal, cardiac, and brain ryanodine receptor Ca^{2+} channels: modulation by the catalytic subunit of cAMP-dependent protein kinase? (1995) *Biochemistry.* **34**, 5120-5129.

Haiech, J., Derancourt, J., Pechere, J-F., & Dedman, J. G. Magnesium and calcium binding to parvalbumins: evidence for differences between parvalbumins and an explanation of their relaxing function. (1979) *Biochemistry.* **18**, 27522758.

Haiech, J., Klee, C. B., & Demaille, J. G. Effect of cations on affinity of calmodulin for calcium: ordered binding of calcium ions allows the specific activation of calmodulin-stimulated enzymes. (1981) *Biochemistry.* **20**, 3890-3897.

Haiech, J., Kilhoffer, M.-C., Lukas, T. J., Craig, T. A., Roberts, D. M., & Watterson, D. M. Restoration of the calcium binding activity of mutant calmodulins toward normal by the presence of a calmodulin binding structure. (1991) *J. Biol. Chem.* **266**, 3427-3431.

Han, C. H., & Roberts, D. M. Altered methylation substrate kinetics and calcium binding of a calmodulin with a Val136→Thr substitution. (1977) *Eur. J. Biochem.* **244**, 904-912.

Hapak, R. C., Lammers, P. J., Palmisano, W. A., Birnbaum, E. R., & Henzl, M. T. Site-specific substitution of glutamate for aspartate at position 59 of rat oncomodulin. (1989) *J. Biol. Chem.* **264**, 18751-18760.

Hashimoto, Y., & Perrino, B. A. Identification of an autoinhibitory domain in calcineurin. (1990) *J. Biol. Chem.* **265**, 1924-1927.

Heidorn, D. B., & Trewhella, J. Comparison of the crystal and solution structures of calmodulin and troponin C. (1988) *Biochemistry*, **27**, 909-915.

Herzberg, O., & James, M. N. G. Structure of the calcium regulatory muscle protein troponin C at 2.8 Å resolution. (1985) *Nature* **313**, 653-658.

Herzberg, O., Moult, J., & James, M. N. G. A model for the Ca^{2+}-induced conformational transition of troponin C: a trigger for muscle contraction. (1986) *J. Biol. Chem.* **261**, 2638-2644.

Herzberg, O., James, M. N. G. Refined crystal structure of troponin C from turkey skeletal muscle at 2.0 Å resolution. (1988) *J. Mol. Biol.* **203**, 761-779.

Hilt, D. C., & Kligman, D. The S-100 protein family: a biochemical and functional overview. (1991) In *Novel Calcium-Binding Proteins.* (Heizmann, C. W. ed) pp65-103. Springer-Verlag, New York, New York.

Hitchamn, A. J., & Harrison, J. E. Calcium binding proteins in the duodenal mucosa of the chick, rat, pig, and human. (1972) *Can J. Biochem.* **50**, 758-765.

Holroyde, M. J., Robertson, S. P., Hohnson, J. D., Solaro, R. J., & Potter, J. D. The calcium and magnesium binding sites on cardiac troponin and their role in the regulation of myofibrillar adenosine triphosphatase. (1980) *J. Biol. Chem.* **255**, 11688-11693.

Hse, Y. -T., & Molday, R. S. Modulation of the cGMP-gated channel of rod photoreceptor cells by calmodulin. (1993) *Nature* **361**, 76-79.

Hubbard, M., Bradley, M., Sullivan, P., Shepherd, M., & Forrester, I. Evidence for the occurrence of calmodulin in the yeasts *Candida albicans* and *Saccharomyces cerevisiae.* (1982) *FEBS Lett.* **137**, 85-88.

Hubbard, S. R., Hodgson, K. O., & Doniach, S. Small-angle X-ray scattering investigation of the solution structure of troponin C. (1988) *J. Biol. Chem.* **263**, 4151-4158.

Hutnik, C. M. L., MacManus, J. P., Banville, D., & Szabo, A.G. Comparison of metal ion-induced conformational changes in parvalbumin and oncomodulin as probed by the intrinsic fluorescence of trptophan 102. (1990) *J. Biol. Chem.* **265**, 11456-11464.

Iio, T., & Hoshihara, Y. Static and kinetic studies on carp muscle parvalbumins. (1984) *J. Biochem.* **96**, 321-328.

Ikura, M., Spera, S., Barbato, G., Kay, L. E., Krinks, M., & Bax, A. Secondary structure and side-chain ^{1}H and ^{13}C resonance assignments of calmodulin in solution by heteronuclear multidimensional NMR spectroscopy. (1991) *Biochemistry* **30**, 9216-9228.

Ikura, M., Clore, G.M., Gronenborn, A.M., Zhu, G., Klee, C.B., & Bax, A. Solution structure of a calmodulin-target peptide complex by multidimensional NMR. (1992) *Science* **256**, 632-638.

Johnson, J. D., Collins, J. H., Robertson, S. P., & Potter, J. D. A fluorescent probe study of Ca^{2+} binding to the Ca^{2+}-specific sites of cardiac troponin and troponin C. (1980) *J. Biol. Chem.* **255**, 9635-9640.

Keller, C. H., Olwin, B. B., LaPorte, D. C., & Storm, D. R. Determination of the free-energy coupling for binding of calcium ions and troponin I to calmodulin. (1982) *Biochemistry.* **21**, 156-162.

Kennedy, M. B., McGuinness, T., & Greengard, P. A calcium/calmodulin dependent protein kinase from mammalian brain that phosphorylates Synapsin I: partial purification and characterization. (1983) *J. Neurosci.* **3**, 818-831.

Kesvatera, T., Jonsson, B., Thulin, E., & Linse S. Binding Ca^{2+} to calbindin D_{9K}: structure stability and function at high salt concentration. (1994) *Biochemistry* **33**, 14170-14176.

Kilby, P. M., Van Eldik, L. J., Roberts, J. C. K. Nuclear magnetic resonance assignments and secondary structure of bovine S100β protein. (1995) *FEBS Lett.* **363**, 90-96.

Kilhoffer, M.-C., Roberts, D.M., Adibi, A.O., Watterson, D.M., & Haiech, J. Investigation of the mechanism of calcium binding to calmodulin: use of an isofunctional mutant with a tryptophan introduced by site-directed mutagenesis. (1988) *J. Biol. Chem.* **263**, 17023-17029.

Kilhoffer, M.-C., Kubina, M., Travers, F., & Haiech, J. Use of engineered proteins with internal tryptophan reporter groups and perturbation techniques to probe the mechanism of ligand-protein interactions: investigation of the mechanism of calcium binding to calmodulin. (1992) *Biochemistry* **31**, 8098-8106.

Klee, C. B., Crouch, T. H., & Krinks, M. H. Calcineurin: a calcium- and calmodulin-binding protein of the nervous system. (1979) *Proc. Natl. Acad. Sci. USA* **76**, 6270-6273.

Klee, C. B. & Vanaman, T. C. Calmodulin. (1982) *Advances in Prot. Chem.* **35**, 213-321.

Klee, C. B. Interaction of calmodulin with Ca^{2+} and target proteins. (1988) In *Calmodulin* (Cohen P., & Klee C. B. eds.) pp35-56. Elsevier, Amsterdam, Netherlands.

Kördel, J., Skelton, N. J., Akke, M. & Chazin, W. J. High resolution solution structure of calcium-loaded calbindin D_{9K}. (1993) *J. Mol. Biol.* **231**, 711-734.

Kretsinger, R. H., & Nockolds, C. E. Carp muscle calcium-binding protein. (1973) *J. Biol. Chem.* **248**, 3313-3326.

Kretsinger, R. H. Structure and evolution of calcium-modulated proteins. (1980) *CRC Crit. Rev. Biochem.* **8**, 119-174.

Kuboniwa, H., Tjandra, N., Grzesiek, S., Ren, H., Klee, C.B., & Bax, A. Solution structure of calcium-free calmodulin. (1995) *Nature Struct. Biol.* **2**, 768-776.

Leavis, P. C., & Kraft, E. L. Calcium binding to cardiac troponin C. (1978) *Arch. Biochem. Biophys.* **186**, 411-415.

Leavis, P. C., & Gergely, J. Thin filament proteins and thin filament-linked regulation of vertebrate muscle contraction. (1984) *CRC Crit. Rev. Biochem.* **16**, 235-305.

Levine, B. A., Coffman, D. M. D., & Thornton, J. M. Calcium binding by troponin C. A proton magnetic resonance study. (1977) *J. Mol. Biol.* **115**, 743-760.

Levine, B. A., & Williams, R. J. P. Calcium binding to proteins and other large biological anion centers. (1982) In *Calcium and Cell Function*. (Cheung, W. Y. ed) **2**, 1-38, Academic Press, New York, New York.

Li, M. X., Chandra, M., Pearlstone, J. R., Racher, K. I., Trio-Gonzalez, G., Borgford, T., Kay, C. M., & Smillie, L. B. Properties of isolated recombinant N and C domains of chicken troponin C. (1994) *Biochemistry* **33**, 917-925.

Lin, Y. M., Liu, Y. P., & Cheung, W. Y. (1974) Cyclic 3',5'-nucleotide phosphodiesterase: purification, characterization, and active form of the protein activator from bovine brain. *J. Biol. Chem.* **249**, 4943-4954.

Linse, S., Brodin, P., Drakenberg, T., Thulin, E., Sellers, P., Elmdén, K., Grundström, T., & Forsén, S. Structure-function relationships in EF-hand Ca^{2+}-binding proteins: protein engineering and biophysical studies of calbindin D_{9K}. (1987) *Biochemistry* **26**, 6723-6735.

Linse, S., Helmersson, A., & Forsén S. Calcium binding to calmodulin and its globular domains. (1991a) *J. Biol. Chem.* **266**, 8050-8054.

Linse, S., Johansson, C., Brodin, P., Grundström, T., Drakenberg, T., & Forsén, S. Electrostatic contribution to the binding of calcium in calbindin D_{9K}. (1991b) *Biochemistry* **30**, 154-162.

Linse, S., Bylsma, N. R., Drakenberg, T., Sellers, P., Forsén, S., Thulin, E., Svensson, L. A., Zajtzeva, I., Zajtsev, V., & Marek, J. A calbindin D_{9K} mutant with reduced calcium affinity and enhanced cooperativity. Metal ion binding, stability, and structural studies. (1994) *Biochemistry* **33**, 12478-12486.

Linse, S., Jonsson, B., & Chazin, W. J. The effect of protein concentration on ion binding. (1995) *Proc. Natl. Acad. Sci. U.S.A.* **92**, 4748-4752.

Linse, S., & Forsen, S. Determinants that govern high-affinity calcium binding. (1995) *Adv. Second Messng. Phosphoprot. Res.* **30**, 89-151.

Liu, Y., & Storm, D. R. Regulation of free calmodulin levels by neuromodulin: neuron growth and regeneration. (1990) *Trends Pharmacol. Sci.* **11**, 107-111.

Lukas, T. J., Craig, T. A., Roberts, D. M., Watterson, D. M., Haiech, J., & Prendergast, F. G. An interdisciplinary approach to the molecular mechanisms of calmodulin action: comparative biochemistry, site-specific mutagenesis, and protein engineering. (1987) In *Calcium-Binding Proteins in Health and Disease* (Norman, A.W., *et al.*, eds.) pp533-543, Academic Press, New York, New York.

MacManus, J. P. Occurrence of a low-molecular-weight calcium binding protein in neoplastic liver. (1979) *Cancer Res.* **39**, 3000-3005.

MacManus, J. P. & Whitfield, J. F. Oncomodulin: a calcium-binding protein from hepatoma. (1983) In *Calcium and Cell Function.* (Cheung, W. Y. ed) **4**, 411-440, Academic Press, New York, New York.

MacManus, J. P., Watson, D. C., & Yaguchi, M. The complete amino acid sequence of oncomodulin — a parvalbumin-like calcium-binding protein from Morris hepatoma 5123tc. (1983) *Eur. J. Biochem.* **136**, 9-17.

MacManus, J. P., Szabo, A. G., & Williams, R. E. Conformational changes induced by binding of bivalent cations to oncomodulin, a parvalbumin-like tumor protein. (1984) *Biochem. J.* **220**, 261-268.

MacManus, J. P. Hutnik, C. M. L., Sykes, B. D., Szabo, A. F., Williams, T. C., & Banville, D. Characterization and site-specific mutagenesis of the calcium-binding protein oncomodulin produced by recombinant bacteria. (1989) *J. Biol. Chem.* **264**, 3470-3477.

Malik, N. A., Anantharamaiah, G. M., Gawish, A., & Cheung, H. C. Structural and biological studies on synthetic peptide analogues of a low-affinity calcium-binding site of skeletal troponin C. (1987) *Biochim. Biophys. Acta* **911**, 221-230.

Mani, R. S., Shelling, J. G., Sykes, B. D., & Kay, C. M. Spectral studies on the calcium binding properties of bovine brain S-100b protein. (1983) *Biochemistry* **22**, 1734-1740.

Marsden, B. J., Hodges, R. S., & Sykes, B. D. ^{1}H NMR studies of synthetic peptide analogues of calcium-binding site III of rabbit skeletal troponin C: effect on the lanthanum affinity of the interchanges of aspartic acid and asparagine residues at the metal ion coordinating positions. (1988) *Biochemistry* **27**, 4198-4206.

Marsden, B. J., Shaw, G. S., & Sykes, B. D. Calcium binding proteins. Elucidating the contributions to calcium affinity from an analysis of species variants and peptide fragments. (1990) *Biochem. Cell Biol.* **68**, 587-601.

Martin, S. R., Linse, S., Johansson, C., Bayley, P. M., & Forsen S. Protein surface charges and Ca^{2+} binding to individual sites in calbindin D_{9K}: stopped-flow studies. (1990) *Biochemistry* **29**, 4188-4192.

Matsushima, N., Izumi, Y., Matsuo, T., Yoshino, H., Ueki, T., & Miyake, Y. Binding of both Ca^{2+} and mastoparan to calmodulin induces a large change in the tertiary structure. (1989) *J. Biochem. (Tokyo)* **105**, 883-887.

Matsuura, I., Ishihara, K., Nakai, Y., Yazawa, M., Toda, H., & Yagi, K. A site-directed mutagenesis study of yeast calmodulin. (1991) *J. Biochem. (Tokyo)* **109**, 190-197.

Matsuura, I., Kimura, E., Tai, K., & Yazawa, M., Mutagenesis of the fourth calcium-binding domain of yeast calmodulin. (1993) *J. Biol. Chem.* **268**, 13267-13273.

Maune, J. F., Klee, C. B., & Beckingham, K. Ca^{2+} binding and conformational change in two series of point mutations to the individual Ca^{2+}-binding sites of calmodulin. (1992) *J. Biol. Chem.* **267**, 5286-5295.

McPhalen, C. A., Strynadka, N. C. J., & James, M. N. G. Calcium-binding sites in proteins: a structural perspective. (1991) *Adv. Prot. Chem.* **42**, 77-144.

Meador, W. E., Means, A. R., & Quiocho, F. A. Target enzyme recognition by calmodulin: 2.4 Å structure of a calmodulin-peptide complex. (1992) *Science* **257**, 1251-1255.

Meador, W. E., Means, A. R., & Quiocho, F. A. Modulation of calmodulin plasticity in molecular recognition on the basis of X-ray structure. (1993) *Science* **262**, 1718-1721.

Menegazzi, P., Larini, F., Treves, S. Guerrini, R., Quadroni, M., & Zorzato, F. Identification and characterization of three calmodulin binding sites of the skeletal muscle ryanodine receptor. (1994) *Biochemistry.* **33**, 9078-9084.

Minowa, O., & Yagi, K. Calcium binding to tryptic fragments of calmodulin. (1984) *J. Biochem.* (Tokyo) **96**, 1175-1182.

Moeschler, H. J., Schaer, J. J., & Cox, J. A. A thermodynamic analysis of the binding of calcium and magnesium ions to parvalbumin. (1980) *Eur. J. Biochem.* **111**, 73-78.

Moews, P. C., & Kretsinger, R. H. Refinement of the structure of carp muscle calcium-binding parvalbumin by model building and difference fourier analysis. (1975) *J. Mol. Biol.* **91**, 201-228.

Muto, S., & Miyachi, S. Properties of a protein activator of NAD kinase from plants. (1977) *Plant Physiol.* **59**, 55-60.

Negele, J. C., Dotson, D. G., Liu, W., Sweeney, H. L., & Putkey J. A. Mutation of the high affinity calcium binding sites in cardiac troponin C. (1992) *J. Biol. Chem.* **267**, 825-831.

Ogawa, Y., & Tanokura, M. Calcium binding to calmodulin: effects of ionic strength, Mg^{2+}, pH and temperature. (1984) *J. Biochem. (Tokyo)* **95**, 19-28.

Ogawa, Y. Calcium binding to troponin C and troponin: effects of Mg^{2+}, ionic strength and pH. (1985) *J. Biochem. (Tokyo)* **97**, 1011-1023.

Ohno, S., Emori, Y., Imajoh, S., Kawasaki, H., Kisargi, M., & Suzuki, K. Calcium-dependent protease (calcium protease). (1984) *Nature* **312**, 566-570.

O'Neil, K. T., & DeGrado, W. F. How calmodulin binds its targets: sequence independent recognition of amphiphilic α-helices. (1990) *Trends Biochem. Sci.* **15**, 59-??.

Palmisano, W. A., Treviño, C. L., & Henzl, M. T. Site-specific replacement of amino acid residues within the CD binding loop of rat oncomodulin. (1990) *J. Biol. Chem.* **265**, 14450-14456.

Parmacek, M. S., & Leiden, J. M. Structure, function, and regulation of troponin C. (1991) *Circulation* **84**, 991-1003.

Pauls, T. L., Durussel, I., Cox, J. A., Clark, I. D., Szabo, A. G., Gagné, S. M., Sykes, B. D., & Berchtold, M. W. Metal binding properties of recombinant rat parvalbumin wild-type and F102W mutant. (1993) *J. Biol. Chem.* **268**, 20897-20903.

Pearlstone, J. R., Borgford, T., Chandra, M., Oikawa, K., Kay, C. M., Herzberg, O., Moult, J., Herklotz, A., Reinach, F. C., & Smillie, L. B. Construction and characterization of a spectral probe mutant of troponin C: application to analyses of mutants with increased Ca^{2+} affinity. (1992) *Biochemistry* **31**, 6545-6553.

Pechère, J. F. The significance of parvalbumins among muscular calciproteins. (1977) In *Calcium Binding Proteins and Calcium Function.* (Wasserman, R. H., Carradino, R. A., Carafoli, E., Kretsinger, R. H., Maclennan, D. H., & Siegal, F. L. eds) pp 212-221, Elsevier North Holland, Inc., New York, New York.

Pedigo, S. & Shea, M.A. Quantitative endoproteinase GluC footprinting of cooperative Ca^{2+} binding to calmodulin: proteolytic susceptibility of E31 and E87 indicates interdomain interactions. (1995) *Biochemistry* **34**, 1179-1196.

Permyakov, E. A., Yarmolenko, V. V., Emelyanenko, V. I., Burstein, E. A., Closset, J., & Gerday, C. Fluorescence studies of the calcium binding to whiting (*Gadus merlangus*) parvalbumin. (1980) *Eur. J. Biochem.* **109**, 307-315.

Permyakov, E. A., Medvedkin, V. N., Kalinichenko, L. P., & Burstein, E. A. Comparative study of physicochemical properties of two pike parvalbumins by means of their intrinsic tyrosyl and phenylalanyl fluorescence. (1983) *Arch. Biochem. Biophys.* **227**, 9-20.

Permyakov, E. A., Shnyrov, V. L., Kalinichenko, L. P., & Orlov, N.Y. Effects of cation binding on the thermal transitions in calmodulin. (1985) *Biochim. Biophys. Acta* **830**, 288-295.

Persechini, A., Stemmer P. M., & Ohashi, I. Localization of unique functional determinants in the calmodulin lobes to individual EF hands. (1996) *J. Biol. Chem.* **271**, 32217-32225.

Potter, J. D., & Gergely, J. The calcium and magnesium binding sites on troponin C and their role in the regulation of myofibrillar adenosine triphosphatase. (1975) *J. Biol. Chem.* **250**, 4628-4633.

Potter, J. D., Seidel, J. C., Leavis, P., Lehrer, S. S., & Gergely, J. Effect of Ca^{2+} binding on troponin C. (1976) *J. Biol. Chem.* **251**, 7551-7556.

Potter, J. D., Johnson, J. D., Dedman, J. R., Schreiber, W. E., Mandel, F., Jackson, R. L., & Means, A. R. Calcium-binding proteins: relationship of binding, structure, conformation and biological function. (1977) In *Calcium Binding Proteins and Calcium Function.* (Wasserman, R. H., Corradino, R. A., Carafoli, E., Kretsinger, R. H., MacLennan, D. H., & Siegel, F. L., eds.) pp239-250, Elsevier North Holland, Inc., New York, New York.

Potts, B. C., Smith, J., Akke, M., Macke, T. J., Okazaki, K., Hidaka, H., Case, D. A., & Chazin, W. J. The structure of calcyclin reveals a novel homodimeric fold for S100 Ca^{2+}-binding proteins. (1995) *Nature Struct. Biol.* **2**, 790-796.

Procyshyn, R. M., & Reid, R. E. A structure/activity study of calcium affinity and selectivity using a synthetic peptide model of the helix-loop-helix calcium-binding motif. (1994a) *J. Biol. Chem.* **269**, 1641-1647.

Procyshyn, R. M., & Reid, R. E. An examination of glutamic acid in the -X chelating position of the helix-loop-helix calcium binding motif. (1994b) *Arch. Biochem. Biophys.* **311**, 425-429.

Putkey, J. A., Draetta, G. F., Slaughter, G. R., Klee, C. B., Cohen, P., Stull, J. T., & Means, A. R. Genetically engineered calmodulins differentially activate target enzymes. (1986) *J. Biol. Chem.* **261**, 9896-9903.

Putkey, J. A., Sweeney, H. L., & Campbell, S. T. Site-directed mutation of the trigger calcium binding sites in cardiac troponin C. (1989) *J. Biol. Chem.* **264**, 12370-12378.

Reid, R. E., & Hodges, R. S. Co-operativity and calcium/magnesium binding to troponin C and muscle calcium binding parvalbumin: an hypothesis. (1980) *J. Theor. Biol.* **84**, 401-444.

Reid, R. E., Clare, D. M., & Hodges, R. S. Synthetic analog of a high affinity calcium binding site in rabbit skeletal troponin C. (1980) *J. Biol. Chem.* **255**, 3642-3646.

Reid, R. E., Gariepy, J., Saund, A. K., & Hodges, R. S. Calcium-induced protein folding: structure-affinity relationships in synthetic analogs of the helix-loop-helix calcium binding unit. (1981) *J. Biol. Chem.* **256**, 2742-2751.

Reid, R. E. Total sequential solid phase synthesis of rabbit skeletal troponin C calcium binding site III. (1987a) *Int. I. Peptide Protein Res.* **30**, 613-621.

Reid, R. E. A synthetic 33-residue analog of bovine brain calmodulin calcium binding site III: synthesis, purification, and calcium binding. (1987b) *Biochemistry* **26**, 6070-6073.

Reid, R E. Synthetic fragments of calmodulin calcium-binding site III: a test of the acid pair hypothesis. (1990) *J. Biol. Chem.* **265**, 5971-5976.

Reid, R. E., & Procyshyn, R. M. Engineering magnesium selectivity in the helix-loop-helix calcium-binding motif. (1995) *Arch. Biochem. Biophys. 323*, 115-119.

Reinach, F. C., & Karlsson, R. Cloning, expression, and site-directed mutagenesis of chicken skeletal muscle troponin C. (1988) *J. Biol. Chem.* **263**, 2371-2376.

Rinaldi,, M. L., Haiech, J., Pavlovitch, J., Rizk, M., Ferraz, C., Derancourt, J., & Demaille, J. G. Isolation and characterization of a rat skin parvalbumin-like calcium-binding protein. (1982) *Biochemistry* **21**, 4805-4810.

Rhyner, J. A., Koller, M., Durussel-Gerber, I., Cox, J. A., & Strehler, E. E. Characterization of the human calmodulin-like protein expressed in *E. coli*. (1992) *Biochemistry* **31**, 12826-12832.

Roberts, D. M., Crea, R., Malecha, M., Alvarado-Urbina, G., Chiarello, R. H., & Watterson, D. M. Chemical synthesis and expression of a calmodulin gene designed for site-specific mutagenesis. (1985) *Biochemistry* **24**, 5090-5098.

Saimi, Y., & Ling, K. -Y. Calmodulin activation of calcium-dependent sodium channels in excited membrane patches of *Paramecium*. (1990) *Science* **249**, 1441-1444.

Sakane, F., Yamada, K., Kanoh, H., Yokoyama, C., & Tanabe, T. Porcine diacylglycerol kinase sequence has zinc finger and E-F hand motifs. (1990) *Nature* **344**, 345-348.

Sambrook, J., Fritsch, E.F., & Maniatis, T. (1989) in *Molecular Cloning: A Laboratory Manual*, 2nd Ed., pp18.51-18.55, Cold Spring Harbor Laboratory, Cold Spring Harbor, New York.

Satyshur, K. A., Rao, S. T., Pyzalska, D., Drendel, W., Greaser, M., & Sundaralingam, M. Refined structure of chicken skeletal muscle troponin C in the two-calcium state at 2-Å resolution. (1988) *J. Biol. Chem.* **263**, 1628-1647.

Schmidt, H. H. H. W., Wilke, P., Evers, B. & Bohme, E. Enzymatic formation of nitrogen oxides from L-arginine in bovine brain cytosol. (1989) *Biochem. Biophys. Res. Commun.* **165**, 284-291.

Seamon, K.B. Calcium- and magnesium-dependent conformational states of calmodulin as determined by nuclear magnetic resonance. (1980) *Biochemistry* **19**, 207-215.

Seaton, B. A., Head, J. F., Engelman, D. M., & Richards, F. M. Calcium-induced increase in the radius of gyration and maximum dimension of calmodulin measured by small-angle X-ray scattering. (1985) *Biochemistry* **24**, 6740-6743.

Sekharudu, Y. C., & Sundaralingam, M. A structure-function relationship for the calcium affinities of regulatory proteins containing 'EF-hand' pairs. (1988) *Prot. Eng.* **2**, 139-146.

Shaw, G. S., Hodges, R. S., & Sykes, B. D. Probing the relationship between α-helix formation and calcium affinity in troponin C: ^{1}H NMR studies of calcium binding to synthetic and variant site III helix-loop-helix peptides. (1991) *Biochemistry* **30**, 8339-8347.

Shea, M. A., Verhoeven, A. S., & Pedigo, S. Calcium-induced interactions of calmodulin domains revealed by quantitative thrombin footprinting of Arg37 and Arg106. (1996) *Biochemistry* **35**, 2943-2957.

Sheng, M., Thompson, M. A., & Greenberg, M. E. CREB: a Ca^{2+}-regulated transcription factor phosphrylated by calmodulin-dependent kinases. (1991) *Science* **252**, 1427-1430.

Sherry, J. M. F., Gorecka, A., Aksoy, M. O., Dabrowska, R., & Hartshorne, D. J. Roles of calcium and phosphorylation in the regulation of the activity of gizzard myosin. (1978) *Biochemistry*. **17**, 4411-4418.

Skelton, N. J., Forsén, S., & Chazin, W. J. ^{1}H NMR resonance assignments, secondary structure, and global fold of apo bovine calbindin D_{9K}. (1990a) *Biochemistry* **29**, 5752-5761.

Skelton, N. J., Kördel, J., Forsén, S., & Chazin, W. J. Comparative structural analysis of the calcium free and calcium bound states of the calcium regulatory protein calbindin D_{9K}. (1990b) *J. Mol. Biol.* **213**, 593-598.

Skelton, N. J., Kördel, J., Akke, M., Forsén, S., & Chazin, W. J. Signal transduction versus buffering activity in Ca^{2+}-binding proteins. (1994) *Nature Struct. Biol.* **1**, 239-245.

Skelton, N. J., Kördel, J., & Chazin, W. J. Determination of the solution structure of apo $calbindin_{9K}$. (1995) *J. Mol. Biol.* **249**, 441-462.

Starovasnik, M. A., Davis, T. N., & Klevit, R. E. Similarities and differences between yeast and vertebrate calmodulin: an examination of the calcium-binding and structural properties of calmodulin from the yeast *Saccharomyces cerevisiae*. (1993) *Biochemistry* **32**, 3261-3270.

Steward, A. A., Ingebritsen, T. S., Manalan, A., Klee, C. B., & Cohen, P. Discovery of a Ca^{2+}- and calmodulin-dependent protein phosphatase: probable identity with calcineurin ($CaM\text{-}BP_{80}$). (1982) *FEBS* Lett. **137**, 80-84.

Stewart, A. A., Ingebritsen, T. S., & Cohen, P. The protein phosphatases involved in cellular regulation. 5. Purification and properties of a Ca^{2+}/calmodulin-dependent protein phosphatase (2B) from rabbit skeletal muscle. (1983) *Eur. J. Biochem.* **132**, 289-295.

Strynadka, N. C. J., & James, M. N. G. Crystal structures of the helix-loop-helix calcium-binding proteins. (1989) *Annu. Rev. Biochem.* **58**, 951-998.

Sundaralingam, M., Bergstrom, R., Strasburg, G., Rao, S. T., Roychowdhury, P., Greaser, M., & Wang, B. C. Molecular structure of troponin C from chicken skeletal muscle at 3-angstrom resolution. (1985) *Science* **227**, 945-948.

Svensson, B., Jönsson, B., & Thulin, E. Binding of Ca^{2+} to calmodulin and its tryptic fragments: theory and experiment. (1993) *Biochemistry*. **32**, 2828-2834.

Szebenyi, D. M. E., Obedorf, S. K., & Moffat, K. Structure of vitamin D-dependent calcium-binding protein from bovine intestine. (1981) *Nature* **294**, 327-332.

Szebenyi, D. M. E., & Moffat, K. The refined structure of vitamin D-dependent calcium-binding protein from bovine intestine. Molecular details, ion binding, and implications for the structure of other calcium-binding proteins. (1986) *J. Biol. Chem.* **261**, 8761-8777.

Taylor, A. N. (1983) In *Calcium Binding Proteins* (De Bernard, B., Sottocasa, G. L., Sandri, G., Carafoli, E., Taylor, A. W. eds) pp207-213, Elsevier Science., Amsterdam, Netherlands.

Teo, T. S., & Wang, J. H. Mechanism of activation of a cyclic adenosine 3':5'-monophosphate phosphodiesterase from bovine heart by calcium ions. Identification of the protein activator as a Ca^{2+} binding protein. (1973) *J. Biol. Chem.* **248**: 5950-5955.

Trigo-Gonzalez, G., Racher, K., Burtnick, L., & Borgford, T. A comparative spectroscopic study of tryptophan probes engineered into high- and low-affinity domains of recombinant chicken troponin C. (1992) *Biochemistry 31*, 7009-7015.

Van Eerd, J.-P., & Takahashi, K. The amino acid sequence of bovine cardiac troponin C. Comparison with rabbit skeletal troponin C. (1975) *Biochem. Biophys. Res. Commun.* **64**, 122-127.

Van Eerd, J.-P., & Takahashi, K. Determination of the complete amino acid sequence of bovine cardiac troponin C. (1976) *Biochemistry.* **15**, 1171-1180.

Vogt, H.-P., Strassburger, W., & Wollmer, A. Calcium binding by troponin-C and homologs is correlated with the position and linear density of "β-turn forming" residues. (1979) *J. Theor. Biol.* **76**, 297-310.

Vyas, M. N., Jacobson, B. L., & Quiocho, F. A. The calcium binding site in the galactose chemoreceptor protein: crystallographic and metal binding studies. (1989) *J. Biol. Chem.* **264**, 20817-20821.

Wallace, R.B., Tallant, E.A., & Cheung, W.Y. Assay of calmodulin by Ca^{2+}-dependent phosphodiesterase. (1983) *Methods in Enzymology* **102**, 39-47.

Waltersson, Y., Linse S., Brodin, P., & Grundström, T. Mutational effects on the cooperativity of Ca^{2+} binding in calmodulin. (1993) *Biochemistry* **32**, 7866-7871.

Wang, C.-L.A., Leavis, P.C., & Gergely, J. Kinetic studies show that Ca^{2+} and Tb^{3+} have different binding preferences toward the four Ca^{2+}-binding sites of calmodulin. (1984) *Biochemistry 23*, 6410-6415.

Wang, C. K., & Cheung, H. T. Energetics of the binding of calcium and troponin I to troponin C from rabbit skeletal muscle. (1985) *Biophys. J.* **48**, 727-739.

Wang, C.-L. A., Zhan, Q., Tao, T., & Gergely, J. pH-dependent structural transition in rabbit skeletal troponin C. (1987) *J. Biol. Chem.* **262**, 9636-9640.

Wasserman, R. H., & Fullmer, C. S. Vitamin D-induced calcium-binding protein. (1982) In *Calcium and Cell Function.* (Cheung, W. Y. ed) **2**, 175-216, Academic Press, New York, New York.

Wasserman, R. H., Shimura, F., Meyer, S. A., & Fullmer, C. S. (1983) In *Calcium Binding Proteins* (De Bernard, B., Sottocasa, G. L., Sandri, G., Carafoli, E., & Taylor, A. W. eds) pp. 183-205. Elsevier Science, Amsterdam, Netherlands.

Watterson, D. M., Sharief, F., & Vanaman, T. C. The complete amino acid sequence of the Ca^{2+}-dependent modulator protein (calmodulin) of bovine brain. (1980) *J. Biol. Chem.* **259**, 13680-13683.

Wegner, M., Cao, Z., & Rosenfeld, M. G. Calcium-regulated phosphorylation within the leucine Zipper of CEBPβ. (1992) *Science* **256** 370-377.

Wilkinson, J. M. The amino acid sequence of troponin C from chicken skeletal muscle. (1976) *FEBS Lett.* **70**, 254-256.

Williams, T. C., Corson, D. C., Oikawa, McCubbin, W. D., Kay, C. M., & Sykes, B. D. ^1H NMR spectroscopic studies of calcium binding proteins. 3. Solution conformations of rat apo-α-parvalbumin and metal-bound rat α-parvalbumin. (1986) *Biochemistry* **25**, 1835-1846.

Wintrode P. L., & Privalov, P. L. Energetics of target peptide recognition by calmodulin: a calorimetric study. (1997) *J. Mol. Biol.* **266**, 1050-1062.

Wnuk, W., Cox, J. A., & Stein, E. A. Parvalbumins and other soluble high-affinity calcium-binding proteins from muscle. (1982) In *Calcium and Cell Function.* (Cheung, W. Y. ed) **2**, 243-278, Academic Press, New York, New York.

Wolff, D. J., Poirier, P. G., Brostrom, C. O., & Brostrom, M. A. Divalent cation binding properties of bovine brain Ca^{2+}-dependent regulator protein. (1977) *J. Biol. Chem.* **252**, 4108-4117.

Wu, X. & Reid, R. E. Conservative D133E mutation of calmodulin site IV drastically alters calcium binding and phosphodiesterase regulation. (1997a) *Biochemistry* 36, 3608-3616.

Wu, X. & Reid, R. E. Structure/calcium affinity relationships of site III of calmodulin: testing the Acid-Pair Hypothesis using calmodulin mutants. (1997b) *Biochemistry* in press.

Wylie, D. C., & Vanaman, T. C. Structure and evolution of the calmodulin family of calcium regulatory proteins. (1988) In *Calmodulin* (Cohen, P., & Klee, C. B. eds) pp1-15, Elsevier, Amsterdam, Netherlands.

Yazawa, M., Kuwayama, H., & Yagi, K. Modulator protein as a Ca^{2+}-dependent activator of rabbit skeletal myosin light-chain kinase. (1978) *J. Biochem. (Tokyo)* **84**, 1253-1258.

Yazawa, M., Ikura, M., Hikichi, K., Ying, L., & Yagi, K. Communication between two globular domains of calmodulin in the presence of mastoparan or caldesmon fragment. (1987) *J. Biol. Chem.* **262**, 10951-10954.

Zhang, M., & Vogel, H. J. Characterization of the calmodulin-binding domain of rat cerebellar nitric oxide synthase. (1994) *J. Biol. Chem.* **269**, 981-985.

Zhang, M., Tanaka, T., & Ikura, M. Calcium-induced conformational transition revealed by the solution structure of apo calmodulin. (1995) *Nature Struct. Biol.* **2**, 758-767.

Zhao, Y., Pokutta, S., Maurer, P., Lindt, M., Franklin, R. M., & Kappes, B. Calcium-binding properties of a calcium-dependent protein kinase from *Plasmodium falciparum* and the significance of individual calcium-binding sites for kinase activation. (1994) *Biochemistry* **33**, 3714-3721.

Zot, A. S., & Potter, J. D. Structural aspects of troponin-tropomyosin regulation of skeletal myuscle contraction. (1987) *Annu. Rev. Biophys. Biophys. Chem.* **16**, 535-559.

APPENDIX

Table 16. One-Site Model Fitting[a]

Protein	Parameter	Value	CV%	Dependency	Fit Coeff. (r^2)[b]
VU-1	n	0.88	6.17	0.1313604	0.986249
	K (μM)	2.99	8.62	0.1313604	
F92W	n	1.72	4.59	0.0990303	0.996092
	K (μM)	1.24	2.78	0.0990303	
F92W/D133E	n	1.07	2.89	0.0018255	0.99125
	K (μM)	1143	2.84	0.0018255	
3xCaM	n	0.82	2.57	0.0534632	0.988929
	K (μM)	589	3.25	0.0534632	
3zCaM	n	0.70	4.14	0.0511166	0.968361
	K (μM)	806	5.78	0.0511166	
4xCaM	n	0.58	4.11	0.2170025	0.976827
	K (μM)	161	7.23	0.2170025	
4zCaM	n	0.43	6.48	0.0765307	0.958424
	K (μM)	109	16.0	0.0765307	
4xzCaM	n	0.44	6.51	0.0804534	0.956373
	K (μM)	72	16.2	0.0804534	

[a] Calcium titration data (average of six to nine separate titrations) were fitted to the one-site model: $f = \frac{[Ca^{2+}]^n}{K^n + [Ca^{2+}]^n}$ where f, n, and K are parameters as defined in section 2.2.17 on pages 73-74. Dependency is an indicator of overparameterization. Parameters with dependency near 1 are strongly dependent on one another. This may indicate that the equation used is too complicated and overparameterized. Data fittings were carried out using the program SigmaPlot for Windows.

[b] The fitting coefficient was obtained by fitting the data using the program SlideWrite for Windows.

Table 17. One-Site Model Fitting (+W4I-M13 Peptide)[a]

Protein	Parameter	Value	CV%	Dependency	Fit Coeff. (r^2)[b]
VU-1	n	1.77	4.68	0.0004903	0.991612
	K (μM)	0.05	2.47	0.0004903	
F92W	n	1.59	2.05	0.0183410	0.9981
	K (μM)	0.09	1.39	0.0183410	
F92W/D133E	n	1.74	4.94	0.0512696	0.990341
	K (μM)	0.46	2.83	0.0512696	
3xCaM	n	2.11	3.15	0.0516508	0.996559
	K (μM)	0.48	1.57	0.0516508	
3zCaM	n	1.52	5.68	0.0846269	0.985006
	K (μM)	0.46	3.83	0.0846269	
4xCaM	n	2.30	2.72	0.0142425	0.996665
	K (μM)	0.24	1.26	0.0142425	
4zCaM	n	2.29	2.19	0.0017240	0.997544
	K (μM)	0.17	0.99	0.0017240	
4xzCaM	n	2.13	2.55	0.0002316	0.996377
	K (μM)	0.14	1.18	0.0002316	

[a] Calcium titration data (average of three to six separate titrations in the presence of the CaM-binding peptide, W4I-M13) were fitted to the one-site model: $f = \frac{[Ca^{2+}]^n}{K^n + [Ca^{2+}]^n}$ where f, n, and K are parameters as defined in section 2.2.17 on pages 73-74. Dependency is an indicator of overparameterization. Parameters with dependency near 1 are strongly dependent on one another. This may indicate that the equation used is too complicated and overparameterized. Data fittings were carried out using the program SigmaPlot for Windows.

[b] The fitting coefficient was obtained by fitting the data using the program SlideWrite for Windows.

Table 18. Two-Site Model Fitting[a]

Protein	Parameter	Value	CV%	Dependency	Fit Coeff. (r^2)[b]
VU-1	f_1	0.65	2.39	0.9507404	0.999748
	n_1	1.84	2.92	0.6464798	
	K_1 (μM)	1.1	2.83	0.8845568	
	n_2	1.29	5.67	0.7418238	
	K_2 (μM)	35	9.48	0.9059047	
F92W	f_1	0.83	2.46	0.9866874	0.999931
	n_1	2.22	1.83	0.8048031	
	K_1 (μM)	1.0	1.48	0.9364767	
	n_2	1.29	10.1	0.8690744	
	K_2 (μM)	11	21.4	0.9635359	
F92W/D133E	f_1	0.43	8.76	0.9879479	0.998902
	n_1	2.41	9.24	0.8158498	
	K_1 (μM)	360	5.91	0.9280067	
	n_2	1.64	6.02	0.8586546	
	K_2 (μM)	3037	8.55	0.9701573	
3xCaM	f_1	0.66	13.3	0.9975455	0.998184
	n_1	0.92	9.67	0.9637509	
	K_1 (μM)	223.5	28.2	0.9946406	
	n_2	1.81	16.0	0.9424526	
	K_2 (μM)	3036	10.5	0.9505089	
3zCaM	f_1	0.52	5.2	0.9778629	0.997278
	n_1	1.19	9.29	0.8632332	
	K_1 (μM)	144.7	10.1	0.9150952	
	n_2	1.85	6.33	0.7163279	
	K_2 (μM)	4627	5.71	0.8900116	

Table 18. Two-Site Model Fitting (Cont'd)[a]

Protein	Parameter	Value	CV%	Dependency	Fit Coeff. (r^2)[b]
4xCaM	f_1	0.47	7.13	0.9730590	0.99846
	n_1	0.94	11.8	0.7986880	
	K_1 (μM)	9.1	22.8	0.8593751	
	n_2	1.16	6.66	0.7568958	
	K_2 (μM)	1137	11.3	0.9217032	
4zCaM	f_1	0.48	2.91	0.8118896	0.996723
	n_1	1.22	9.96	0.4285614	
	K_1 (μM)	3.0	10.0	0.5578276	
	n_2	1.12	6.65	0.5079639	
	K_2 (μM)	1860	7.77	0.6819909	
4xzCaM	f_1	0.46	3.02	0.7961683	0.996622
	n_1	1.81	10.6	0.2804821	
	K_1 (μM)	2.2	7.01	0.4490961	
	n_2	1.0	6.17	0.5203869	
	K_2 (μM)	1104	8.90	0.7069097	

[a] Calcium titration data (average of six to nine separate titrations) were fitted to the two-site model: $f = f_1 \cdot \frac{[Ca^{2+}]^{n_1}}{K_1^{n_1} + [Ca^{2+}]^{n_1}} + (1 - f_1) \cdot \frac{[Ca^{2+}]^{n_2}}{K_2^{n_2} + [Ca^{2+}]^{n_2}}$ where f, f_1, n_1, n_2, K_1 and K_2 are parameters as defined in section 2.2.17. on pages 73-74. Dependency is an indicator of overparameterization. Parameters with dependency near 1 are strongly dependent on one another. This may indicate that the equation used is too complicated and overparameterized. Data fittings were carried out using the program SigmaPlot for Windows.

[b] The fitting coefficient was obtained by fitting the data using the program SlideWrite for Windows.

Table 19. Two-Site Model Fitting (+W4I-M13 Peptide)[a]

Protein	Parameter	Value	CV%	Dependency	Fit Coeff. (r^2)[b]
VU-1	f_1	0.79	2.18	0.9945576	0.999944
	n_1	2.63	1.54	0.8663398	
	K_1 (μM)	0.04	0.99	0.9511106	
	n_2	1.58	8.05	0.9385505	
	K_2 (μM)	0.26	11.1	0.9805911	
F92W	f_1	0.21	28.5	0.9949956	0.999559
	n_1	3.71	21.0	0.8911652	
	K_1 (μM)	0.03	7.35	0.9215887	
	n_2	1.89	5.27	0.9270642	
	K_2 (μM)	0.13	8.30	0.9892696	
F92W/D133E	f_1	0.82	3.67	0.9872655	0.999579
	n_1	2.40	3.42	0.8496879	
	K_1 (μM)	0.36	1.38	0.8313160	
	n_2	0.87	1.67	0.9103438	
	K_2 (μM)	8.0	4.84	0.9671991	
3xCaM	f_1	0.84	7.54	0.9957339	0.999666
	n_1	2.62	5.25	0.9429294	
	K_1 (μM)	0.41	1.85	0.9239582	
	n_2	1.15	22.6	0.9327959	
	K_2 (μM)	2.74	68.4	0.9901544	
3zCaM	f_1	0.74	6.36	0.9879677	0.998991
	n_1	2.42	5.75	0.8582079	
	K_1 (μM)	0.31	2.40	0.8450535	
	n_2	0.92	17.3	0.9090757	
	K_2 (μM)	6.1	47.7	0.9676558	

Table 19. Two-Site Model Fitting (+W4I-M13 Peptide) (Cont'd)[a]

Protein	Parameter	Value	CV%	Dependency	Fit Coeff. (r^2)[b]
4xCaM	f_1	0.84	6.55	0.9080420	0.999843
	n_1	2.89	3.86	0.9590695	
	K_1 (μM)	0.20	1.53	0.9631692	
	n_2	1.52	21.9	0.9693827	
	K_2 (μM)	1.02	44.3	0.9946517	
4zCaM	f_1	0.88	6.21	0.9984974	0.999855
	n_1	2.73	3.29	0.9591408	
	K_1 (μM)	0.16	1.59	0.9732460	
	n_2	1.47	29.5	0.9736358	
	K_2 (μM)	0.72	58.8	0.9960414	
4xzCaM	f_1	0.85	2.82	0.9972766	0.999934
	n_1	2.69	1.54	0.9147057	
	K_1 (μM)	0.12	1.08	0.9745741	
	n_2	1.73	12.6	0.9610817	
	K_2 (μM)	0.61	18.2	0.9904187	

[a] Calcium titration data (average of three to six separate titrations in the presence of the CaM-binding peptide, W4I-M13) were fitted to the two-site model: $f = f_1 \cdot \frac{[Ca^{2+}]^{n_1}}{K_1^{n_1} + [Ca^{2+}]^{n_1}} + (1 - f_1) \cdot \frac{[Ca^{2+}]^{n_2}}{K_2^{n_2} + [Ca^{2+}]^{n_2}}$ where f, f_1, n_1, n_2, K_1 and K_2 are parameters as defined in section 2.2.17. on pages 73-74. Dependency is an indicator of overparameterization. Parameters with dependency near 1 are strongly dependent on one another. This may indicate that the equation used is too complicated and overparameterized. Data fittings were carried out using the program SigmaPlot for Windows.

[b] The fitting coefficient was obtained by fitting the data using the program SlideWrite for Windows.

Table 20. Three-Site Model Fitting[a]

Protein	Parameter	Value	CV%	Dependency
VU-1	f_1	0.48	5.85×10^9	1.0000000
	K_1 (μM)	2.45	2.56×10^9	1.0000000
	f_2	0.48	5.85×10^9	1.0000000
	K_2 (μM)	2.45	2.56×10^9	1.0000000
	K_3 (μM)	6584	3428	0.0000066
F92W	f_1	0.51	714	0.9999500
	K_1 (μM)	1.57	3129	0.9999500
	f_2	0.51	714	0.9999500
	K_2 (μM)	1.57	3129	0.9999500
	K_3 (μM)	-7.6×10^5	519	0.0000000
F92W/D133E	f_1	0.96	14.4	0.9970520
	K_1 (μM)	1127	16.7	0.9719705
	f_2	0.24	152	0.9940040
	K_2 (μM)	29420	390	0.9984918
	K_3 (μM)	6.68×10^6	19.2	0.0000000
3xCaM	f_1	0.10	2.03×10^5	1.0000000
	K_1 (μM)	52.5	21130	0.9999984
	f_2	0.14	1.45×10^5	1.0000000
	K_2 (μM)	49.3	22180	0.9999988
	K_3 (μM)	1138	19.6	0.9826917
3zCaM	f_1	0.18	1.16×10^7	1.0000000
	K_1 (μM)	85.4	3.55×10^5	1.0000000
	f_2	0.17	1.2×10^7	1.0000000
	K_2 (μM)	82.0	3.58×10^5	1.0000000

Table 20. Three-Site Model Fitting (Cont'd)[a]

Protein	Parameter	Value	CV%	Dependency
3zCaM	K_3 (μM)	2504	29.4	0.9726996
4xCaM	f_1	0.20	4.18×10^6	1.0000000
	K_1 (μM)	6.86	1.35×10^5	1.0000000
	f_2	0.21	3.92×10^6	1.0000000
	K_2 (μM)	6.87	1.21×10^5	1.0000000
	K_3 (μM)	907	8.55	0.8549076
4zCaM	f_1	0.39	2.36×10^7	1.0000000
	K_1 (μM)	3.18	3.4×10^5	1.0000000
	f_2	0.08	1.19×10^8	1.0000000
	K_2 (μM)	3.21	1.74×10^6	1.0000000
	K_3	1698	10.1	0.6475435
4xzCaM	f_1	0.40	3.51×10^9	1.0000000
	K_1 (μM)	3.01	8.68×10^6	1.0000000
	f_2	0.10	1.4×10^{10}	1.0000000
	K_2 (μM)	3.06	3.36×10^7	1.0000000
	K_3 (μM)	1275	12.9	0.6385749

[a] Calcium titration data (average of six to nine separate titrations) were fitted to the three-site model: $f = f_1 \cdot \frac{[Ca^{2+}]}{K_1 + [Ca^{2+}]} + f_2 \cdot \frac{[Ca^{2+}]}{K_2 + [Ca^{2+}]} + (1 - f_1 - f_2) \cdot \frac{[Ca^{2+}]}{K_3 + [Ca^{2+}]}$ where f, f_1, f_2, K_1, K_2, and K_3 are parameters as defined in section 2.2.17. on pages 73-74. Dependency is an indicator of overparameterization. Parameters with dependency near 1 are strongly dependent on one another. This may indicate that the equation used is too complicated and overparameterized. Data fittings were carried out using the program SigmaPlot for Windows.

Table 21. Three-Site Model Fitting (+W4I-M13 Peptide)[a]

Protein	Parameter	Value	CV%	Dependency
VU-1	f_1	0.64	6.34×10^7	1.0000000
	K_1 (μM)	0.05	6.4×10^5	1.0000000
	f_2	0.36	1.11×10^8	1.0000000
	K_2 (μM)	0.05	1.12×10^6	1.0000000
	K_3 (μM)	-0.13	14.2	0.9997320
F92W	f_1	0.55	2.71×10^{11}	1.0000000
	K_1 (μM)	0.10	2.78×10^9	1.0000000
	f_2	0.51	5.86×10^{10}	1.0000000
	K_2 (μM)	0.10	1.41×10^{10}	1.0000000
	K_3 (μM)	0.10	6.01×10^{10}	1.0000000
F92W/D133E	f_1	2.01	1.13×10^{11}	1.0000000
	K_1 (μM)	1.18	1.34×10^8	1.0000000
	f_2	1.88	1.21×10^{11}	1.0000000
	K_2 (μM)	1.18	1.33×10^8	1.0000000
	K_3 (μM)	1.67	6439	0.9999996
3xCaM	f_1	2.23	2689	0.9999660
	K_1 (μM)	1.59	756	0.9999568
	f_2	3.02	1953	0.9999662
	K_2 (μM)	1.58	540	0.9999543
	K_3 (μM)	2.19	274	0.9998907
3zCaM	f_1	0.41	2.24×10^5	0.9999662
	K_1 (μM)	0.54	3468	0.9999687
	f_2	0.55	73760	0.9999685
	K_2 (μM)	0.54	1715	0.9999334

Table 21. Three-Site Model Fitting (+W4I-M13 Peptide) (Cont'd)[a]

Protein	Parameter	Value	CV%	Dependency
	K_3 (μM)	0.53	24780	0.9999556
4xCaM	f_1	-0.53	8.98×10^6	1.0000000
	K_1 (μM)	0.18	8.0×10^5	1.0000000
	f_2	-0.01	5.24×10^{13}	1.0000000
	K_2 (μM)	0.25	9.99×10^{10}	1.0000000
	K_3 (μM)	0.25	9.15×10^8	1.0000000
4zCaM	f_1	0.53	7.27×10^{11}	1.0000000
	K_1 (μM)	0.17	8.71×10^9	1.0000000
	f_2	0.47	1.95×10^{10}	1.0000000
	K_2 (μM)	0.19	3.84×10^8	1.0000000
	K_3 (μM)	0.17	2.72×10^{11}	1.0000000
4xzCaM	f_1	2.49	1535	0.9999652
	K_1 (μM)	0.45	567	0.9999552
	f_2	2.52	1518	0.9999652
	K_2 (μM)	0.45	560	0.9999551
	K_3 (μM)	0.65	257	0.9998803

[a] Calcium titration data (average of three to six separate titrations in the presence of the CaM-binding peptide, W4I-M13) were fitted to the three-site model: $f = f_1 \cdot \frac{[Ca^{2+}]}{K_1 + [Ca^{2+}]} + f_2 \cdot \frac{[Ca^{2+}]}{K_2 + [Ca^{2+}]} + (1 - f_1 - f_2) \cdot \frac{[Ca^{2+}]}{K_3 + [Ca^{2+}]}$ where f, f_1, f_2, K_1, K_2, and K_3 are parameters as defined in section 2.2.17. on pages 73-74. Dependency is an indicator of overparameterization. Parameters with dependency near 1 are strongly dependent on one another. This may indicate that the equation used is too complicated and overparameterized. Data fittings were carried out using the program SigmaPlot for Windows.

Table 22. Four-Site Model Fitting[a]

Protein	Parameter	Value	CV%	Dependency
VU-1	f_1	0.15	67.4	0.9481909
	K_1 (μM)	65.0	109	0.8662069
	f_2	0.33	2.06×10^5	0.9999686
	K_2 (μM)	2.0	3120	0.9999655
	f_3	0.50	5.52×10^5	0.9999682
	K_3 (μM)	2.0	2289	0.9999686
	K_4 (μM)	2.0	19670	0.9999686
F92W	f_1	-7.4×10^{-6}	1.51×10^{17}	1.0000000
	K_1 (μM)	5.97	8.59×10^{12}	1.0000000
	f_2	0.27	1.07×10^5	0.9999999
	K_2 (μM)	0.69	27510	0.9999953
	f_3	0.28	66170	0.9999995
	K_3 (μM)	1.41	74240	0.9999993
	K_4 (μM)	6.0	2.61×10^8	1.0000000
F92W/D133E	f_1	-0.01	3.96×10^7	0.9999662
	K_1 (μM)	1122	4981	0.9999662
	f_2	0.12	2.1×10^5	0.9999707
	K_2 (μM)	1151	5360	0.9999690
	f_3	0.24	58660	0.9999698
	K_3 (μM)	1175	1817	0.9999324
	K_4(μM)	1122	799	0.9999658
3xCaM	f_1	0.12	909	0.9999501
	K_1 (μM)	51.4	3676	0.9999500
	f_2	0.12	909	0.9999501
	K_2 (μM)	51.4	3676	0.9999500
	f_3	0.11	42750	0.9999625

Table 22. Four-Site Model Fitting (Cont'd)[a]

Protein	Parameter	Value	CV%	Dependency
3xCaM	K_3 (μM)	1102	2029	0.9999337
	K_4 (μM)	1146	368	0.9999287
3zCaM	f_1	0.07	2843	0.9999619
	K_1 (μM)	70.3	12590	0.9999507
	f_2	0.07	2843	0.9999619
	K_2 (μM)	70.3	12590	0.9999507
	f_3	0.22	858	0.9999636
	K_3 (μM)	88.5	551	0.9988340
	K_4 (μM)	2500	21.4	0.9438083
4xCaM	f_1	0.21	425	0.9999500
	K_1 (μM)	6.93	2839	0.9999500
	f_2	0.21	425	0.9999500
	K_2 (μM)	6.93	2839	0.9999500
	f_3	-0.14	3782	0.9999510
	K_3 (μM)	521	1316	0.9998399
	K_4 (μM)	828	195	0.9997860
4zCaM	f_1	0.24	4.8×10^9	1.0000000
	K_1 (μM)	3.48	2.09×10^9	1.0000000
	f_2	0.24	4.8×10^9	1.0000000
	K_2 (μM)	3.48	2.09×10^9	1.0000000
	f_3	-0.70	2593	0.9999853
	K_3 (μM)	712	750	0.9999485
	K_4 (μM)	1094	379	0.9999379
4xzCaM	f_1	0.25	580	0.9999500
	K_1 (μM)	3.06	3128	0.9999500
	f_2	0.25	580	0.9999500
	K_2 (μM)	3.06	3128	0.9999500

Table 22. Four-Site Model Fitting (Cont'd)[a]

Protein	Parameter	Value	CV%	Dependency
4xzCaM	f_3	0.11	98370	0.9999625
	K_3 (μM)	1257	3769	0.9998933
	K_4 (μM)	1271	989	0.9998951

[a] Calcium titration data (average of six to nine separate titrations) were fitted to the four-site model:

$$f = f_1 \cdot \frac{[Ca^{2+}]}{K_1 + [Ca^{2+}]} + f_2 \cdot \frac{[Ca^{2+}]}{K_2 + [Ca^{2+}]} + f_3 \cdot \frac{[Ca^{2+}]}{K_3 + [Ca^{2+}]} + (1 - f_1 - f_2 - f_3) \cdot \frac{[Ca^{2+}]}{K_4 + [Ca^{2+}]}$$

where f, f_1, f_2, f_3, K_1, K_2, K_3 and K_4 are parameters as defined in section 2.2.17. on pages 73-74. Dependency is an indicator of overparameterization. Parameters with dependency near 1 are strongly dependent on one another. This may indicate that the equation used is too complicated and overparameterized. Data fittings were carried out using the program SigmaPlot for Windows.

Table 23. Four-Site Model Fitting (+W4I-M13 Peptide)[a]

Protein	Parameter	Value	CV%	Dependency
VU-1	f_1	1.33	3888	0.9999690
	K_1 (μM)	0.13	1168	0.9999649
	f_2	1.31	3963	0.9999690
	K_2 (μM)	0.13	1191	0.9999649
	f_3	1.95	2653	0.9999692
	K_3 (μM)	0.13	794	0.9999636
	K_4 (μM)	0.18	310	0.9999200
F92W	f_1	0.002	4.15×10^{14}	1.0000000
	K_1 (μM)	0.06	1.03×10^{12}	1.0000000
	f_2	0.45	1.26×10^{8}	1.0000000
	K_2 (μM)	0.09	8.54×10^{8}	1.0000000
	f_3	0.81	7.0×10^{10}	1.0000000
	K_3 (μM)	0.09	5.37×10^{8}	1.0000000
	K_4 (μM)	0.06	1.49×10^{10}	1.0000000
F92W/D133E	f_1	1.51	1098	0.9999675
	K_1 (μM)	0.15	532	0.9999638
	f_2	1.44	1156	0.9999675
	K_2 (μM)	0.15	563	0.9999640
	f_3	1.43	1159	0.9999675
	K_3 (μM)	0.15	565	0.9999640
	K_4 (μM)	0.10	148	0.9998887
3xCaM	f_1	0.17	7.49×10^{6}	1.0000000
	K_1 (μM)	0.26	1.38×10^{6}	1.0000000
	f_2	-0.33	36230	0.9999998
	K_2 (μM)	0.06	17590	0.9999953
	f_3	1.16	5.61×10^{13}	1.0000000

Table 23. Four-Site Model Fitting (+W4I-M13 Peptide) (Cont'd)[a]

Protein	Parameter	Value	CV%	Dependency
3xCaM	K_3(μM)	0.40	6.86×10^9	1.0000000
	K_4 (μM)	0.40	1.02×10^{12}	1.0000000
3zCaM	f_1	0.00002	4.87×10^{10}	0.9999689
	K_1 (μM)	0.52	3.11×10^6	0.9999689
	f_2	-0.08	1979	0.9981552
	K_2(μM)	2.27	1598	0.9913446
	f_3	4.32	25100	0.9999686
	K_3 (μM)	0.52	348	0.9999681
	K_4 (μM)	0.52	470	0.9999689
4xCaM	f_1	0.008	1.97×10^{15}	1.0000000
	K_1 (μM)	0.17	1.91×10^{11}	1.0000000
	f_2	7.71	3.74×10^8	1.0000000
	K_2 (μM)	0.16	8.41×10^6	1.0000000
	f_3	-1.03	46110	1.0000000
	K_3 (μM)	0.05	12160	0.9999994
	K_4 (μM)	0.17	9.46×10^8	1.0000000
4zCaM	f_1	-0.02	1.58×10^{14}	1.0000000
	K_1 (μM)	0.26	1.79×10^{11}	1.0000000
	f_2	-1.13	1.02×10^5	1.0000000
	K_2 (μM)	0.10	21150	0.9999999
	f_3	-1.16	12270	0.9999999
	K_3 (μM)	1.11	3957	0.9999958
	K_4 (μM)	0.26	1.68×10^9	1.0000000
4xzCaM	f_1	0.22	1.48×10^6	1.0000000
	K_1 (μM)	0.05	2.99×10^5	0.9999999
	f_2	0.18	3.75×10^5	1.0000000

Table 23. Four-Site Model Fitting (+W4I-M13 Peptide) (Cont'd)[a]

Protein	Parameter	Value	CV%	Dependency
4xzCaM	K_2 (μM)	0.09	1.50×10^6	1.0000000
	f_3	0.006	6.94×10^{10}	1.0000000
	K_3 (μM)	0.36	5.19×10^9	1.0000000
	K_4 (μM)	0.31	1.99×10^7	1.0000000

[a] Calcium titration data (average of three to six separate titrations in the presence of the CaM-binding peptide, W4I-M13) were fitted to the four-site model:

$$f = f_1 \cdot \frac{[Ca^{2+}]}{K_1 + [Ca^{2+}]} + f_2 \cdot \frac{[Ca^{2+}]}{K_2 + [Ca^{2+}]} + f_3 \cdot \frac{[Ca^{2+}]}{K_3 + [Ca^{2+}]} + (1 - f_1 - f_2 - f_3) \cdot \frac{[Ca^{2+}]}{K_4 + [Ca^{2+}]}$$

where f, f_1, f_2, f_3, K_1, K_2, K_3 and K_4 are parameters as defined in section 2.2.17. on pages 73-74. Dependency is an indicator of overparameterization. Parameters with dependency near 1 are strongly dependent on one another. This may indicate that the equation used is too complicated and overparameterized. Data fittings were carried out using the program SigmaPlot for Windows.